The role of c-FLIP in anti-viral immunity

Von der Fakultät für Lebenswissenschaften

der Technischen Universität Carolo-Wilhelmina zu Braunschweig

zur Erlangung des Grades einer

Doktorin der Naturwissenschaften

(Dr. rer. nat.)

genehmigte

D i s s e r t a t i o n

von Neda Tafrishi
aus Mashhad, Iran

1. Referent: Prof. Dr. Michael Meyer-Hermann
2. Referent: Prof. Dr. Martin Korte
eingereicht am: 14.11.2016
mündliche Prüfung (Disputation) am: 10.02.2017

Druckjahr 2018

Vorveröffentlichungen der Dissertation

Teilergebnisse aus dieser Arbeit wurden mit Genehmigung der Fakultät für Lebenswissenschaften, vertreten durch den Mentor der Arbeit, in folgenden Beiträgen vorab veröffentlicht:

Tagungsbeiträge

- **Tafrishi, N**.; Plaza-Sirvent, C.; Meyer-Hermann, M.; Schmitz, I.; (2016) The role of c-FLIP in anti-viral immunity. (poster) 46th Annual Meeting of the German Society for Immunology, Hamburg, Germany.
- **Tafrishi, N**.; Plaza-Sirvent, C.; Schmitz, I.; (2016) The role of c-FLIP in anti-viral immunity. 10th German Meeting on Immune Regulation, Schmöckwitz, Germany.
- **Tafrishi, N**.; Plaza-Sirvent, C.; Schmitz, I.; (2016) The role of c-FLIP in anti-viral immunity. (Poster) Annual Retreat of the Helmholtz Graduate School for Infection Research, Goslar, Germany.
- **Tafrishi, N**.; Plaza-Sirvent, C.; Schmitz, I.; (2015) The role of c-FLIP in anti-viral immunity. (Poster) 6th International PhD Symposium of the Helmholtz Graduate School for Infection Research, Braunschweig, Germany.
- **Tafrishi, N**.; Plaza-Sirvent, C.; Schmitz, I.; (2015) The role of c-FLIP in anti-viral immunity. 19th Joint Meeting Signal Transduction – Receptors, Mediators and Genes, Weimar, Germany.
- **Tafrishi, N**.; Plaza-Sirvent, C.; Schmitz, I.; (2014) The role of c-FLIP in anti-viral immunity. Annual Retreat of the Helmholtz Graduate School for Infection Research, Braunschweig, Germany.
- **Tafrishi, N**.; Plaza-Sirvent, C.; Schmitz, I.; (2013) The role of c-FLIP in anti-viral immunity. (Poster) Annual Retreat of the Helmholtz Graduate School for Infection Research, Bad Bevensen, Germany.

Abstract

Preventing and treating influenza virus infection remains challenging. Influenza is a considerable cause of morbidity and mortality all around the world. Programmed cell death is deeply related to different aspects of Influenza A Virus (IAV) infection. Subsequent to efficient antigen clearance, it is crucial that excessive cells are deleted by apoptosis to maintain cell homeostasis. c-FLIP is an inhibitor of death receptor-mediated apoptosis, of which three isoforms have been characterized so far. While the isoforms c-$FLIP_L$ and c-$FLIP_S$ are well characterized, the function of c-$FLIP_R$ remains poorly understood. To study the regulation of the extrinsic pathway of apoptosis by c-$FLIP_R$, we employed transgenic mice that constitutively express murine c-$FLIP_R$ in all hematopoietic cells, called vav$FLIP_R$ mice. In the steady state, transgenic mice had normal immune cell numbers. However, when challenged with influenza virus more weight loss and higher concentrations of IFN-γ and TNF-α were observed at the peak of infection. Moreover, a higher viral load was detected in vav$FLIP_R$ mice at the peak of infection. Analysis of immune cells during IAV infection indicated that although the frequency and the absolute cell number of most of the immune cells were similar, vav$FLIP_R$ mice have a higher number of NK cells at the peak of Infection. Natural killer (NK) cells play a pivotal role in immune response against IAV infection. The exact role of NK cells in IAV infection is not clear since both protective and immunopathogenic roles were reported. To investigate the influence of a higher number of NK cells on host outcome during influenza infection, vav$FLIP_R$ and WT mice were treated with Anti-Asialo-GM1 to deplete NK cells *in vivo* prior to and during influenza infection. Since the differences in viral load disappeared, it was concluded that NK cells contribute to a higher viral load in vav$FLIP_R$ mice at the peak of IAV infection. Finally, it was demonstrated that influenza virus can directly infect and replicate in primary murine NK cells. It is likely that influenza A virus targets and kills NK cells, in order to evade the NK cell innate immune defense. In turn, however, preventing NK cell apoptosis may provide a reservoir for influenza virus to replicate more efficiently.

Zusammenfassung

Influenza-Infektionen tragen weltweit zur Morbidität und Mortalität bei. Influenza-Infektionen zu verhindern und zu behandeln ist noch immer eine große medizinische Herausforderung. Der programmierte Zelltod ist eng mit verschiedenen Aspekten der Influenza A Virus (IAV) Infektion verbunden. Nachdem das Antigen erfolgreich beseitigt wurde, ist es erforderlich, dass überschüssige Immunzellen durch Apoptose entfernt werden, um die Zell-Homöostase zu erhalten. c-FLIP ist ein Inhibitor der Todesrezeptor-gesteuerten Apoptose. Drei verschiedene Isoformen von c-FLIP wurden bis jetzt beschrieben. Während die Isoformen c-$FLIP_L$ und c-$FLIP_S$ sehr gut untersucht sind, ist über die Funktion von c-$FLIP_R$ bisher nur wenig bekannt. Um die Regulation des extrinsischen Signalwegs der Apoptose durch c-$FLIP_R$ zu untersuchen, wurden transgene Mäuse genutzt, die das murine c-$FLIP_R$ konstitutiv in allen hämatopoetischen Zellen exprimieren. Im stationären Zustand zeigen diese Tiere eine normale Anzahl der verschiedenen Immunzellen. Wenn sie jedoch mit IAV infiziert wurden, zeigten sie am Höhepunkt der Infektion einen höheren Gewichtsverlust und höhere Konzentrationen der inflammatorischen Zytokine IFN-γ und TNF-α. Zu diesem Zeitpunkt war auch die Virusbelastung in vav$FLIP_R$ Mäusen deutlich erhöht. Die Analyse der Immunzellen während der IAV Infektion wies darauf hin, dass, obwohl der Anteil und die absolute Zellzahl der meisten Immunzellen sehr ähnlich war, die vav$FLIP_R$ Mäuse mehr NK Zellen am Höhepunkt der Infektion aufwiesen. Obwohl Natürliche Killer (NK) Zellen ein entscheidender Bestandteil der Immunantwort gegen IAV Infektion sind, ist deren genaue Rolle bei der IAV Infektion noch nicht geklärt, da sowohl eine schützende als auch eine immunpathologische Rolle beschrieben wurden. Um den Einfluss einer höheren NK Zellzahl auf die Folgen einer Influenzainfektion für den Wirt zu untersuchen, wurden vav$FLIP_R$ und Kontrolltiere mit Anti-Asialo Antikörper GM1 behandelt, um NK Zellen *in vivo* vor und während der Influenzainfektion zu depletieren. Da die Unterschiede in der Viruslast verschwanden, wurde geschlussfolgert, dass NK Zellen zu einer höheren Virusbelastung in vav$FLIP_R$ Mäusen während einer IAV Infektion beitragen. Schlussendlich wurde gezeigt, dass IAV primäre NK Zellen direkt infizieren und sich in diesen replizieren kann. Es ist wahrscheinlich, dass IAV auf NK Zellen zielt und diese zerstört, um der NK Zell-basierten Immunantwort zu entgehen. Mit der Vermeidung der Apoptose von NK Zellen schafft sich das Influenzavirus ein Reservoir für die effiziente Replikation.

Acknowledgements

Completing my PhD has been a challenging journey. I would not have been able to complete this journey without the aid and support of a countless number of people over the past three years. First and foremost, I am grateful to my supervisors, Professor Dr. Ingo Schmitz and Professor Dr. Michael Meyer Hermann for their trust, support, time, and guidance. They lead me to an amazing research field of infection and immunity. I am so fortunate to have excellent supervisors.

I am thankful to Prof. Dr. Martin Korte who kindly accepted to review and evaluate my thesis, and to Prof. Dr. Stefan Dübel and Dr. Simone Bergmann for kindly accepting to take part to the oral examination.

I would also like to thank Professor Dr. Dunja Bruder for providing helpful feedback in my thesis committee meetings.

Thanks to my colleagues Frida, Michaela, Yvonne, Marc, Carlos, Sabrina, Christian, Alisha, Tobias, Svenja, Konstantinos, Anne-Marie and Daniela for their help and wonderful working atmosphere. I particularly want to acknowledge Carlos and Lisa for their support. Thank you for your encouragement, advice and friendship.

Special thanks to my Persian friends Parvin, Azadeh, Saham, Jaber and Bahram for all the good memories that we have made in Braunschweig.

I would like to thank my family, whose love and support have made this possible. My parents for instilling in me, the confidence, and drive for pursuing my aims, no matter how high and far. My brothers Nima and Navid for helping me laugh through the tough times. I am so happy to have you in my life.

Finally, I would like to thank Nima, whom I share my life. His endless love, have paved the road to my success. He is always there to offer me a hug at the end of the day.

Table of Contents

1. Introduction

1.1. Cell death

The importance of cell death in tissue homeostasis and embryonic development has been demonstrated for many years. So far, several types of cell death have been defined, amongst them, there are five main forms: apoptosis, autophagic cell death, necroptosis, pyroptosis and necrosis. This division is based on important criteria such as mode of cell death (program/accidental), initiators and production of inflammation [1]. Apoptosis and necrosis are differentiated according to the distinct morphological and biochemical characteristics [2]. In 1972 Kerr *et al*., described apoptosis, which illustrates a specific morphological pattern of dying cells that is distinct from necrosis. Apoptotic cells are characterized by cell size reduction, chromatin condensation, nuclear fragmentation, membrane blebbing and formation of apoptotic bodies, which subsequently can be phagocytosed [3] (Figure 1). In contrast, swelling of the cytoplasm and organelles, enormous oxidative stress, rupture of the plasma membrane and release the intracellular contents are the main necrosis specifications [4].

Autophagy is a fundamental catabolic mechanism that is evolutionarily conserved [5]. It is a self-digestive process where metabolites are recycled in the cells. Upon induction of autophagy, double-membrane autophagosomes sequester organelles or a part of the cytosol. Autophagosomes go through a series of maturation processes, then they are delivered to the endosomal lumen. When an endosome fuses with an autophagosome, the product is called amphisome [6–8]. Upon fusion of lysosomes to amphisomes, the internal contents are degraded [9].

Recent studies show some forms of necrosis which are regulated on the molecular level similary to apoptosis. This regulated necrosis was named necroptosis to discriminate between the regulated forms and uncontrolled necrosis [10,11]. Another highly inflammatory form of programmed cell death is pyroptosis, which is triggered by different pathological stimuli such as stroke and cancer. Pyroptosis has a pivotal role in controlling microbial infections. Pyroptosis features include rapid plasma membrane rupture and release of pro-inflammatory intracellular contents, which is in contrasts to apoptosis [12]. Unlike passive cell death, all active forms of cell death are tightly

regulated. Any variation in the physiologic harmony between cellular proliferation and cell death may lead to malignant diseases [13].

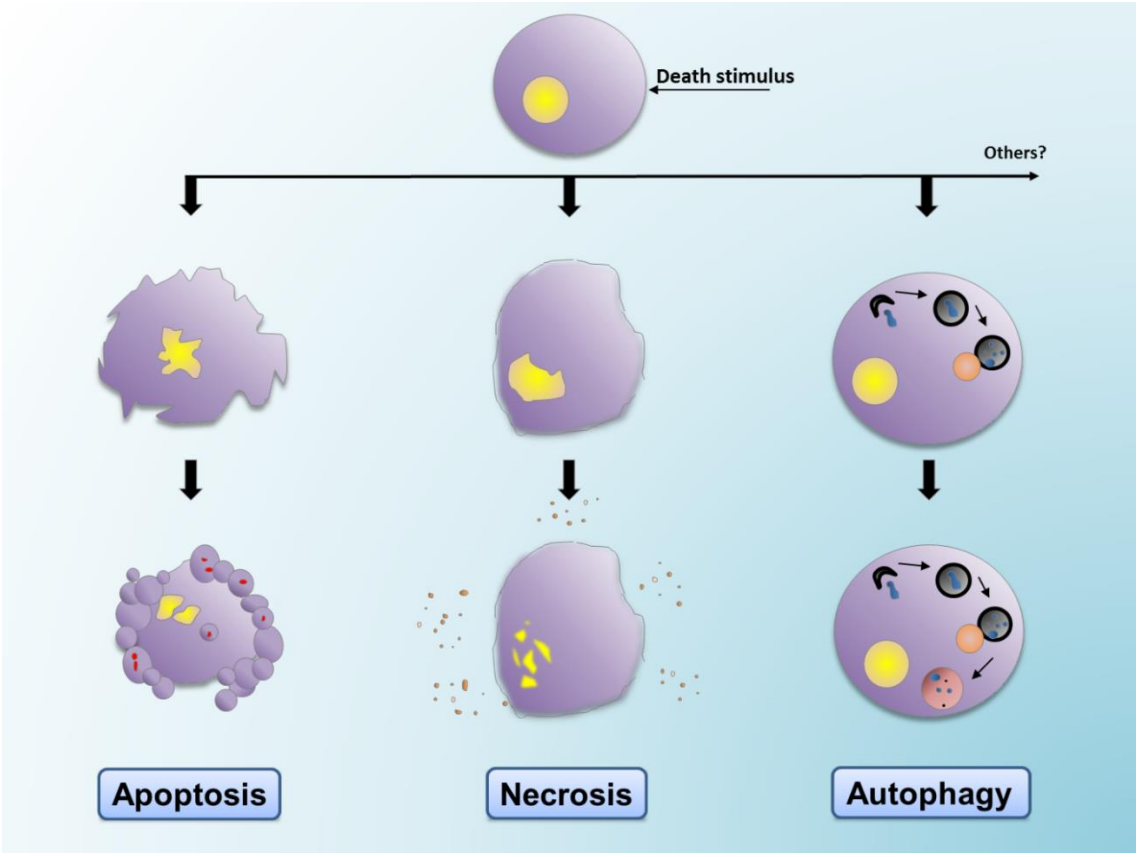

Figure 1. Forms of cell death. Cells death can happen in multiple forms. Type I (apoptosis), Type II (autophagic cell death) and Type III (necrosis), showed in (left), (right) and (middle) of the picture respectively. The apoptotic cell shrinks, DNA is fragmented and the membrane blebs. Further along, apoptotic bodies are formed to facilitate phagocytosis. Autophagic cells include cell material into autophagosomes, while necrosis refers to vacuolation of the cytoplasm, plasma membrane rupture and subsequent loss of intracellular contents, which induce inflammation around the dying cell.

1.2. Apoptosis

Apoptosis is a complex, tightly regulated series of cellular events that is essential for multicellular organisms to eliminate undesirable cells during development, maintenance of tissue homeostasis, and immune system reactions. Dysregulation of apoptosis can lead to malignant disease, including cancer and autoimmune diseases [14,15]. Moreover, the role of apoptosis is substantial in the immune response against viral and bacterial

pathogens by the elimination of infected cells before pathogens spread to other cells [4,16]. There are two main pathways which result in apoptosis, the intrinsic or mitochondrion-initiated pathway and the extrinsic or cell surface death receptor-mediated pathway [17]. In both pathways, there are signals that activate the family of cysteine proteases (caspases) that act as proteolytic machinery. The extrinsic pathway (the death receptor pathway), is activated by binding of death receptors (DRs) which exist on the cell surface. The intrinsic (mitochondrial) apoptotic pathway is activated by different cell stressors such as DNA damage, pH alteration, UV radiation or growth factor withdrawal [18].

1.2.1. Caspases – mediators of apoptosis

Caspases, **c**ysteine-**asp**artic prote**ases** or **c**ysteine-dependent **asp**artate-specific prote**ases**, play a fundamental role in apoptosis. Up to now, 11 murine caspases (caspase 1, 2, 3, 6, 7, 8, 9, 11, 12, 14 and 16) and 12 functional human caspases (caspase 1-10, 14 and 16) have been described [19,20]. According to their function, caspases are categorized into two groups, one of which is involved in the apoptotic action (caspases 2, 3, 6, 7, 8, 9 and 10), and the other is related to inflammation (caspases 1, 4, 5, 11 and 12). The apoptotic caspases are further divided into the initiator and effector caspases. The initiator caspases consist of caspases 2, 8, 9 and 10, and the effector caspases are caspase 3, 6 and 7. Initially, all the caspases are produced as inactive single chain polypeptide precursors (zymogen). Caspases contain three structural domains, a N-terminal pro-domain and two protease domains namely a large subunit (p20) and a small subunit (p10) with a cleavage site that is between the large and small subunits [21]. The N-terminal domain in the initiator caspases, which is crucial for protein interactions, consisting of a caspase recruitment domain (CARD) or death effector domains (DED). In the initial step of activation, these domains mediate dimerization or binding to larger complexes. The initiator caspases are activated with homodimerization of the caspase monomers [22]. Caspases are recruited to the death inducing signaling complex through the interaction of adaptor proteins with CARD or DED domains on initiator caspases [23]. Homodimerization of caspases leads to auto-proteolytic cleavage of the bond between the small and the large subunits, and subsequently cleavage between the pro-domain and the large subunit [21,24]. On the other hand, the effector caspases contain shorter pro-domains and form inactive pro-caspase dimers. Effector caspases

can get activated by activated initiator caspases via proteolytical cleavage of the linker between large and small subunits. The activated effector caspases can then cleave and activate other effector caspases, resulting in a caspase cascade, as well as their other physiological substrates [21,25].

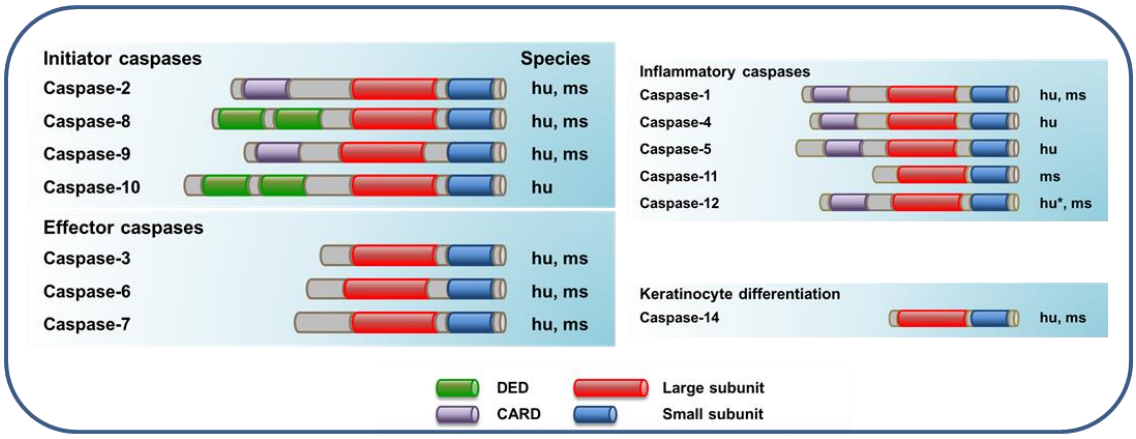

Figure 2. Domain organization of caspases. Three main groups of caspases are presented. Group I: apoptosis initiator caspases. Group II: apoptosis effector caspases. Group III: inflammatory caspases. The caspase activation recruitment domain (CARD), the death effector domain (DED), the large (p20), and the small (p10) catalytic subunits are indicated.

1.2.2. Perforin/granzyme B pathway

In the granzyme B pathway, perforin and granzyme B are released by cytotoxic T lymphocytes (CTL) and Natural Killer (NK) cells, which conjugated to the target cells such as virus-infected cells and tumor cells [26]. Perforin creates large transmembrane pores that mediate the diffusion of serine proteases, known as granzymes into the target cell cytosol [27]. Granzymes then mediate apoptosis by direct activation of caspase 3 or particularly cleavage of Bid and initiation of the intrinsic pathway of apoptosis of the target cell [28]. Afterward, cytotoxic lymphocytes are detached from the dying cell [29,30].

1.2.3. The intrinsic pathway of apoptosis

Several non-receptor-mediated stimuli such as DNA damage, free radicals, toxins and radiation can initiate the intrinsic pathway of apoptotic. Following stimulation,

the intrinsic intracellular signals are produced, approach the mitochondria and impact on the function and integrity of it [31]. The main regulators of this pathway are Bcl-2 (B-cell lymphoma 2) family proteins. All proteins which belongs to the Bcl-2 family contain Bcl-2 homology (BH) domains. Based on their function and number of the BH domains, the Bcl-2 family is divided into three groups [32,33]. The first group contains the anti-apoptotic proteins Bcl-2, Bcl-2-like protein 2 (Bcl-w), B cell lymphoma extra-large (Bcl-xL), myeloid cell leukaemia 1 (Mcl-1) and Bcl-2-related protein A1 (A1). These proteins contain all four BH domains (BH 1-4) and are located in the outer mitochondrial membrane, where the dimerization with other Bcl-2 proteins occurs. The two remaining groups are pro-apoptotic. The second group comprise Bcl-2-associated x protein (Bax), Bcl-2 antagonist killer 1 (Bak) and Bcl-2-related ovarian killer (Bok) [32]. In this group, proteins contain BH domains 1-3. In order for cells to survive, Bax and Bak must constantly be inhibited by anti-apoptotic Bcl-2 members. Alternatively, when apoptosis is needed, Bax and Bak mediate the permeabilization of the outer mitochondrial membrane (OMM), which results in the release of apoptogenic molecules such as cytochrome c from the mitochondria [34]. Release of the cytochrome c induces the formation of the wheel-like structure complex, which contains several molecules of cytochrome c, apoptotic peptidase activating factor 1 (APAF1) and caspase 9 (apoptosome) [35,36]. Active caspase 9 can mediate activation of the executioner caspases 3 and 7 that cause apoptosis [37]. The last group contains the BH3-only proteins, which, as defined by the name, only have the BH3 domain. The proteins, which belong to this group are Bcl-2 antagonist of cell death (Bad), Bcl-2-interacting killer (Bik), Bcl-2 interacting domain death agonist (Bid), Harakiri (Hrk, also known as death protein 5, (DP5), Bcl-2-interacting mediator of cell death (Bim), Bcl-2 modifying factor (Bmf), Noxa, p53-upregulated modulator of apoptosis (Puma) and Mcl-1 ubiquitin ligase E3 (Mule) [38].

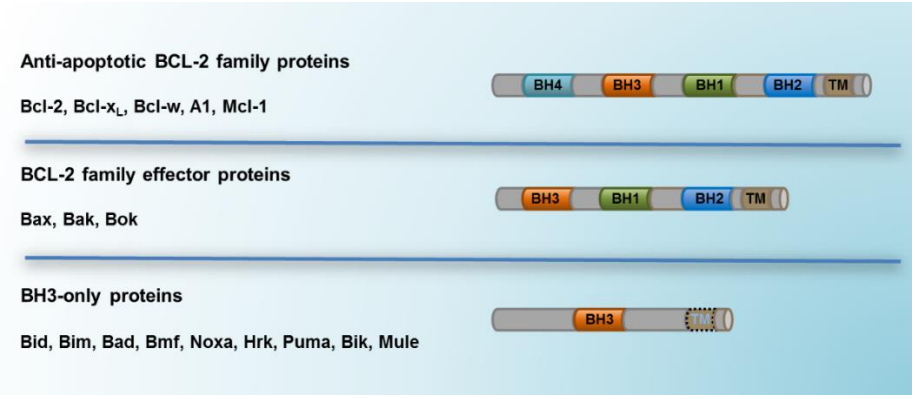

Figure 3. The Bcl-2 family proteins. The proteins are divided into the anti-apoptotic Bcl-2 homologues, the effector proteins, and the pro-apoptotic BH3-only proteins.

1.2.4. Activation of Bak and Bax

During apoptosis, Bax and Bak are subjected to conformational changes and oligomerize at discrete sites on the mitochondria [39]. The oligomerization of Bax and Bak results in the permeabilization of the mitochondrial membrane and releases pro-apoptotic molecules, which lead to apoptosis [40]. Cells that lack both Bax and Bak, but not cells lacking only one of them, are totally resistant to tBID-induced cytochrome c release and apoptosis [41]. Notably, double deficient cells are resistant to various intrinsic apoptotic stimuli. Because of the pivotal role in the induction of mitochondrial apoptosis, Bax and Bak should be tightly regulated by other members of the Bcl-2 family [42].

1.2.5. The extrinsic pathway of apoptosis

Binding extracellular death ligands to their transmembrane death receptors (DRs) can initiate extrinsic apoptosis. Death receptors belong to the tumor necrosis factor (TNF) receptor superfamily [43]. TNF superfamily consists of the number of plasma membrane receptors with an important homology in their extracellular domain, defined by the presence of up to six cysteine-rich domains (CRD), which describe their ligand specificity [44–46]. Among them, Fas (CD95/APO-1), TNF-receptor 1 (TNF-R1/p55/CD120a), TNF-related apoptosis-inducing ligand receptor 1 [TRAIL-R1/Death Receptor 4 (DR4)], and TRAIL-receptor 2 (TRAIL-R2/DR5/APO-2/KILLER), Death Receptor 3 (DR3/APO 3/TRAMP/WSL-1/LARD) and 6 (DR6) have been extensively

studied [47,48]. Notably, an intracellular 80-amino acid motif, called death domain is indicative for the death receptors and has an important role in transducing signals upon activation by the respective death ligand [49]. Apoptosis can be initiated by various death ligands such as CD95 ligand. The death receptor CD95 is activated by its cognate ligand, binding of which results in oligomerization and activation of the intracellular death domain. Ligand binding induces binding of the adaptor molecule FADD (Fas-associated-protein with DD) to the death domain of the CD95 receptor. Afterwards, procaspase 8 or 10 is recruited to the platform via their death effector domain and dimerization occurs. The death receptor, the adaptor molecule FADD and procaspase 8 or 10 form a multi protein complex called death-inducing signaling complex (DISC) [50]. The induced proximity initiates activation and autoproteolytical cleavage of the caspases in the DISC. Active caspase 8 and 10 can further activate effector caspases, which cleave of the numerous substrates and cause apoptosis [51]. TNF is a transmembrane protein, which can be further processed into a soluble form (sTNF) [52]. TNF can apply its function via two receptors, TNF receptor 1 (TNFR1) and TNFR2. TNFR1 is mainly associated with inflammation and tissue degeneration. However, TNFR2 is predominantly involved in tissue regeneration and immune modulation [53]. Notably, sTNF and Membrane-bound TNF (memTNF) both can activate TNFR1 whereas TNFR2 can only get fully activated by memTNF [54]. Deregulation of TNF expression and signaling can lead to chronic inflammation, which can mediate the development of autoimmune diseases and tissue damage [55].

1.2.6. Cross talk between intrinsic and extrinsic pathway of apoptosis

The extrinsic pathway can crosstalk to the intrinsic pathway by caspase 8-mediated cleavage of BID [54]. In type I cells, high levels of DISC formation boost high amounts of active caspase 8, which can activate effector caspases [55,56]. In contrast, type II cells assemble low amounts of DISC and therefore, less active caspase 8 is formed [56]. Since this amount of active caspase 8 is not enough to directly process caspase 3, hence amplification of the death receptor signal is needed to induce apoptosis. This amplification occurs by caspase 8 mediated processing of the BH3-only protein Bid [57]. The anti-apoptotic Bcl-2 family members are inhibited by the active protein truncated Bid (tBid), which results in permeabilization of the outer mitochondrial membrane with Bax and Bak proteins [58,59]. Because of the disruption in mitochondrial integrity,

cytochrome c is released into the cytosol and induces the formation of the apoptosome and activation of caspase 9, which mediates activation of caspase 3 and caspase 7 causing apoptosis. In type II cells, overexpression of the Bcl-2 or Bcl-XL can block death-receptor-mediated apoptosis, which demonstrates the necessity of the interplay between the extrinsic and intrinsic apoptosis pathways in these cells [56].

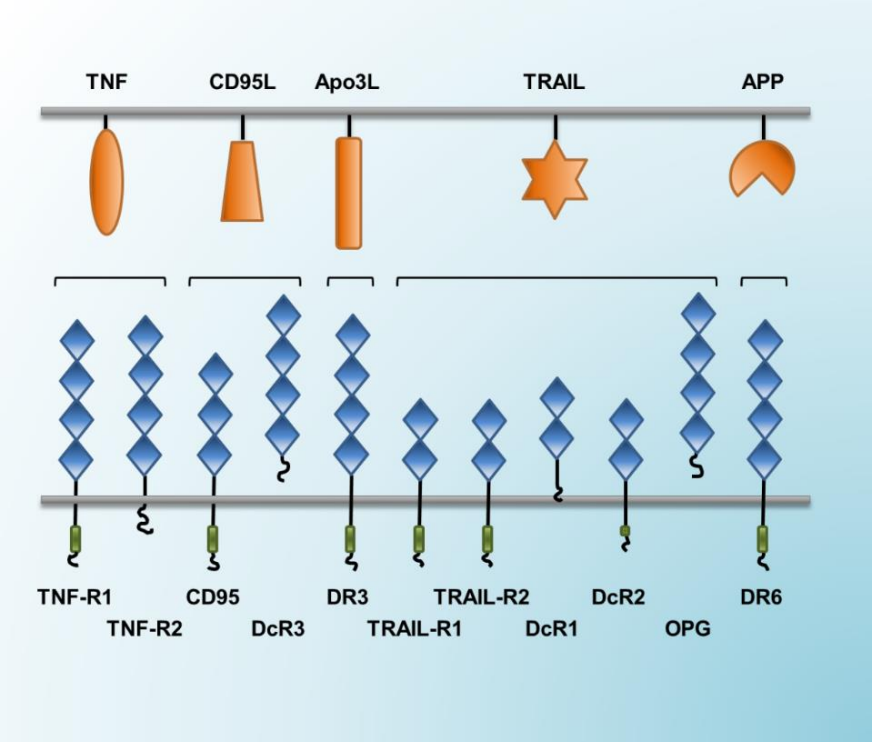

Figure 4. The death receptor superfamily and their ligands. The death and decoy receptors are illustrated at the bottom, with the extracellular cysteine-rich domains in blue and death domains (DDs) in green. TNF-R1 (p55/p60 TNF-R), CD95 (Fas, APO-1), death receptor 3 (DR3, TRAMP), TRAIL-R1 (DR4), TRAIL-R2 (DR5) DcR1, DcR2 and OPG and DR6 are activated by their respective ligands, which are indicated in orange.

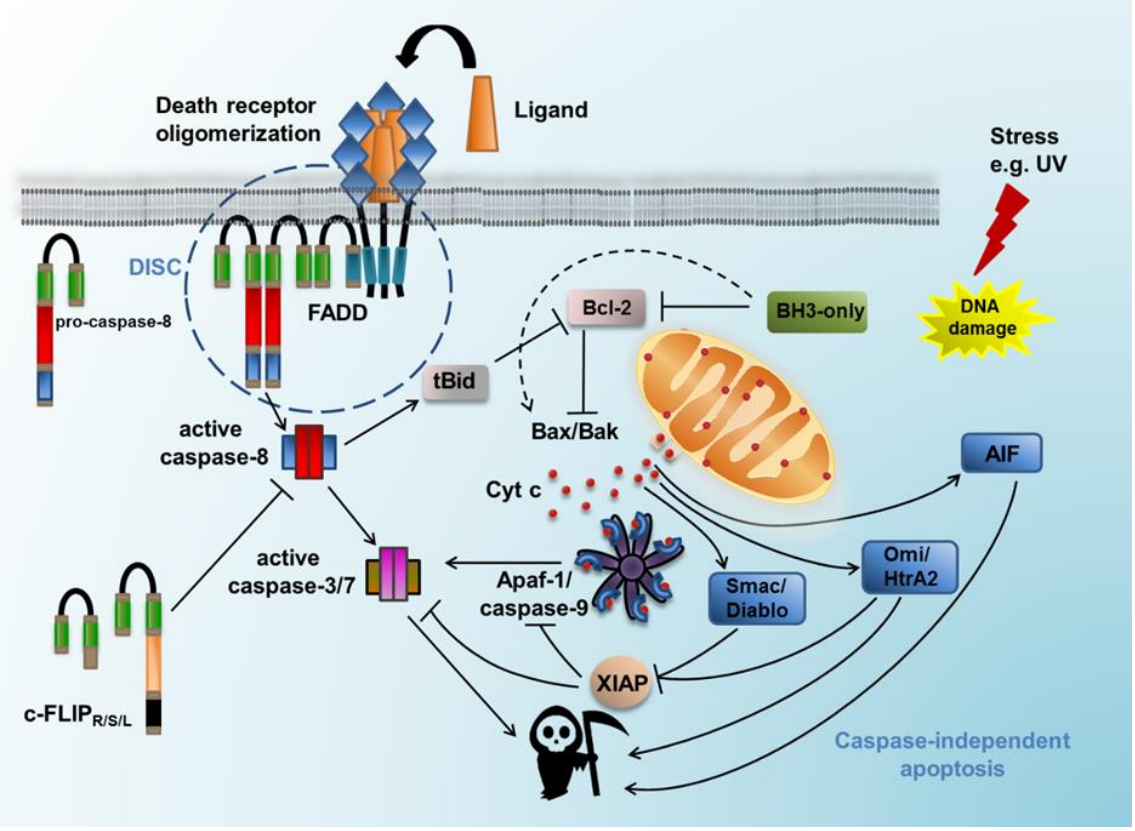

Figure 5. The extrinsic and intrinsic apoptosis pathways**.** The connection of the intrinsic (mitochondrial) and death receptor pathways in the caspase cascade system is indicated. APAF1, apoptotic peptidase activating factor 1; Bak, Bcl-2 antagonist/killer 1; Bax, Bcl-2-associated X protein; Bcl-2, B-cell leukemia/lymphoma 2; BID, BH3-interacting domain death agonist; BH, Bcl-2 homology domain; DIABLO, diablo homolog (Drosophila); DISC, death-inducing signaling complex; FAS, tumor necrosis factor receptor superfamily member 6; FASL, Fas ligand (TNF superfamily, member 6); IAP, inhibitor of apoptosis.

1.2.7. FLICE-inhibitory proteins (FLIPs)

In 1997 the cellular FLICE-inhibitory protein (c-FLIP) was reported by several groups as a cellular homologue to viral FLIPs [57,58]. Although thirteen c-FLIP splice variants have been identified, presently only three proteins have been isolated, namely c-FLIP long (c-FLIP$_L$), c-FLIP short (c-FLIP$_s$) and c-FLIP Raji (c-FLIP$_R$), which have 55 kDa, 26 kDa and 24 kDa molecular weight, respectively [56,59]. c-FLIP$_L$ is structurally similar to pro-caspase 8 consisting of two death effector domains (DED) at the N-terminus and the C-terminal caspase-like domains. However, because of the substitution of several amino acids in the active site, including the catalytic residues His-237 and Cys-285, it is

catalytically inactive [60]. The structures of c-FLIP$_S$ and the viral FLIP (v-FLIP) proteins are comparable [61]. However, following the two DEDs of c-FLIP$_S$, there are 20 amino acids that are essential for its ubiquitination and targeting for proteasomal degradation [62–64]. c-FLIP$_R$ also consists of two DEDs but lacks the additional carboxy (C)-terminal amino acids that are present in c-FLIP$_S$. C-FLIP is expressed abundantly in many tissues, for instance in neurons, cardiac myocytes, skeletal muscle, kidney, epithelial cells, macrophages, T and B cells [65,66]. c-FLIP proteins control death receptor-mediated apoptosis by interfering with caspase 8 activation [67,68]. C-FLIP$_S$ inhibits DR-mediated apoptosis by preventing processing of caspase 8 at the DISC [56,69]. C-FLIP$_L$ has a controversial role and acts in a pro or anti-apoptotic manner, leading to activation or inhibition of apoptosis [70]. In the presence of high levels of c-FLIP$_S$ or c-FLIP$_R$ or strong death receptor stimulation, c-FLIP$_L$ works like a pro-apoptotic molecule whereas high c-FLIP$_L$ levels inhibit apoptosis [70].

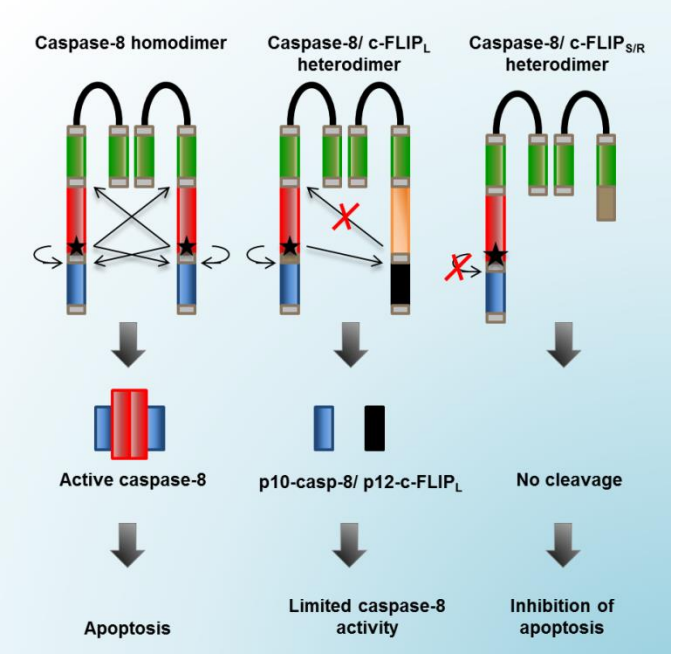

Figure 6. c-FLIP proteins regulate caspase 8 activity [63,71,72]. Caspase 8 homodimers initiate activation and autoproteolytical cleavage of the caspase 8 molecules, which lead to apoptotic signaling, whilst the short c-FLIP isforms block apoptosis [73]. Heterodimers of caspase 8 and c-FLIP$_L$ result in activation of caspase 8, but only partial cleavage and therefore only limited caspase 8 activity. Adapted from reference [74]

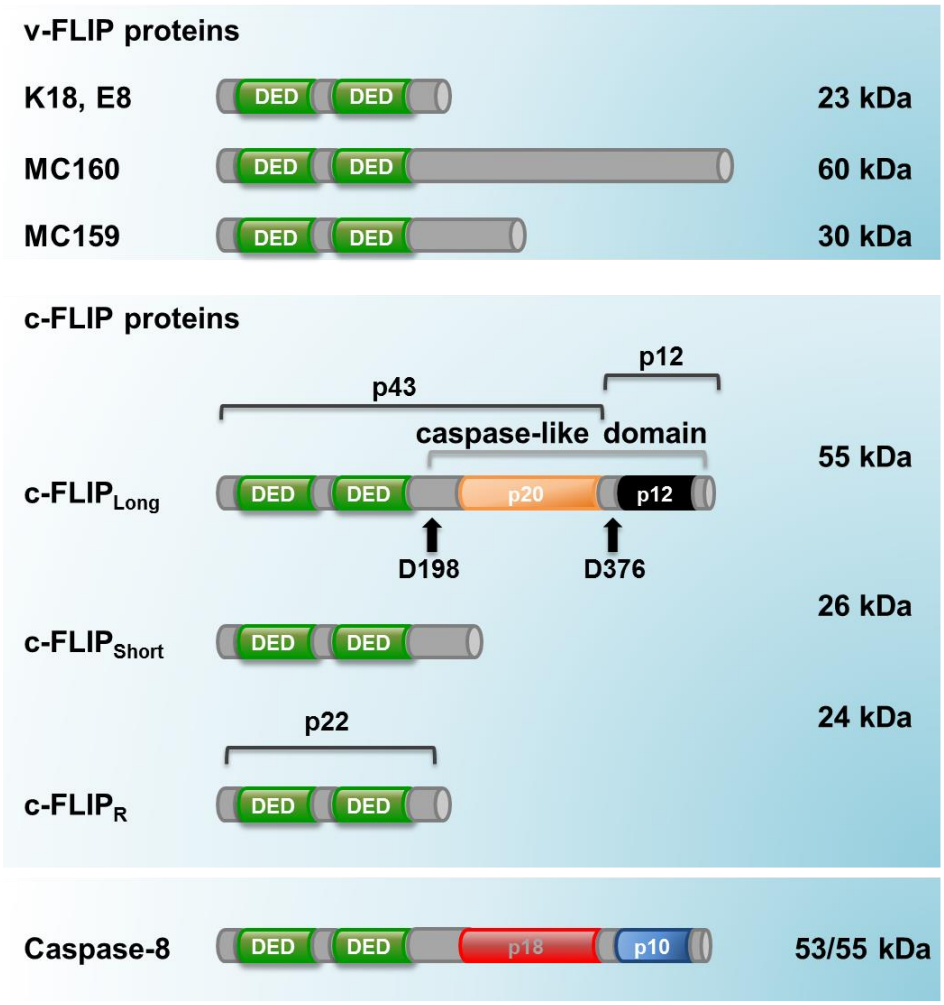

Figure 7. Structure of c-FLIP proteins. The v-FLIP proteins are expressed in γ-herpesviruses such as Kaposi's-sarcoma-associated human herpesvirus-8 (HHV8), herpesvirus saimiri and equine herpesvirus-2 as well as in molluscipoxviruses. Three isoforms of cellular caspase 8 (FLICE)-inhibitory protein (cFLIP) are known: $cFLIP_{long}$ ($cFLIP_L$) $cFLIP_{short}$ ($cFLIP_S$) and cFLIP $_{Raji}$ ($cFLIP_R$). All viral and cellular FLIP proteins include tandem DED domains. Adapted from reference [16]

1.3. Biology of influenza virus and replication

Influenza viruses are negative-sense single-stranded, segmented RNA genome viruses, which belong to the family of orthomyxoviridae. The family of orthomyxoviridae includes Influenza virus A, Influenza virus B, Influenza virus C, Isavirus and Thogotovirus. Antigenic differences in nucleoproteins and matrix proteins have been used to distinguish Influenza A virus, Influenza B virus and Influenza C virus. In addition, further classification of influenza A viruses (IAV) is based on two important surface glycoproteins, hemagglutinin (HA) and neuraminidase (NA) [75,76].

1.3.1. Influenza A virus

Influenza is a respiratory pathogen, which causes considerable morbidity and mortality all around the world, resulting in 3-5 million infections and 250,000-350,000 deaths annually [77,78]. All age groups can get infected by influenza. However, some people like the elderly or pregnant women, are more susceptible to get flu complications that result in hospitalization and sporadically even death [79,77]. There are two important mechanisms by which influenza A viruses change their antigenic properties. These are commonly referred to as "antigenic drift" and "antigenic shift [80,81]. Influenza can change substantially with recombination (antigenic shift). Therefore, the host has no protective immunity, which results in increasing influenza mortality rate even among healthy young adults. Moreover, because of low fidelity of the RNA polymerase and the lack of proofreading mechanism, antigenic drift (mutation) happens in the IAV virus genome frequently [82]. Recombination of RNA or antigenic shift happens when two or more different strains of the virus combine and form a new subtype, which is showing a mixture of the surface antigens from each strain. As a consequence of the antigenic shift and antigenic drift, the potential host will be without protective immunity, which increases dramatically the morbidity and mortality rates of influenza infection.

1.3.2. Viral genome organization

The influenza A genome is approximately 13.6 kb in size and comprises eight viral RNA (vRNA) segments which encode 11 proteins including: matrix 1 (M1), matrix 2 (M2), nucleoprotein (NP), non-structural protein 1 (NS1), non-structural protein 2 (NS2), polymerase acidic protein (PA), polymerase basic protein 1 (PB1), polymerase basic protein 2 (PB2), and polymerase basic protein 1-F2 (PB1-F2) hemagglutinin (HA), neuraminidase (NA)[83]. HA and NA are two surface glycoproteins that have substantial roles in viral replication and pathogenicity. Eighteen IAV HA (H1-H18) and eleven IAV NA (N1-N11) subtypes have been identified so far [84,85]. Hemagglutinin is a membrane glycoprotein (MW 61.5 kDa monomer) and the main surface antigen of the influenza virus. Synthesis of HA occurs in the rough endoplasmic reticulum of the infected cells [86,87]. This protein has a homotrimer structure, which forms a spike shape. HA has two main functions. Helping the virus to attach to the cell, by binding to host sialic acid-containing receptors and then intermediating membrane fusion between the endocytic vesicle and the viral membrane during viral penetration [88]. Neuraminidase

intercedes enzymatic cleavage of the viral receptor, which results in release of the newly assembled virus. The molecular mass of the monomer is 60 kDa. In general, there is four times more HA than NA on the surface of the influenza A virus, which makes the HA glycoprotein the prominent part of the external structure of the influenza A virus [89,90].

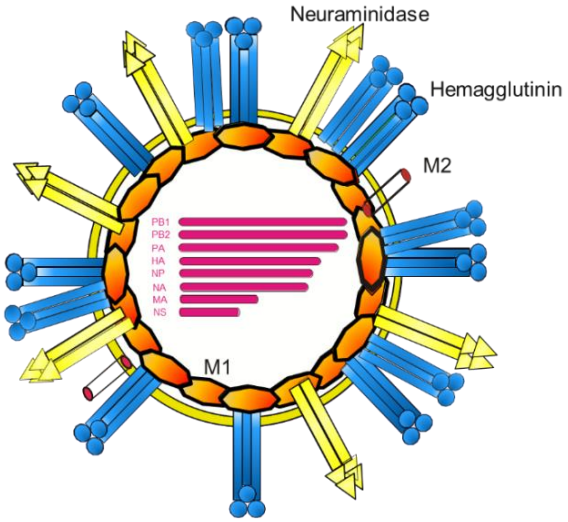

Figure 8. Morphology and genome structure of Influenza A genome. The influenza A genome consists of 8 negative-strand RNA segments. The hemagglutinin protein (HA) and neuraminidase (NA) that are present on the surface of the viral envelope are used to classify influenza A into different subtypes.

Replication of the influenza A virus is a multi-step process. In the first step of viral replication cycle, the virus attaches and enters the host cell. This initial step is followed by fusion of the viral and endosomal membrane, uncoating, transcription, protein synthesis, assembly and finally exiting of the host cell [91]. The main target of the Influenza virus is the epithelial cells. This attachment happens through sialic acid receptors on the surface of the target cells in the airway. The attached virus particle enters the host cell through receptor-mediated endocytosis [92]. The low pH in the resulting endosome leads to a conformational change in the hemagglutinin protein, which mediates the fusion of viral and endosomal membranes. The low pH also increases the proton flux into the virus via the M2 ion channel. The M2 ion channel pumps protons into the endosomes, therefore dissociating the vRNPs from M1 matrix proteins and releasing the viral ribonucleoproteins into the cytoplasm and then

transporting them into the cell nucleus [93]. In the nucleus (-) sense influenza-viral RNAs are used as a template for the RNA-dependent RNA polymerase complex to generate two different kinds of RNA. Viral messenger RNA (mRNA) is produced for the synthesis of viral proteins, and complementary RNA (cRNA) is transcribed to produce genomic vRNA [75]. The influenza virus polymerase complex expresses PB2, PB1 and PA subunits and use 5´-capped primers from host mRNA to transcribe viral genomic RNAs into mRNA. The viral mRNA is transported back to the cytoplasm for translation into viral proteins. HA, NA and M2 envelope proteins are translated on the membrane-bound ribosomes. Afterwards, these proteins are transferred to the endoplasmic reticulum (ER), glycosylated in the Golgi apparatus and transported to the cell membrane. The other viral proteins (M1, PB1, PB2, NP, PA, NS1 and NS2) are transported to the host nucleus. In the host nucleus, there are newly synthesized vRNA available. This vRNA is coated with M1 protein and transferred to the plasma membrane [94,95]. A high amount of M1 protein at the cytoplasmic side of the lipid bilayer, mediates viral budding. Finally, the cellular membrane covers the nucleocapsid and the virions exit the cell [96].

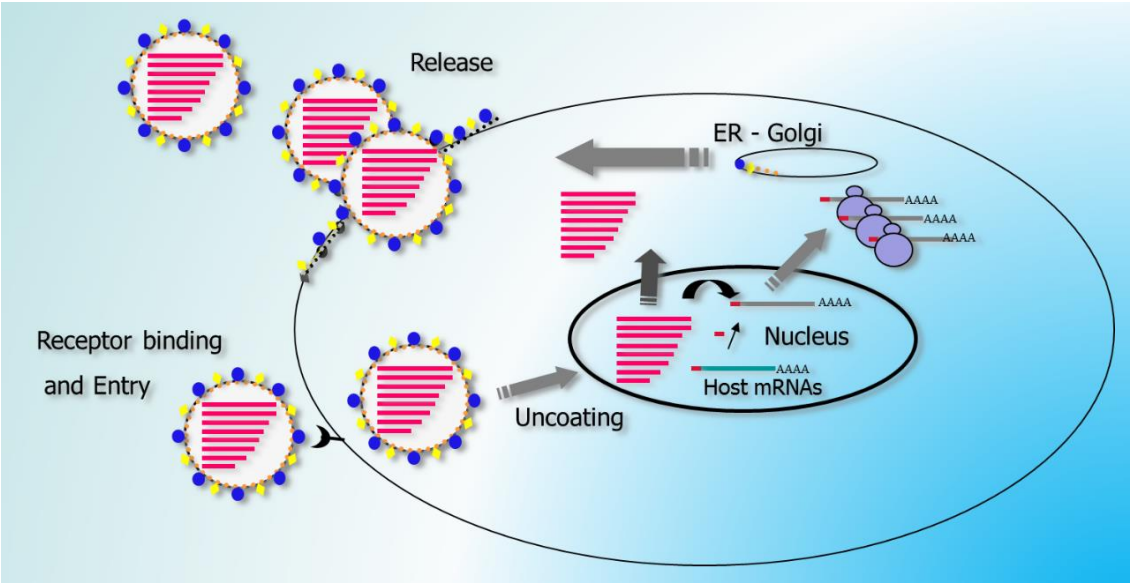

Figure 9. Replication of influenza A virus. After attachment to the target cell receptor containing sialic acid, the virus particle goes through the processes, consisting of fusion, endocytosis, uncoating, and subsequently replication by the RNA polymerase. Afterwards, surface protein-coated envelope forms around the genome to produce a complete virion, which can then leave the cell and infect other cells.

1.4. Innate immune response to IAV

The innate and adaptive immune system work together to clear the viral infection. In recent years, appreciation of the role of innate immunity in defense against influenza A virus (IAV), has grown exponentially [97–100]. Innate immune responses are not specific to a particular pathogen. However, it plays an important role as the first line of defense. Innate immunity against influenza consists of physical barriers and innate cellular immune responses [101]. Skin and lung are the only organs that directly contact the external environment. The airway tract mucosa has a substantial role in protecting the lung from pathogens that have been inhaled [102]. If the virus successfully passes the mucous layer, it will bind and attack the respiratory epithelial cells [103]. Henceforth the virus can spread to immune and non-immune cells. Infected cells present the viral RNA which is called pathogen-associated molecular patterns (PAMPs) [104]. Recognition of (PAMPs) by pattern recognition receptors (PRRs) on the innate immune cells, mediates signaling cascades. The signaling cascades result in the production of interferons (IFNs), cytokines and chemokines [105]. Three different classes of PRRs have been shown to play a role in recognition of an influenza A infection and the induction of an IFN response: Toll-like receptors (TLRs), retinoic acid inducible gene-I (RIG-I) receptors and the nucleotide oligomerization domain (NOD)-like receptor family pyrin domain containing protein 3 (NLRP3) inflammasome [106–108].

TLRs are the first receptors that were identified as having the ability to sense the viral nucleic acids [109]. TLR7 is an intracellular receptor that recognizes single-stranded viral RNA (ssRNA) that are taken up into the endosome [110]. Double-stranded viral RNA (dsRNA) is recognized by another intracellular receptor TLR3, which leads to the production of type I IFN and proinflammatory cytokines [111,112]. Viral surface glycoproteins, HA and NA are recognized by TLR2 and TLR4, which are present on the cell surface [113]. RIG- I recognize the 5′-triphosphate viral ssRNA that is generated after viral replication. At the later stage of infection, the uncapped 5′-triphosphate viral ssRNA, which was generated after viral replication, is recognized by RIG-I in the cytoplasm [114,115]. The intracellular recognition by the PRRs results in the production of interferons (IFNs), cytokines and chemokines, which leads to transcription of hundreds of interferon-stimulated genes (ISGs) that significantly limit viral infection of target cells [105]. However, by using NS1 protein, which interferes with the RIG-1 system, the

virus can inhibit the type I interferon response. Previous studies have shown that the inflammasome responds to influenza virus [116]. There are two main signals responsible for activation of the inflammasome. The first signal is produced as a result of the presence of foreign particles in the airway epithelial cells. This signal, which constitutively stimulates the NLRP3 inflammasome, is called signal 1 [117,118]. The first signal mediates the production of pro-IL-1β and pro-IL-18. Signal 2 can be provided with ssRNA of IAV or IAV M2-induced proton flux or PB1-F2 aggregates in lysosomes [119,120,121]. Signal 2 can activate the inflammasome and mediate caspase 1 activation. Caspase 1 activation is necessary for the cleavage of the pro-IL-1β and pro-IL-18 into their active forms [122,123].

Different immune cells are involved in the innate immunity against influenza. The high level of cytokines and chemokines such as type I IFN, IL-1 and IL-6 at the site of infection attracts innate immune cells consisting of natural killer (NK) cells, neutrophils, macrophages and dendritic cells [103] . Following IAV infection, neutrophils are recruited to the infection area and mediate viral clearance through phagocytosis of apoptotic IAV-infected cells and secretion of pro-inflammatory cytokines [124–126]. Neutrophils also play an important role in regulating IAV-specific CD8 T cells in the periphery, which indicates the role of neutrophils in connecting innate and adaptive immune responses against IAV [127]. Alveolar macrophages (AM) are one of the main phagocytic and prominent antigen presenting cells in the lungs. In steady state condition, AM are relatively inactive and show regulatory cell phenotypes [128]. The phagocytic property and cytokine production is relatively low in these homeostatic AM. Notably, these AM play a role in the suppression of the induction of the innate and adaptive immunity [129,130]. During IAV infection, homeostatic AM can get activated and converted into extremely phagocytic cells that can produce a solid amount of inflammatory cytokines. Moreover, during infection, macrophages are also recruited to the lung and assist both innate and adaptive immune responses. Macrophages secrete pro-inflammatory cytokines and chemokines such as IL-1, IL-6, IL-8, IL-12, TNFα, and IFN-γ. Additionally, they also work as antigen presenting cells to activate the IAV-specific T cell response [76]. Depletion of AM suggested that these cells are crucial in the early protection of influenza infection. AM depletion before day three post infection causes uncontrolled viral replication and escalates mortality [76]. Although neutrophils

and macrophages have a substantial role in controlling IAV infection, some studies, which illustrate the contribution of macrophages to the "cytokine storm", which can cause morbidity [76]. Therefore, these cells can demonstrate both beneficial and detrimental roles during IAV infection.

The role of natural killer (NK) cells in controlling IAV infection have been demonstrated for many years [131]. NK cells are granular lymphocytes that are part of the innate immunity through their natural cytokine and chemokine production [132,133]. NK cells circulate all over the body. In mice, NK cell frequencies oscillate from 1% to 10% in lymph nodes and lung respectively. Notably, the spleen has the largest absolute NK cell number [134]. As a part of the innate immune response, NK cells have the ability to respond immediately to any unusual changes in the host such as infection. Activation of NK cells can be regulated by activating and inhibitory receptors, such as inhibitory receptors KLRG1, CD94/NKG2-A and 2B4 and activating receptors NKG2D, NKp46, and CD16 [135]. Moreover, in mouse NK cells, the family of lectin-like receptors Ly49 is expressed, which act as activating and inhibitory receptors [136]. The inhibitory part of Ly49 recognizes major histocompatibility complex (MHC) class I. Recognition of MHC class I on a target cell by an NK cell produces an inhibitory signal. However, by sensing the ligands with the activating receptor, an activation signal is produced. The balance between activation or inhibitory signals controls the NK cell activation. In the virally infected cell, MHC class I is downregulated, which leads to an increase in sensitivity to NK cell-mediated killing. Beside this downregulation, activation of NK cell requires signals via activating receptors, which mediate production of cytokines and cytolytic activity [137].

It has been described that NK cells can get activated via binding to HA proteins, which are expressed on the surface of IAV-infected cells to the NK receptors NKp44 and NKp46 [138,139]. This activation mediates direct killing of IAV infected cells via a perforin/granzyme mechanism, which controls the spread of the virus [140,132].

Dendritic cells (DCs) belong to the antigen-presenting cells and fundamental mediators of immunity and tolerance. Respiratory dendritic cells (rDC) are present in the lung and check the airway for any foreign particles. In the steady state, the migration rate of rDCs to the lung draining lymph nodes (DLN) is low. However, following IAV infection this

migration is accelerated [141]. Depending on the viral dose and virus strain this high level of migration can continue up to 7 days post infection [138,142]. DCs can present the antigen via MHC class I and II [143]. This antigen can be directly taken up from the infected cell, which is called direct presentation or via using the antigen from an apoptotic IAV-infected cell, named cross-presentation [144]. However, the exact source of this antigen has been difficult to ascertain. It has been shown that most of the influenza viruses are able to infect DCs and lead to viral protein synthesis, however, infection is generally abortive and does not produce infectious particles[145]. Following infection with IAV, DCs mediate production of proinflammatory cytokines and chemokines including type-I IFN (IFN-α and IFN-β), IL-6, IL-12, TNF-α, IL-8, IP-10, RANTES and MIP-1β [146].

1.5. Cellular adaptive response

1.5.1. $CD8^+$ T cell effector functions in the lung

In the presence of IAV infection, one of the main goals of the immune system is to clear the infected epithelial cells by $CD8^+$ T cells [147]. $CD8^+$ T cells perform this duty with either FasL or perforin/granzyme-mediated mechanisms [148]. Around day four post-infection, the number of influenza-specific $CD8^+$ T cells is increased [149,150]. In the lung, they expand and accumulate in order to clear the viral infection. Notably, in the absence of $CD4^+$ T cells, B cells, and neutralizing antibody, $CD8^+$ T cells can take over and control the influenza virus infections, which emphasizes the importance of CD8 cells [151,152]. This hypothesis that $CD8^+$ T cells employ perforin and Fas ligand to initiate killing of influenza-virus-infected targets was verified by Topham *et al*. They illustrated that viral clearance was delayed in perforin$^{-/-}$ or Fas$^{-/-}$ IAV infected mice. In these mice, pulmonary influenza virus titers were detectable for longer durations. Remarkably chimeric mice, which contain perforin$^{-/-}$ $CD8^+$ T cells and Fas$^{-/-}$ respiratory epithelium cells showed significantly higher viral load even up to 14 days post infection. However, despite lacking both perforin and Fas, some of these mice showed less viral titers on day 14 compared to day 10 post infection [148]. One possible explanation for these data is that there might be another mechanism, which $CD8^+$ T cells use for killing the influenza infected target cells.

1.5.2. CD4+ T cell responses to influenza virus

In addition to $CD8^+$ T cells, which play an important role during IAV infection, $CD4^+$ T cells also provide support in the primary response to IAV infection. Among the plenty of activities that $CD4^+$ cells perform, providing potent help for priming of $CD8^+$ T cell responses has been shown to be the most important one. Lack of $CD4^+$ T cells results in significantly less production of IL-2 and IFN-γ in the lung-draining lymph node and the bronchoalveolar lavage [153,154]. Although $CD4^+$ T cells and the chemokines that they produce are not absolutely essential for controlling the primary infection, the absence of $CD4^+$ T cells affect the cytolytic function of the $CD8^+$ T cells, antibody production of B cells and memory formation of both $CD8^+$ T cells and B cells [155,156]. Moreover, $CD4^+$ T cells also provide effector functions and assist with the clearance of the virus during primary and memory responses. These $CD4^+$ effector cells employ perforin-mediated cytotoxic pathways to ameliorate host survival [157,158].

1.5.3. Humoral immune response

IAV infection advocates both a local and systemic humoral response. During influenza infection or vaccination activated B cells produce influenza directed antibodies[159]. This humoral response is pivotal for the clearance of the virus in the primary infection as well as for long-term immunity [159]. It has been shown that there is a correlation between the titers of serum neutralizing specific antibody for the HA and NA proteins and protective immunity. Anti-HA antibodies can interrupt viral attachment to host cells and inhibit receptor-mediated endocytosis [160]. Another type of antibodies has been described, which is related to the NA protein. This protein is required for the release of newly synthesized virions. Antibodies against NA do not neutralize the virus but limit the spread of the virus [81,161].

All natural infections with any strain of influenza virus are able to exploit the long-lived antibody-mediated defense against a similar infection [162,163]. The humoral response against respiratory viruses can be produced locally in the nasal-associated lymphoid tissue (NALT) and bronchus-associated lymphoid tissue (BALT) [164,165]. By day three post infection, DCs, which have migrated from the infection area, present viral antigen to B cells in mediastinal lymph node. B cells can also directly take the viral antigens in the mediastinal lymph nodes (MLN) or at the site of infection in order to transport it to

the lymph nodes [166]. Formation of germinal centers, which contains B and T cell zones, in BALT support B cell proliferation. Furthermore, in the absence of peripheral lymphoid organs such as lymph nodes, spleen and Peyer's patches, the isolated immune response in the BALT could clear influenza infection and results in a small measure of protective immunity [167]. Both germinal center and extrafollicular B cell responses can be derived by Influenza A infection. However, memory B cells and long-lived plasma cells are mainly produced by the germinal center reaction [168].

1.6. Aim of the thesis

Cell fate decisions in response to influenza virus infection have an important role in elimination and control of the infection. On the other hand, apoptosis can cause tissue damage and multiple organ disfunction at the peak of infection [169]. Although many aspects of apoptosis have been identified, regulation of apoptosis, especially by c-FLIP proteins remains a matter of interest in experimental research [170,171]. It has been shown that c-FLIP proteins act at the level of the CD95 DISC and that c-$FLIP_{long}$ and c-$FLIP_{short}$ inhibit caspase 8 activation via two different mechanisms [56]. Further studies on c-FLIP protein expression in cell lines of various species led to the outstanding knowledge that only humans are able to express c-$FLIP_{short}$, while the only short c-FLIP isoform that other species can express is c-$FLIP_R$ [172]. Although the physiological roles of c-$FLIP_L$ and c-$FLIP_S$ are well characterized, the function of c-$FLIP_R$ in the immune system is poorly understood. In 2013, Telieps *et al*., showed that adult vavFLIP$_R$ mice, in which c-$FLIP_R$ was constitutively expressed in all hematopoietic cells, had normal numbers of immune cells in the steady condition. However, when challenged with *Listeria monocytogenes* vavFLIP$_R$ mice showed better bacterial clearance, less liver necrosis and less caspase 3 activation compared with infected wild-type littermates [173]. Thus, it seems that early apoptosis occurring during *Listeria monocytogenes* infection is restricting bacterial clearance. The death receptor-mediated signaling pathway can contribute to the pathology of IAV infection. TNF-α, Fas ligand, and TRAIL are known to be death ligands, and recognized by TNFR1, Fas, DR4, and DR5, respectively. In lethal IAV infections, elevated expression of these death ligands was reported. Impairment in the induction of apoptosis caused by these death ligands can affect the morbidity of IAV infection. Viruses infect host cells in order to use cellular proteins and

enzymes for replication. For a long time, apoptosis was known as a host defense mechanism, which can limit virus replication. However, recent evidence supports the hypothesis that viruses have a mechanism to utilize apoptosis and take advantage of it. c-FLIP is known as an inhibitor of death receptor-mediated apoptosis. This project aims to elucidate the role of c-$FLIP_R$ in anti-viral immunity and the consequences of the constitutive expression of c-$FLIP_R$ for the host and the influenza virus. Additionally, this thesis evaluated the contribution of the higher number of natural killer cells during influenza virus infection and examined the direct effect of influenza virus on NK cells.

2. Materials and Methods

2.1. Materials

2.1.1. Mice

The mouse strain vavFLIP$_R$ was generated by the transgenic core facility of the University of Duesseldorf, Germany from a transgenic construct with murine c-FLIP$_R$ cDNA in the vector HS21/45 vav-hCD4 [174]. Mice carrying the transgenic construct were backcrossed for more than ten generations to C57BL/6 mice. WT littermates were used as control animals. All mice were maintained under specific pathogen free conditions at the animal facilities of the Helmholtz Centre for Infection Research. All experiments were approved by an external committee according to the national guidelines of the animal welfare law in Germany. The protocol used in these experiments has been reviewed by an ethics committee and approved by the 'Niedersächsisches Landesamt für Verbraucherschutz und Lebensmittelsicherheit, Oldenburg, Germany' (Permit Number :15042). Genotyping was performed by PCR on tail biopsies using KAPA Mouse Genotyping Hot Start Kit (PEQLAB) according to manufacturer's protocol.

2.1.2. Influenza A virus

Original stocks of viruses were obtained from Prof. Dr. Dunja Bruder, University of Magdeburg (PR8, A/Puerto Rico/8/34 H1N1). Virus stocks were propagated in the chorioallantoic cavity of ten-day-old pathogen-free embryonated chicken eggs for 48 h at 37 °C. Viral titer was determined by focus-forming unit (FFU) assay.

2.1.3. Chemicals

Chemicals were purchased from Sigma Aldrich (Munich, Germany) or Roth (Karlsruhe, Germany) if not stated otherwise. Phosphate buffered saline (PBS), Tween-20, Bovine serum albumin (BSA), N-Acetylated Trypsin (NAT), Penicillin and Streptomycin were purchased from Invitrogen, Merck, Sigma-Aldrich and Bulldog Bio. Ketamine and Xylazine for mice anesthesia were ordered from Invesa Arzneimittel GmbH. RNAlater® solution was ordered from Qiagen. True Blue substrate was purchased from KPL.

2.1.4. Cell culture materials and devices

Cells were cultured in cell culture flasks, 10 cm dishes, 6-well, 12-well, 24-well, 48-well or 96-well plates from NUNC – Thermo Scientific (Waltham, MA, USA) in the incubator HERAcell 240 i (Thermo scientific) at 37°C, 5% CO2 and 95% air humidity. Materials used for handling of cells were: 1.5 ml and 2 ml reaction tubes (Sarstedt, Nuembrecht, Germany), sterile 10 µl, 200 µl and 1000 µl pipette tips (Starlab, Ahrensburg, Germany), 5 ml, 10 ml and 25 ml pipettes (Sterilin - Thermo Scientific), 15 ml and 50 ml reaction tubes (Greiner-bio-one, Frickenhausen, Germany), 45 µm and 22 µm sterile syringe filters (Merck Millipore, Billerica, MA, USA). Centrifuges used were 5810R from Eppendorf (Hamburg, Germany) and Megafuge 1.0 from Heraeus SEPATECH (Osterode, Germany). Cells were handled in sterile hoods SterilGARD® III Advance° (The Baker Company, Sanford, ME, USA). Cell numbers were determined by Neubauer improved cell counting chambers (BRAND scientific, Wertheim, Germany) or CellometerTM Auto T4 (Nexcelom Bioscience, Lawrence, MA, USA).

2.1.5. Medium for cell culture

Reagent	Order No.	Company
MEM 31095	31095	GIBCO_Life Technologies
DMEM 11965	11965	GIBCO_Life Technologies
RPMI 1640	41965	GIBCO_Life Technologies
Fetal Calf Serum (FCS)	A15-101	PAA (Pasching, Austria)
Sodium-Pyruvate (100 mm)	11360	GIBCO_Life Technologies
Non-essential amino acids (100 X)	11140	GIBCO_Life Technologies
Penicillin / Streptomycin (5µg/ml)	15070	GIBCO_Life Technologies
β-mercaptoethanol (50 mM)	31350	GIBCO_Life Technologies

2.1.6. Solutions

The frequently used buffers are as follows.

Buffers	Components
Washing buffer for FFU assay	0.5% Tween-20 in PBS
Blocking buffer for FFU assay	0.5% Tween-20, 1 % BSA in PBS
Fixative	4% Formalin in PBS
Quencher	0.5% Triton X-100, 20 mM Glycine in PBS
Explant culture medium	DMEM with 10% FCS, 5% L-Glutamine, 1% Penicillin / Streptomycin
MDCK culture medium	MEM with 10%FCS and 1% Penicillin / Streptomycin

2.1.7. Influenza A virus antibodies

In order to detect the virus, the following antibodies were used.

Antibody	Catalogue number	Company
Goat anti-influenza virions (H1N1)	1301	Virostat
Anti-goat-IgG [H+L] Antibody-HPR	14-13-06	KPL

2.1.8. Oligonucleotides for PCR

HPLC-purified oligonucleotides were supplied by Eurofins MWG Operon (Ebersberg, Germany).

Name	Sequence (5´-3´)
UBC fwd	AAG AGA ATC CAC AAG GAA TTG AAT G
UBC rev	CAA CAG GAC CTG CTG AAC ACTG
NP fwd	GAG GGG TGA GAA TGG ACG AAA AAC
Np rev	TTC AGG ACG GAC GGA CGG AC

2.1.9. Oligonucleotides for mouse genotyping

Name	Sequence (5´-3´)
c-FLIP fwd	GCC TGA AGA ACA TCC ACA GAA TAG
SV40 poly A rev	CTC ATC AAT GTA TCT TAT CAT GTC
β-actin fwd	TGT TAC CAA CTG GGA CGA CA
β-actin rev	TCT CAG CTG TGG TGG TGA AG

2.1.10. Flow cytometery devices

Labelled samples were analyzed on BD LSR Fortessa and BD LSR II by Becton Dickinson (New Jersey, USA). Cell purification was performed using FACS Aria II (Becton Dickinson) or Moflo (Beckman Coulter, Indianapolis, USA) devices.

2.1.11. Flow cytometry murine antibodies

Reactivity	Fluorochrome	Clone/ notation	Isotype	Company
CD3	V500	500A2	Syrian Hamster IgG2, κ	BD Biosciences
CD4	Pacific blue	RM4-5	rat IgG2a, κ	BioLegend
CD8	PE/Cy7	53-6.7	rat IgG2a, κ	BioLegend
CD8	APC/Cy7	YTS156.7.7	rat IgG2b, κ	Biolegend
CD335-NKp46	eflur660	29A1.4	rat IgG2a, κ	eBioscience
CD11b	Pacific blue	M1/70	rat IgG2b, κ	eBioscience
CD11c	APC eFluor 780	N418	hamster IgG	eBioscience
CD19	PerCP Cy5.5	1D3	rat IgG2a, κ	eBioscience
CD49b	APC	Dx5	rat IgM, κ	eBioscience
CD62L	PerCP Cy5.5	MEL-14	rat IgG2a, κ	eBioscience
CD95	PE	Jo-2	hamster IgG2, λ2	BD Biosciences
F4/80	PE	BM8	rat IgG2a, κ	eBioscience
Ly6C	APC	HK1.4	rat IgG2c, κ	Biolegend
Ly6G	PE/Cy7	1A8	rat IgG2a, κ	Biolegend

2.2. Methods

2.2.1. RNA isolation

Total RNA was prepared from lungs using the RNeasy Midi kit (Qiagen, Germany) following the manufacturer's protocol

2.2.2. Reverse transcription and Quantitative real-time polymerase chain reaction (qRT-PCR)

PR8 and mock-infected mice were euthanized by CO_2 asphyxiation; heart blood was taken (for hematological analysis) and each entire lung was extracted and immediately stored in RNAlater reagent following Qiagen's instruction. For each group, 5-7 mice were prepared as independent biological replicates. Total RNA from the lung was prepared according to the detailed protocol from RNeasy Mini Kit (Qiagen) including an on-column genomic DNA digestion step (Qiagen's instruction). The concentration of these materials was measured by Nanodrop 2000c (Thermo Scientific). 100 ng of purified RNA were used as template to generate a complementary DNA (cDNA) strand by means of RevertTM Premium First Strand cDNA Synthesis Kit (Thermo Scientific). NP primers were used for RNA transcription according to supplier protocol. cDNA was used as a template for real-time PCR using SYBR Green (Roche). Ubiquitin-conjugating enzyme E2D 2A (UBC) was used as a housekeeping gene for normalization. qPCR was implemented in a Roche LightCycler® Real-Time device using Roche FastStart SYBRgreen Master (Roche, #04673484001). Measurements were run in duplicates in the LightCycler 96 system using the following primers (NP) (*5′-GAG GGG TGA GAA TGG ACG AAA AAC* and *3′-CAG GCA GGC AGG CAG GAC TT*). Incubation were done in peqSTAR thermocycler.

Time	Temperature	Function	Cycles #
1 minute	95 °C	Preincubation	1
10 seconds	95 °C	Single	45
10 seconds	60 °C	Mode of	
10 seconds	72 °C	Acquisition	
10 seconds	95 °C	Continuous	1
60 seconds	65 °C	Mode of	
1 second	97 °C	Acquisition	

2.2.3. Photometric determination of DNA/RNA concentration

DNA/RNA concentrations were measured with the Nanodrop 2000c (Thermo Scientific). The Beer-Lambert equation is used to correlate the calculated absorbance with concentration.

$$c = \varepsilon \times d \times E^{-1}$$

c = concentration (mol/l)

ε = coefficient of extinction (M^{-1} x cm^{-1})

d = density of the cuvette (cm)

E = extinction

d = the pathlength in cm (cm)

2.2.4. Influenza virus isolation in MDCK cell

MDCK cells were incubated in DMEM with 10% FCS, 5% L-Glutamine, 5% P/S and 1% NEAA at 37ºC in 5% CO2 incubator for 1-2 days. Then growth medium was replaced with infection medium (MEM containing 2.5 µg/ml NAT (N-Acetylated Trypsin, Sigma), 0.1% BSA, 1% penicillin/streptomycin). Infection medium was decanted and washed three times with 10 ml DPBS. DPBS was removed from flask with a sterile pipette. 5 µl virus stock (PR8 in egg allantoic fluid) was inoculated in 20 ml infection media to each flask using sterile pipettes including positive and negative control. After 1 hr of incubation at 37ºC in 5% CO2 incubator, virus suspension was removed and cells were washed once with 10ml DPBS (0.2 % BSA). Afterwards, 30 ml of the infection culture media was added to each flask. Cells were checked for clear cytopathic effects in the virus-infected flasks (otherwise waited another half day or day). When cytopathic effects were observed, the supernatant was collected and centrifuged to remove debris. Small aliquots of virus were kept at -80 °C.

2.2.5. Infection of cells

For infections where the determination of infectious virus was not required, no trypsin was added to the medium. Monolayers of sorted immune cells were infected with virus diluted in serum-free DMEM at an appropriate multiplicity of infection (MOI). Monolayers were washed prior to infection in PBS to remove all traces of serum. After an adsorption period of 1-2 hour on a rocking platform at 37°C, the virus inoculum (or

DMEM only for mock infections) was removed and replaced with serum-free DMEM. Cells were incubated at 37°C/5% CO2 until harvested.

2.2.6. In vitro stimulation with death ligands

Sorted NK cells from the spleen of vavFLIP$_R$ mice and WT littermates were stimulated with 20 ng/ml CD95L, 20 ng/ml TRAIL, 20 ng/ml TNF-α or PBS for 16 hours. After incubation, cells were harvested and analyzed by flow cytometry.

2.2.7. Cell isolation by flow cytometry

Primary cells were stained with the respective surface markers and were sorted by means of a FACS Aria II or Moflo device and collected in tubes containing PBS. This procedure was performed in cooperation with Dr. Lothar Gröbe, head of the flow cytometry and cell sorting facility at the Helmholtz Center for Infection Research (Braunschweig, Germany).

2.2.8. Flow cytometry analysis

For flow cytometry analysis, 1×106 cells were washed in 1 ml PBS at 4 °C, 1500 rpm, 5 min. Cells were resuspended in 100 µl PBS and stained with LIVE/DEAD for 30 min, 4 °C in the dark. Thereafter, cells were washed in 1 ml PBS as above. Next, cells were resuspended in FACS buffer containing Fc Block antibodies and incubated for 15 minutes at 4ºC in the dark. Surface markers were stained in 100 µl FACS buffer. Cells were incubated with appropriate dilutions of fluorochrome-conjugated or unconjugated antibodies at 4 °C for 20 min in the dark. Unbound antibodies were washed away with 1 ml FACS buffer. For intracellular staining cell were fixed and permeabilised with FoxP3 Staining Buffer Set by Miltenyi Biotec (Mönchengladbach, Germany) according to supplier's instructions.

2.2.9. Mouse infection

Female animals (12–17 week of age) were anesthetized by intra-peritoneal injection of Ketamin-Xylazine solution (10% (v/v) 100 mg/ml ketamine and 5% (v/v) 20 mg/ml xylazine in 0.9% (w/v) NaCl) with a dose adjusted to the individual body weight (200 µl per 20 g body weight) and infected intranasally with the specified dose of virus in 20 µl sterile PBS. Weight loss and survival of infected mice were monitored over a 14-day

period. In addition to mice that were found dead, animals showing more than 20% of body weight loss were euthanized and documented as dead.

2.2.10. Isolation of mouse organ

Mice were sacrificed by cervical dislocation or CO2. Spleen, peripheral and mediastinal lymph nodes were isolated from mice. Organs were homogenized through a 70 µm nylon mesh and washed with PBS. Erythrocytes were removed by 2 min incubation in ACK lysis buffer (0.15 M NH4Cl, 1 mM KHCO3, 0.1 mM EDTA, pH adjusted to 7.3 with NaOH) at room temperature followed by a further washing step. Lungs were removed aseptically, and perfused through the right ventricle with 1 mL PBS. Each lung was stored in 2ml RNA later buffer (RNA stabilization buffer) in -20 °C until used for RNA isolation.

2.2.11. Histology and immunohistochemistry

c-FLIP$_R$ and WT mice were sacrificed and lung was isolated. Samples were fixed with 4% formaldehyde and embedded in paraffin. 3µm sections were cut, deparaffinized and stained with hematoxilin and eosin for histological analysis. Furthermore, they were stained with NP antibody. Histological analysis and immunohistochemistry determinations were done in cooperation with Dr. Ulrike Heise and the mousepathology facility at the Helmholtz Center for Infection Research (Braunschweig, Germany).

2.2.12. Determination of cytokines

Blood was obtained by means of the final heart puncture method. Samples were incubated at 37ºC for 1 hour, then 10 minutes at 4ºC and finally centrifuged. The supernatant was transferred to another tube and stored at -80ºC. Broncho-alveolar lavage (BAL) fluid was collected from an 1 ml PBS instillation and subsequent aspiration from the lung of each mouse. Supernatants were aliquoted, stored at -80ºC. Spleen was isolated from the mice and milled through a 45 µm filter. Cells were diluted in 1 ml PBS and centrifuged. The supernatant was transferred to another tube and stored at -80ºC. Cytokine levels from serum, spleen and BAL were determined using procartaplex mix & match/ mouse 17-plex contains TNF-α, IFN-γ, IFN-α, IL-6, IL-12p70, IL-17A, IL-10, IL-2, IL-1α, IL-1β, IL-4, IL-21, RANTES, MCP-1, IP-10, MIP-

1α and MIP-1β in a Luminex® Instrument of the Luminex Corporation (Austin, USA) following supplier's protocol.

2.2.13. Focus forming assay

Lungs from infected mice were collected at different time points p.i. and homogenized in PBS + 0.1% BSA. Virus titers in these homogenates were determined by FFU assay on MDCK (Madin–Darby Canine Kidney) cells. Briefly, 6×10^4 MDCK cells per well were seeded in 96-well culture plates and incubated at 37 °C and 5% CO_2 for 24 h. Serial 10-fold dilutions of extracts were prepared in MEM containing 2.5 µg/ml NAT (N-Acetylated Trypsin, Sigma), 0.1% BSA, 1% penicillin/streptomycin (infection medium) and added to MDCK cells. Specific virus stocks (virus in embryonated chicken eggs) were used as positive controls for the assay. After 1h of incubation at 37 °C in 5% CO2, the inoculates were replaced with 100 µl of 1% Avicel overlay prepared in DMEM containing 2.5% NAT, 0.1% BSA and the cells were incubated for 24 h. Subsequently, the cells were washed twice with PBS and fixed with 4% formalin in PBS (100 µl/well) for 10 min at room temperature. Then, the cells were washed twice and incubated with Quencher (100 µl/well; 0.5% Triton X-100, 20 mM Glycine in PBS) for 10 min at room temperature. Afterwards, the cells were washed with Washing Buffer (100 µl/well, 0.5% Tween20 in PBS). The primary antibody (anti-influenza Nucleocapsid NP polyclonalgoat antibody, Virostat) and the secondary antibody (anti-goat-HRP from KPL, MA, USA) were diluted 1:1000 in Blocking Buffer (50 µl/well; 0.5% Tween, 20% BSA in PBS). 50 µl of the primary antibody was added to each well and incubated at room temperature. After 45 min, the cells were washed with Washing Buffer, incubated with 50 µl of secondary antibody for 45 min, then washed again and incubated with 30 µl of True Blue substrate and exposed until blue spots from infected cells appeared (about 30 min). foci were counted under microscopy and viral titers were calculated as focus formation units (FFU) per lung [175].

2.2.14. *In vivo* NK cell depletion

In order to deplete NK cells in mice with influenza infection, mice were i.p. injected with 50 µL Anti-Asialo-GM1 every 3 days, starting on day before infection. Control mice were treated with IgG. After depletion treatments, NK cells in lung and spleen were examined by flow cytometry on day 7.

2.3. Software

qPCR and flow cytometry data were analyzed by the Light cycler 96 version 1.1.0.1320 and FlowJo 10.1r7 respectively.

2.4. Statistical Analysis

Statistical analyses were performed using Mann-Whitney-tests to determine statistical significance, using Graph Pad Prism (Graph-Pad-Software Inc., La Jolla, CA, USA). Standard error of the mean (SEM) was represented as error bars in the graphs

3. Results

3.1. Constitutive expression of c-FLIP$_R$ does not alter lymphocyte populations in vavFLIP$_R$ mice in steady state

Considering the physiological importance of apoptotic responses, it is clear that tight regulations of the signaling cascades are needed. The important role of regulatory apoptosis signaling molecules has been shown for many years [176]. Among several regulators of death receptor signaling, c-FLIP has been a matter of interest over the last decade [63,177–179]. The physiological role of c-FLIP$_L$ and c-FLIP$_S$ has been well characterized in the past few years [70,177,180–182]. However, the function of c-FLIP$_R$ in the immune system is poorly understood. A comprehensive analysis of c-FLIP protein expression in cell lines of different species illustrated that only humans express c-FLIP$_{short}$, while other species, even the closely related chimpanzee, express c-FLIP$_R$. Therefore c-FLIP$_R$ is the only short c-FLIP isoform expressed in mice [172]. A c-FLIP$_R$ transgenic mouse model (vavFLIP$_R$), was used to further examine the role of murine c-FLIP$_R$ in the immune system. In this mouse model, murine c-FLIP$_R$ is under control of the vav-promoter and therefore expressed in all hematopoietic compartments. The plasmid used for generating the transgenic construct was described by Ogilvy and colleagues [174]. It was already shown that c-FLIP$_R$ expression in vavFLIP$_R$ mice was comparable to the endogenously expressed c-FLIP$_R$ in splenocytes induced by Con A[173,183]. To investigate whether the inhibition of death receptor-induced apoptosis results in any alterations in lymphocyte numbers, lymphocyte populations in the spleen, lymph nodes and bronchoalveolar lavage of 12-17 week old vavFLIP$_R$ mice (n=6) and WT littermates (n=6) were analyzed. Both frequencies and total cell numbers of CD3$^+$ T cells, CD19$^+$ B cells, NKp46$^+$ NK cells, Ly6G$^+$ neutrophils and F4/80$^+$ macrophages were comparable between 12-17 week old littermate WT and vavFLIP$_R$ mice (Figure 10, table 1). Furthermore, the activation status of T cells was analysed in spleen and lymph nodes from 12-17 week old WT and vavFLIP$_R$ mice by CD44 and CD62L staining. No difference in CD44$^+$ antigen-experienced T cells or CD62L$^+$ naïve T cells could be observed (Figure 10B). The results indicated that in the steady state condition, there is no effect on the lymphocyte populations in vavFLIP$_R$ mice compared to WT littermates. This is consistent with previous studies where 7 week old vavFLIP$_R$ mice and WT littermates were analyzed [173].

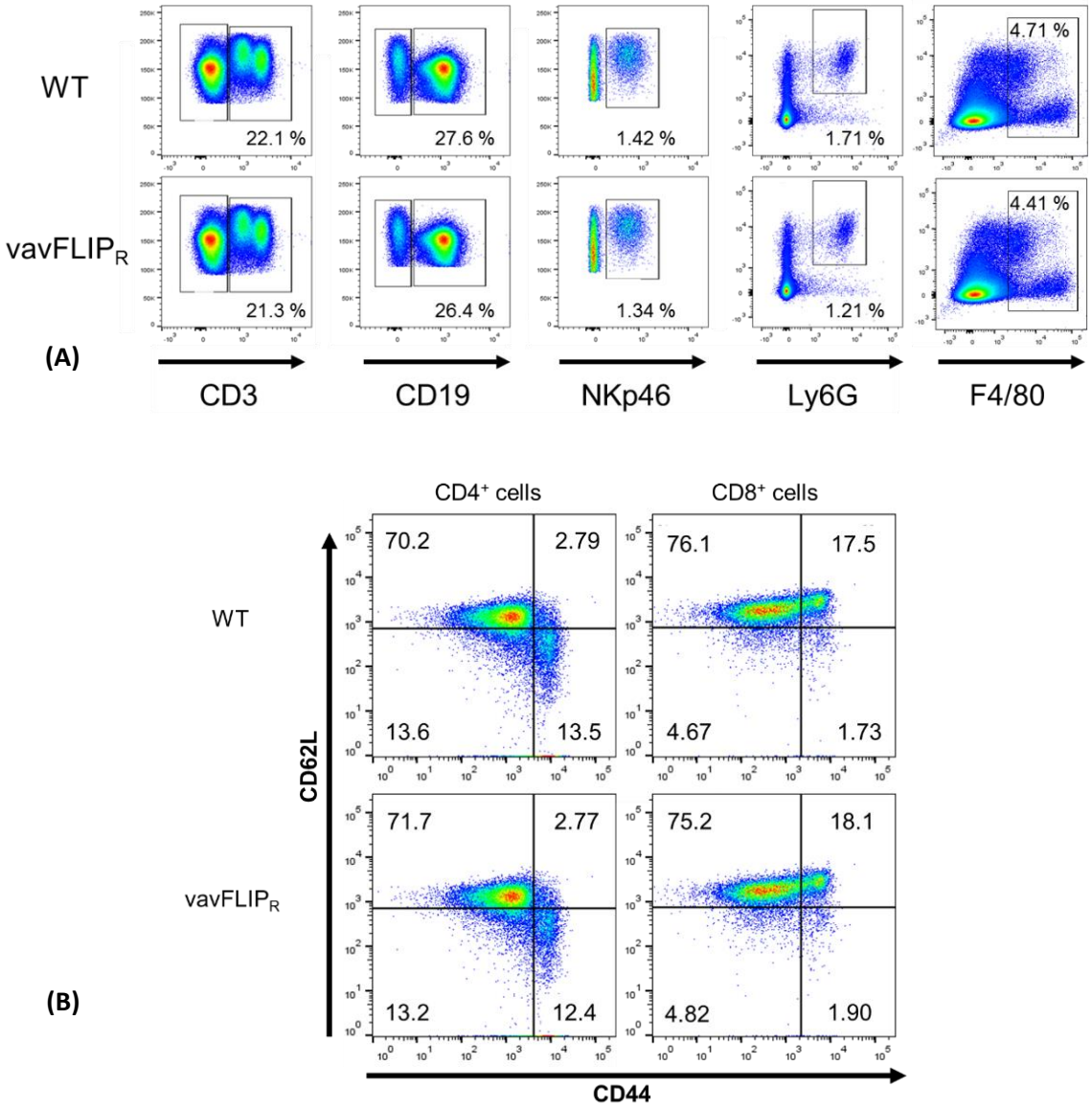

Figure 10. Flow cytometry analyses of CD3$^+$, CD19$^+$, NKp46$^+$, Ly6G$^+$ and F4/80$^+$ cells and activation status of CD4+ and CD8+ cells in vavFLIP$_R$ and WT littermates. (A) Representative dot plots for spleen cellularity in 12-17 week old wildtype (n=6, upper panel) and vavFLIP$_R$ mice (n=6, lower panel). Cells from freshly isolated spleens were stained for CD3, CD19, NKp46, Ly6G and F4/80. Adult vavFLIP$_R$ mice had normal numbers of immune cells in the steady state. (B) Representative dot plots of CD44 and CD62L cells within the CD4$^+$ and CD8$^+$ compartment from spleen. The frequency of CD44$^+$ antigen-experienced T cells and CD62L$^+$ naïve T cells were comparable in vavFLIP$_R$ mice and WT littermates.

Mouse strain	Organ	Percentage of all acquired cells					Absolute numbers x 1.0E+07
		CD3	CD4	CD8	CD19	NKp46	
WT	Spleen	20.6 (±4.7)	10.3 (±2.7)	8.20 (±1.0)	23.4 (±6.7)	0.92 (±0.5)	6.7 (±1.4)
vavFLIP$_R$	Spleen	21.7 (±3.5)	11.6 (±2.3)	7.45 (±1.5)	22.7 (±6.4)	0.87 (±0.3)	6.3 (±2.3)
WT	Lymph node	33.9 (±3.7)	23.8 (±2.5)	16.0 (±2.2)	10.5 (±1.1)	0.21 (±0.03)	1.6 (±0.6)
vavFLIP$_R$	Lymph node	34.1 (±2.9)	22.1 (±2.0)	17.7 (±1.0)	12.1 (±1.6)	0.19 (±0.04)	1.4 (±1.3)

Table 1. Percentage and absolute cell number of CD3$^+$, CD19$^+$, NKp46$^+$, Ly6G$^+$ and F4/80$^+$ cells in vavFLIP$_R$ mice and WT littermates. (Standard deviation).

3.2. vavFLIP$_R$ mice are more susceptible to influenza virus infection

Death receptor-mediated apoptosis is a key mechanism for the control of immune responses and dysregulation of this pathway is associated with many pathogenic conditions and may even be central in the pathogenesis of many diseases [176]. The death receptor-mediated signaling pathway has been shown to be closely related to the pathology of IAV infection [184–186]. Abnormally elevated expression of death ligands has been found in lethal IAV infections. Aberrant induction of apoptosis caused by death ligands is related to multi organ disorders, which occur in severe IAV infections [187]. Apoptosis is also known as a major mechanism of elimination of activated T cells during an immune response to viral infection [188].

It has been demonstrated that c-FLIP$_S$ is crucial during the early phase of an immune response in humans [180]. To study whether expression of c-FLIP$_R$ modulates the immune response during viral infection, vavFLIP$_R$ mice were challenged with IAV. Influenza was chosen since it is still not well known how apoptosis signaling affects IAV infection and replication. vavFLIP$_R$ and WT female mice in the age of 12-17 week were intranasally infected with 2x10^3 FFU PR8 (H1N1) virus. Control mice were given an equal volume of PBS for mock infection. Body weight and sickness score of mice were recorded daily over a period of 14 days post infection (Figure 11). As illustrated in Figure 11, in the early phase of infection, weight loss curves in vavFLIP$_R$ and WT mice were similar. However, vavFLIP$_R$ mice showed slightly higher body weight loss

compared to WT mice at the peak of infection. Notably, 100% of the WT, as well as vavFLIP$_R$ mice, were able to recover and regain body weight.

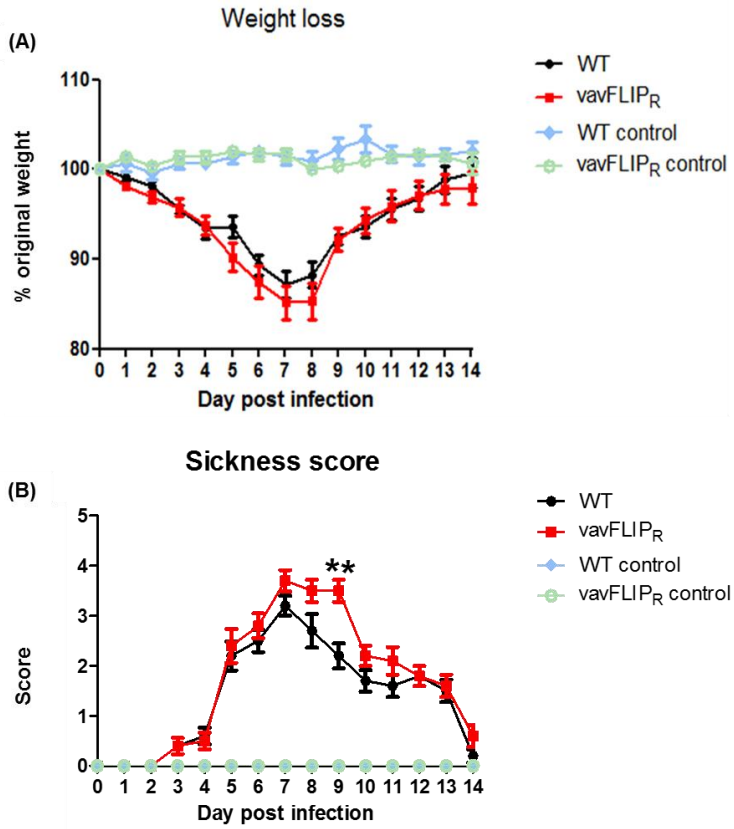

Figure 11. Morbidity and weight loss comparison during influenza A virus infection. vavFLIP$_R$ and WT female mice at the age of 12-17 week were infected intranasally with 2x10^3 FFU PR8 (H1N1) influenza A virus. Following infection, mice were checked daily for weight loss. (A) The weight of vavFLIP$_R$ mice (Red) was a bit lower than the WT littermates (black) at the peak of infection. Mock infected animals from WT and vavFLIP$_R$ mice did not lose weight or showed signs of disease. Data are presented as mean value +/- SEM. (B) Mice were evaluated daily and scored for individual symptoms. Ruffled fur (absent = 0; present = 1), hunched back (absent = 0; present = 1) and activity (normal = 0; reduced = 1; severely reduced = 2) were evaluated. The final score was the addition of each individual symptom score. The minimum score was 0 for the control mice and 1-4 for the IAV infected mice, depending on the severity.

3.3. vavFLIP$_R$ mice have a higher viral load compared to WT mice at the peak of infection

To investigate whether the high susceptibility of vavFLIP$_R$ mice is partially due to enhancing viral replication and associated tissue damage or a detrimental immunopathology of the host response, or both, viral load was analyzed by determining mRNA copies of the (NP) gene in the lung. In the early phase of infection (day 1-2 post infection), the number of NP copies was comparable between littermate WT and vavFLIP$_R$ infected mice. However, the virus replicated to a significantly higher titer in vavFLIP$_R$ mice compared to WT mice at the peak of infection. This was additionally confirmed by foci assays indicating replication-competent virus (Figure 12B). Notably, the virus titers in vavFLIP$_R$ mice, as well as WT mice, were below the level of detection at day 10 post infection.

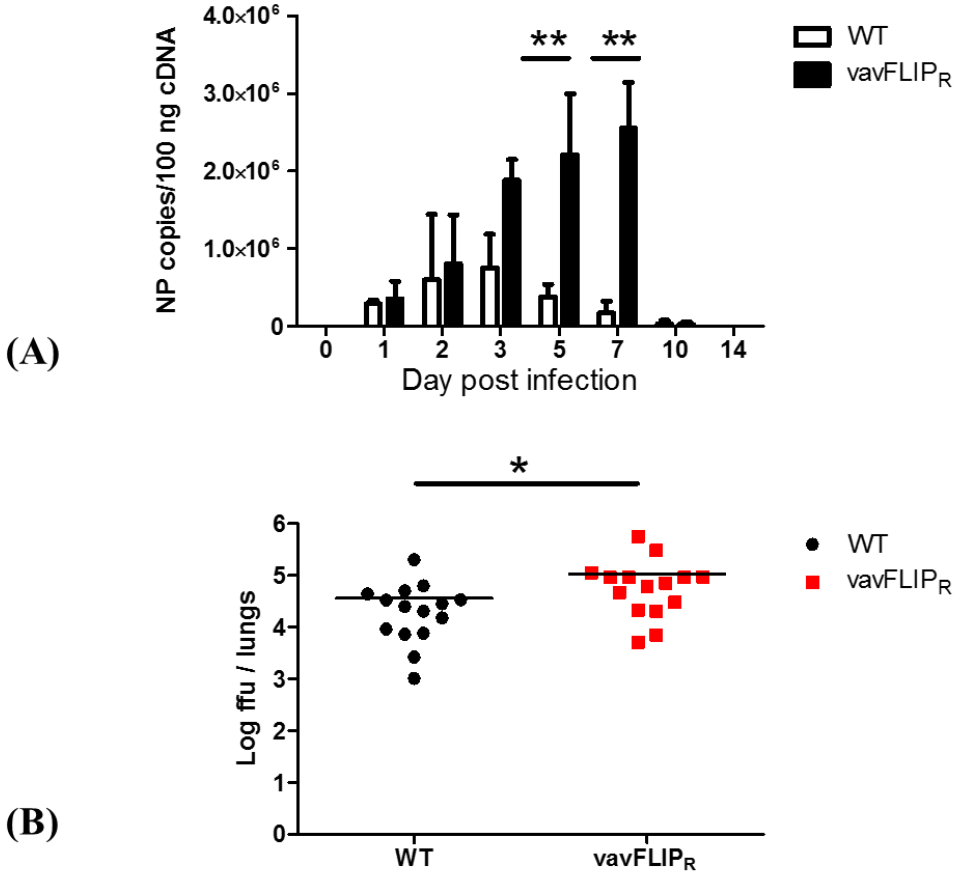

Figure 12. (A) Viral load kinetics in the lungs of the vavFLIP$_R$ mice and WT littermates. After intranasal infection of female mice at the age of 12-17 week with 2x10^3 FFU PR8. Influenza virus titers were evaluated in lung supernatants of WT (white bars) and vavFLIP$_R$ (black bars) mice by qPCR with at least two technical replicates for each sample. vavFLIP$_R$ mice had a higher virus titer in the lungs. Bar graphs represent the mean; error bars represent SEM. Statistical analyses were performed using two-tailed Mann-Whitney tests; (*) indicate $p < 0.05$. (B) Viral load in the lungs of influenza infected vavFLIP$_R$ (n=5) and WT (n=5) mice were measured on day 7 p.i. by focus formation assay indicating replication-competent virus. foci assay recapitulated the qPCR results. vavFLIP$_R$ mice had a higher viral titer in the lungs. foci assay was performed with three technical replicates for each sample. Statistical analyses were performed using two-tailed Mann-Whitney tests; (*) indicates $p < 0.05$.

3.4. Histological analysis confirmed the observed higher viral load in vavFLIP$_R$ mice

To verify the results of the qPCR analysis, a histological study was performed. Histological sections of the lungs from influenza infected vavFLIP$_R$ and WT mice, were examined on day 7 post infection. Large patches of virus-infected cells (brown staining) were detected in vavFLIP$_R$ mice compared to WT mice. This data recapitulated the qPCR data which showed a higher viral titer in vavFLIP$_R$ mice at the peak of infection. All infections were performed at an infection dose of 2×10^3 FFU. Control mice were given an equal volume of PBS for mock infection.

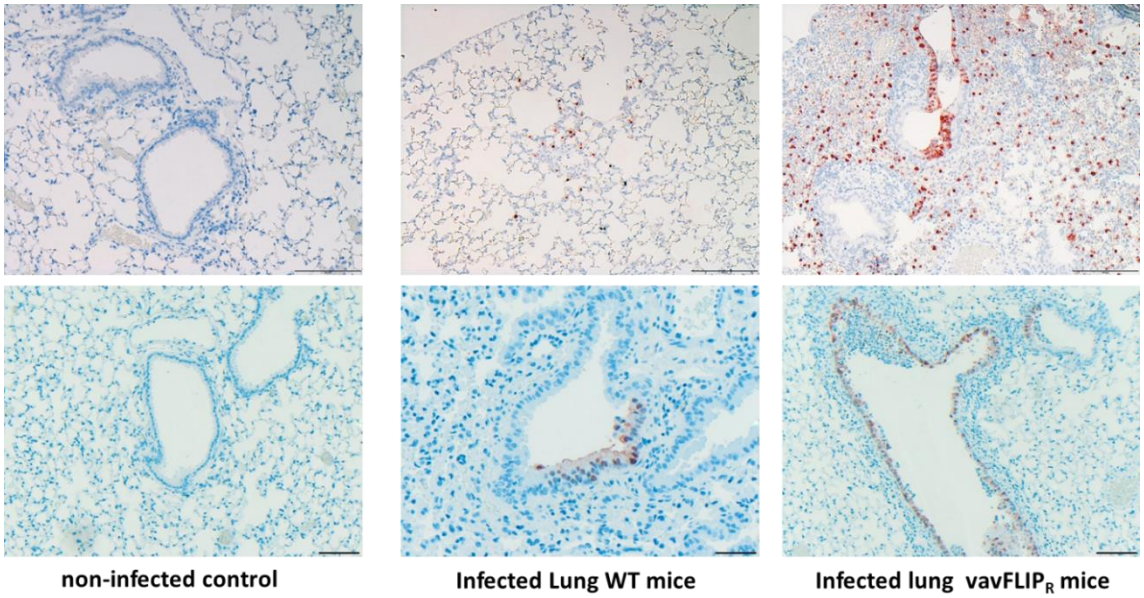

Figure 13. Histological sections of lungs of WT and vavFLIP$_R$ mice infected with the PR8 virus. Mice were infected intranasally with 2×10^3 FFU of H1N1 virus. Control mice were given an equal volume of PBS for mock infection. 7 days post infection, lung sections were stained with hematoxilin and eosin for histological analysis. Furthermore, they were stained with anti-influenza NP antibody. PR8 infected cells were observed in the lungs of the vavFLIP$_R$ and WT littermates (Red dots). Large patches of virus-infected cells were detected in vavFLIP$_R$ mice compared to WT mice.

3.5. Immune cell composition in vavFLIP$_R$ and WT littermates following IAV infection

In response to influenza A infection, the host develops a complicated antiviral response to fight against the virus. Both the innate and adaptive immune system participate in the containment and clearance of viral infection, which takes place in about a week [189]. For a long time, apoptosis was regarded mainly as a host cell defense mechanism, as many viruses express antiapoptotic proteins to prevent this cellular response. It has been shown that three of the 11 viral gene products, namely NS1, PB1 and M2 ion channel, were implicated in the manipulation of programmed cell death [190,191]. More recent data illustrated, however, that viruses can also take advantage of proapoptotic signaling events to increase the efficiency of their replication machinery within the apoptotic cell [185]. Furthermore, apoptosis induced by extracellular death signals is now regarded as a crucial event that occurs regularly during innate and adaptive immune responses toward several kinds of pathogens, including IAV. To understand whether the observed differences in the host suseptibility, following influenza infection, are due to innate or adaptive immunity, vavFLIP$_R$ and WT female mice at the age of 12-17 week were intranasally infected with $2x10^3$ FFU of PR8 (H1N1) virus. The composition of immune cells was analyzed in influenza infected vavFLIP$_R$ and WT littermates on day 7 post infection. Flow cytometry data from spleen (Figure 14A) and the mediastinal lymph node (Figure 14B) indicated that both, frequencies and total cell numbers of CD19$^+$ B cells, CD3$^+$ T cells as well as the CD4$^+$ helper T cell and CD8$^+$ cytotoxic T cell subsets were comparable between infected vavFLIP$_R$ mice and the WT littermates. Furthermore, the activation status of T cells was analysed in spleen and mediastinal lymphnodes from 12-17 week old infected WT and vavFLIP$_R$ mice by CD44 and CD62L staining on day 7 post infection. No difference in CD44$^+$ antigen-experienced T cells or CD62L$^+$ naïve T cells could be observed.

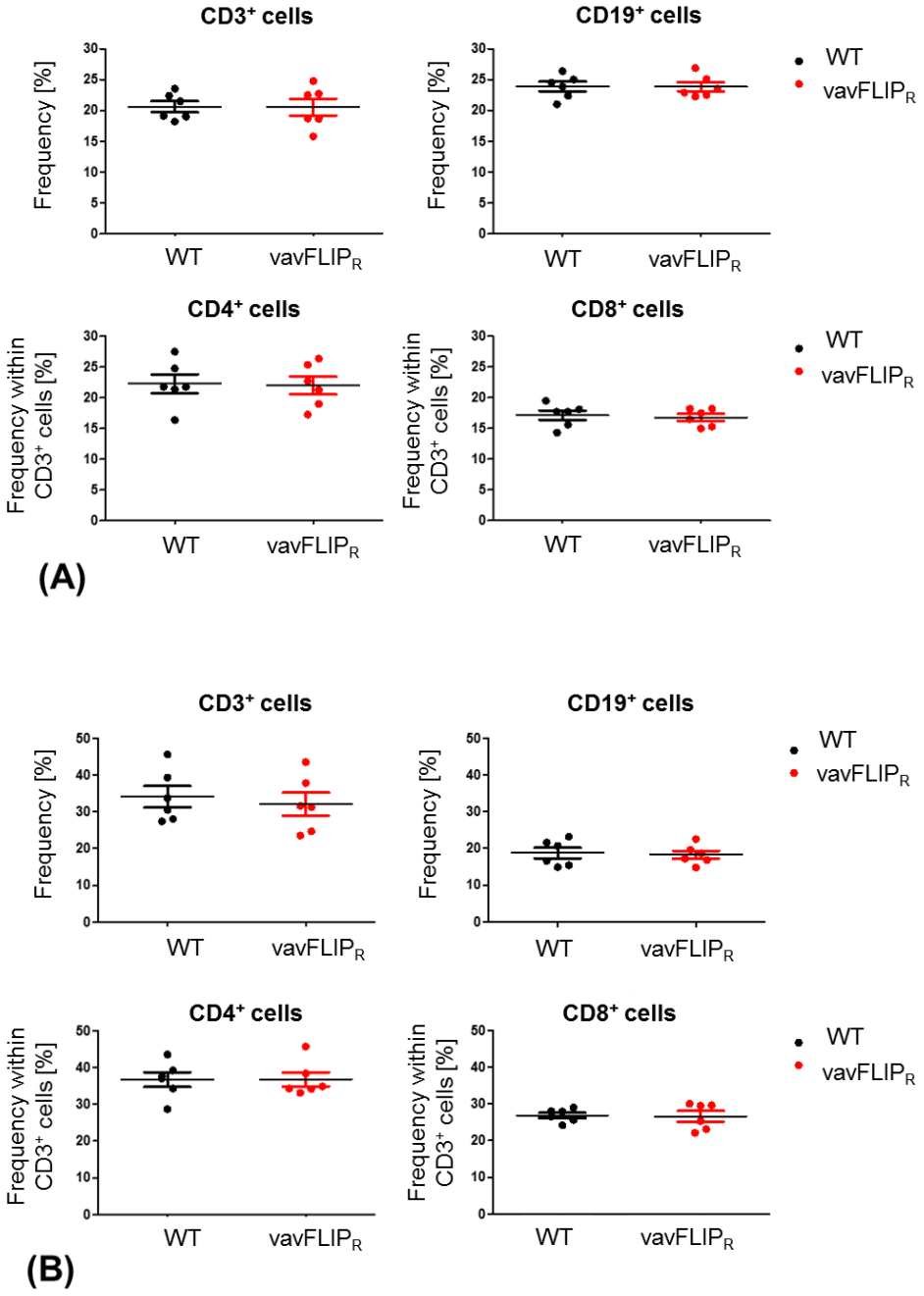

Figure 14. Freshly isolated splenocytes and lung draining lymph node cells (DLN) from WT (n=6) and vavFLIP$_R$ (n=6) mice were stained with antibodies directed against CD3, CD4, CD8 and CD19 followed by FACS analysis. Individual mice are shown as separate symbols. Horizontal lines represent the mean of frequencies from three independent experiments; error bars display s.e.m. $CD3^+$ T cells, $CD19^+$ B cells, $CD4^+$ T helper cells within the $CD3^+$ compartment and $CD8^+$ cytotoxic T cells within the $CD3^+$ subset in spleen **(A)** and mediastinal lymph node **(B)**.

3.6. IAV infected vavFLIP$_R$ mice have a higher number of NK cells compared to WT littermates

Natural killer cells are a population of innate lymphoid cells, which exhibits potent cytotoxic activity and cytokine production [192]. NK cells also have a role in the regulation of the adaptive immune response, and have been shown, in different contexts, to stimulate or inhibit T cell responses [193]. In many virus infections, natural killer cells are critical for the rapid containment of virus replication [194–196] . However, the exact role of NK cells in IAV infection is still a matter of debate [197,198]. In this study, upon IAV infection, the frequency and total NK cell number in vavFLIP$_R$ mice and WT littermates were analyzed, using NKp46 flow cytometry antibody. The lymphocytes were live gated during acquisition using the side and forward scatter dot plot display. Furthermore, by using the negative gating strategy, CD3$^-$ and CD19$^-$ lymphocyte populations were identified. The NK cell population was further identified by NKp46$^+$ cells (Figure 15). Interestingly, Flow cytometry analysis illustrated that, at the peak of infection, the frequency and total numbers of NK cells were higher in the spleen (Figure 16A). Similarly, the percentages and absolute numbers of NK cells were higher in the mediastinal lymph node (Figure 16 B) and bronchoalveolar lavage fluid (Figure 16C) of vavFLIP$_R$ mice compared to WT littermates.

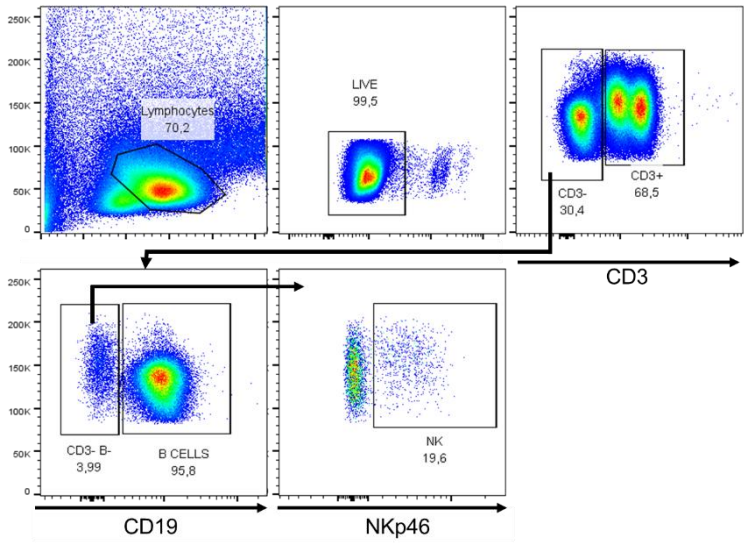

Figure 15. Flow cytometry gating and identification strategy for NK cells. Mice were intranasally infected with PR8 influenza. On day seven post-infection, mediastinal lymph node NK cells were examined for NKp46 marker by flow cytometry.

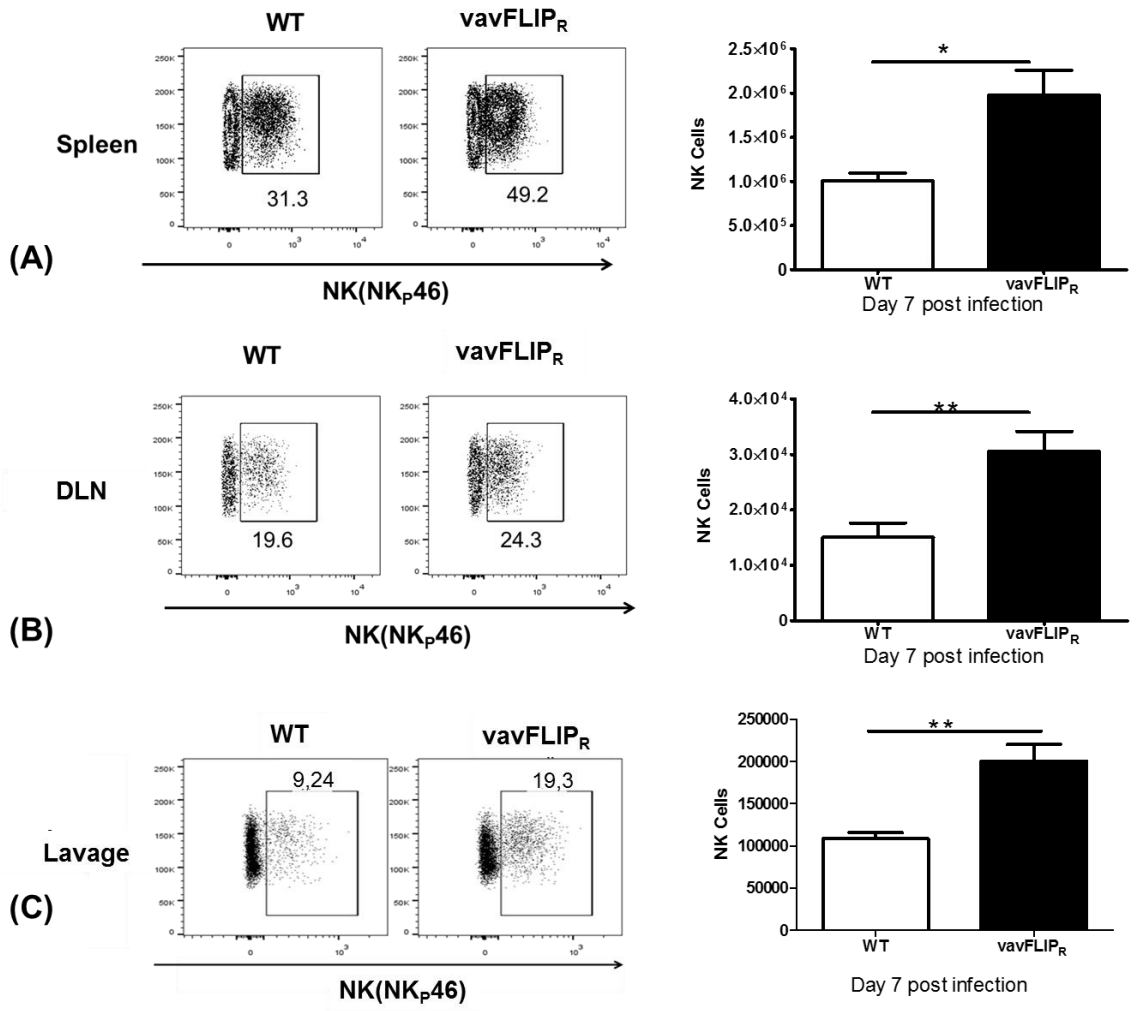

Figure 16. vavFLIP$_R$ mice had a higher number of NK cells at the peak of IAV infection. Single cell suspensions from spleen (A) and the mediastinal lymph node (B) and bronchoalveolar lavage (C) of infected vavFLIP$_R$ (black) and WT (white) mice stained with the NKp46 marker. NK cell frequencies and cell numbers were determined. Representative dot plots are shown in (A-C). Horizontal lines represent the mean of frequencies from three independent experiments; error bars display SEM. Statistical analyses were performed with two-tailed nonparametric Mann Whitney U tests. *p<0.05, ***p<0.001. WT (n=6), vavFLIP$_R$ (n=7)

Next, to compare NK cell apoptosis in IAV infected vavFLIP$_R$ and WT mice, Sorted NKp46$^+$ cells, CD4$^+$ and CD8$^+$ T cells from infected vavFLIP$_R$ and WT mice were stained with active caspase 3/7 stain for 10 minutes and analyzed with flow cytometry. The result indicated that the frequency of active caspase 3/7 in CD4 and CD8 cells were comparable in IAV infected vavFLIP$_R$ and WT mice. However, vavFLIP$_R$ mice have a lower frequency of active caspase 3/7 in NK cells (Figure 17).

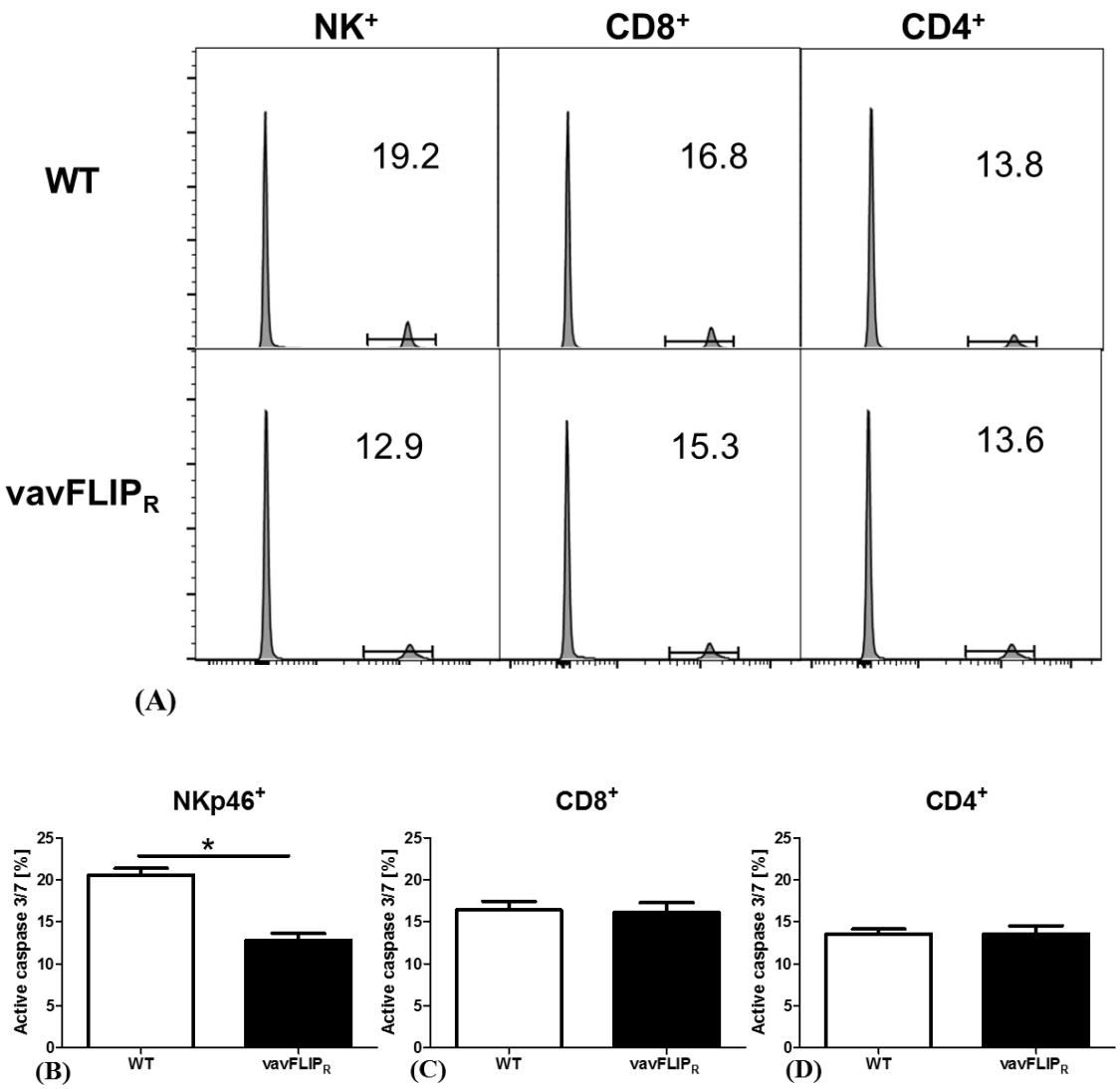

Figure 17. (A) Representative flow cytometry histogram of active caspase 3/7 in NKp46$^+$, CD8$^+$ and CD4$^+$ cells in vavFLIP$_R$ and WT mice on day 7 post infection. (B-C) Summary graph of frequencies of active caspase 3/7 in NKp46$^+$, CD8$^+$ and CD4$^+$ cells in bronchoalveolar lavage. Active caspase 3/7 is comparable in CD8$^+$ and CD4$^+$ cells. However, NKp46$^+$ cells in vavFLIP$_R$ mice showed significantly lower active caspase 3/7. Active caspase 3/7 is displayed as the mean ± SEM. from three independent experiments. Statistical analyses were performed with two-tailed nonparametric Mann Whitney U tests. *p<0.05, ***p<0.001.

3.7. Kinetics of NK cell accumulation does not alter in vavFLIP$_R$ mice

Prior studies examinied the contribution of NK cells to IAV immunity have shown disparate results [195,197,199,200]. Therefore, to determine if the kinetics and location of NK cells during IAV infection are altered in vavFLIP$_R$ mice, vavFLIP$_R$ mice and WT littermates were infected with 2x10^3 FFU PR8 (H1N1) influenza A virus and then NK cell numbers were quantified in the lung draining lymph node (DLN) and spleen by flow cytometry. Following infection, both groups of mice showed similar kinetics till day 10 post infection. Notably, on days 7 and 10 post infection, the numbers of NK cells were higher in vavFLIP$_R$ mice compared to WT littermates (Figure 18).

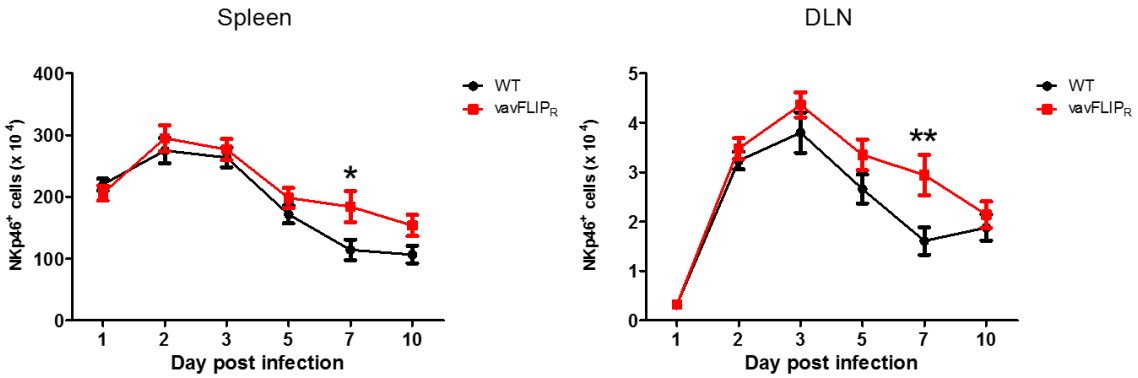

Figure 18. Kinetics of NK cell accumulation during IAV infections. vavFLIP$_R$ (n=6) and WT (n=6) mice were infected with IAV infection. NK cells were enumerated in the lung draining lymph node (DLN) and spleen at the indicated time points by flow cytometry. Shown are NKp46$^+$ cells. Statistical analyses were performed using two-tailed Mann-Whitney tests; *p<0.05, ***p<0.001.

3.8. vavFLIP$_R$ mice have a higher level of proinflammatory cytokines compared to WT mice at the peak of infection

Following influenza infection, activated immune cells produce different cytokines and chemokines [201]. Cytokines such as TNF-α and IFN-γ have important roles in coordinating the antiviral immune response and can also have direct antiviral effects. Although TNF-α was first noted for its role in the killing of tumor cells [202], it has pleiotropic functions that include the inflammatory response and host resistance to pathogens [203,204]. IFN-γ is primarily produced by T cells and NK cells and its function is to activate macrophages. It has been shown that IFN γ treatment at the early stages of influenza virus infection protects mice from death in a NK cell-dependent manner [205].

However, excessive inflammation due to the overabundant production of proinflammatory cytokines and chemokines has been shown as one of the main factors in disease pathogenesis [82,123,206]. Because both apoptosis and the pro-inflammatory response have a definitive role in the pathogenesis of influenza virus, to assess the contribution of the proinflammatory cytokine responses in the severity of influenza infection in vavFLIP$_R$ mice, cytokine protein levels in bronchoalveolar lavage, spleen and serum were assessed by Bio-plex cytokine assay and the Luminex® instrument. Compared with the infected WT mice, infected vavFLIP$_R$ mice had a higher level of IFN-γ and TNF-α in bronchoalveolar lavage (Figure 19A), spleen (Figure 19B) and serum (Figure 19C) on day 7 post infection.

In addition to cytokines, multiple chemotactic molecules are induced following influenza virus infection. In fact, the production of several chemokines, both locally and systemically, correlate with influenza virus pathogenesis [207–209]. Chemokines and their receptors play an important role in site-directed migration and activation of immune cells. Elevated levels of MCP-1 (CCL2) and IP-10 (CXCL10) were reported in the serum of patients infected with H5N1compared to patient infected with H1N1 [210]. Moreover, elevated levels of RANTES (CCL5) mRNA were detected in human primary macrophages following infection with H5N1 as compared to H1N1 or H3N2 infection [211]. To examine the contribution of the chemokine production in the severity of influenza infection in vavFLIP$_R$ mice, chemokine protein levels in bronchoalveolar lavage, spleen and serum were assessed by Bio-plex cytokine assay and the Luminex® instrument. Infected vavFLIP$_R$ mice had higher levels of MIP-1α and RANTES in bronchoalveolar lavage (Figure 20A), spleen (Figure 20B) and serum (Figure 20C) on day 7 post infection. Furthermore, the concentration of IFN-α, IL-6, IL-12p70, IL-17A, IL-10, IL-2, IL-1α, IL-1β, IL-4, IL-21, MCP-1, IP-10, MIP-1β were analyzed on different time points (day 0, 1, 2, 3, 5, 7, 10, 14 p.i.). However, no differences could be identified between WT and vavFLIP$_R$ mice.

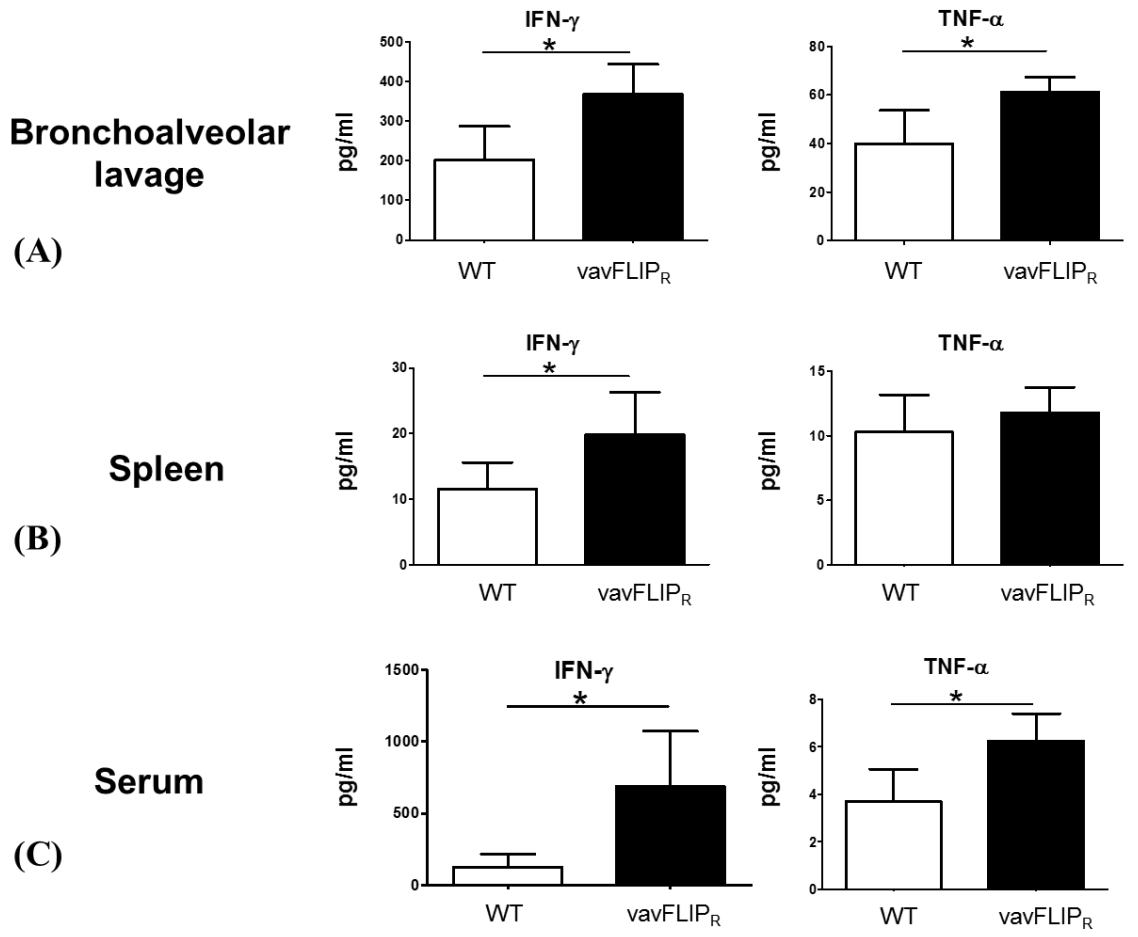

Figure 19. Comparison of proinflamatory cytokines in vavFLIP$_R$ and WT littermates at the peak of IAV infection. Concentration of IFN-γ and TNF-α were determined in the bronchoalveolar lavage (A), spleen (B) and serum (C) of IAV infected vavFLIP$_R$ (black) and WT (white) mice on day 7 post infection, by Luminex® assay (n=4 each). Bar graphs represent the mean; error bars represent SEM. Statistical analyses were performed using two-tailed Mann-Whitney tests; *p<0.05, ***p<0.001. Higher levels of the IFN-γ and TNF-α were detected in vavFLIP$_R$ mice.

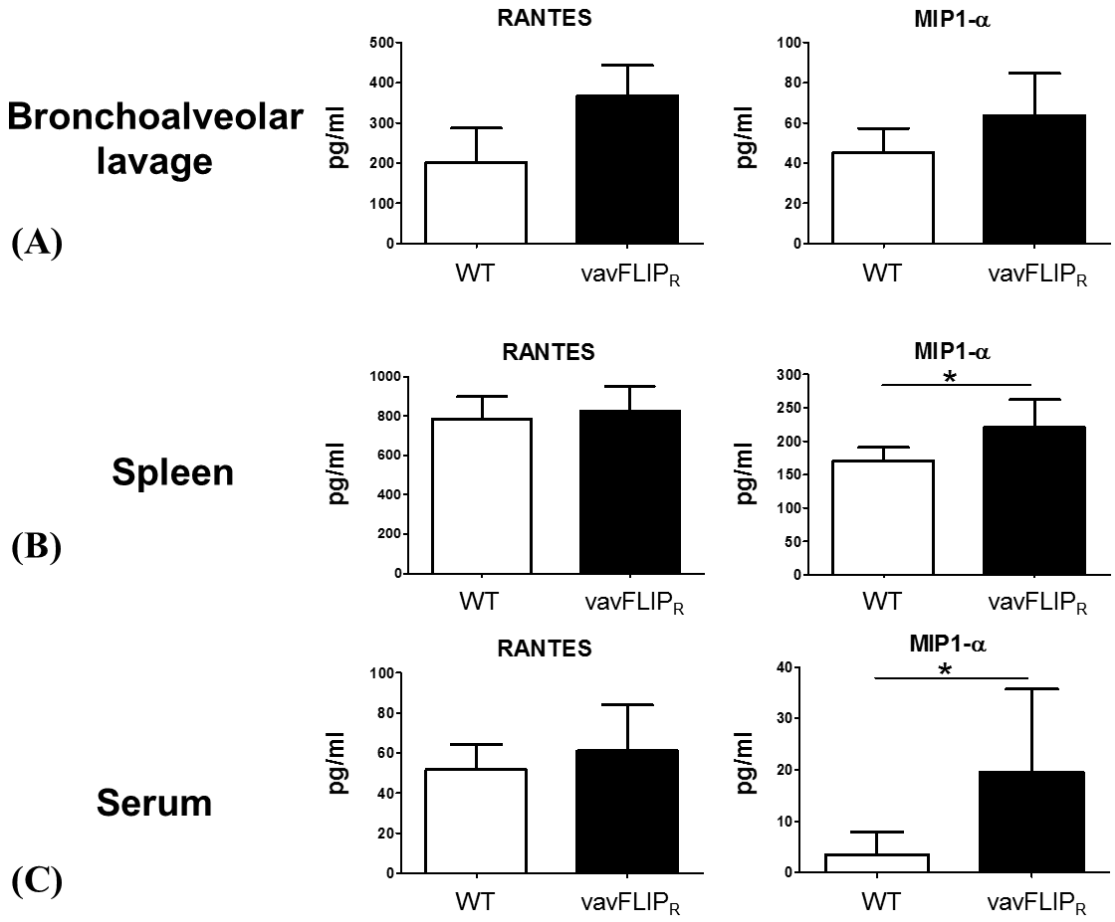

Figure 20. Chemokine concentrations in the vavFLIP$_R$ and WT littermates at the peak of IAV infection. Concentrations of RANTES and MIP1-α were determined in the bronchoalveolar lavage (A), spleen (B) and serum (C) of IAV infected vavFLIP$_R$ (black) and WT (white) mice on day 7 post infection, by luminex assay (n=4 each). Bar graphs represent the mean; error bars represent SEM. Statistical analyses were performed using two-tailed Mann-Whitney tests; *p<0.05, ***p<0.001. Higher level of MIP-1α was detected in vavFLIP$_R$ mice.

3.9. Degranulation is impaired in NK cells of vavFLIP$_R$ mice during influenza infection

In order to functionally characterize NK cells of the vavFLIP$_R$ mice, NK cells from vavFLIP$_R$ and WT mice were isolated from spleen. A standard cytotoxicity assay with YAC-1 target cells was employed to assess NK cytotoxicity. The result indicated that the cytotoxicity of NK cells in vavFLIP$_R$ and WT mice were comparable (Figure 21). In addition, to further assess FLIP$_R$-related changes in NK cell function, degranulation was measured with the CD107a assay. CD107a is localized to lysosomes and cytolytic granules in resting NK cells [212,213]. Upon activation, NK cells degranulate their cytolytic contents and CD107a appears on the NK cell surface. First, the degranulation response of wildtype and vavFLIP$_R$ NK cells upon co-culturing with YAC-1 target cells was analyzed. Cell-surface exposure of CD107a was determined by flow cytometry. In order to compare degranulation of natural killer cells following interaction with influenza-infected cells, the expression level of CD107a was analyzed in vavFLIP$_R$ mice and WT littermates during the course of IAV infection. Percentages of the CD107a$^+$ NK cells were similar in uninfected mice however, CD107a$^+$ were significantly lower in the NK cells of the infected vavFLIP$_R$ mice compared to WT littermates (Figure 22).

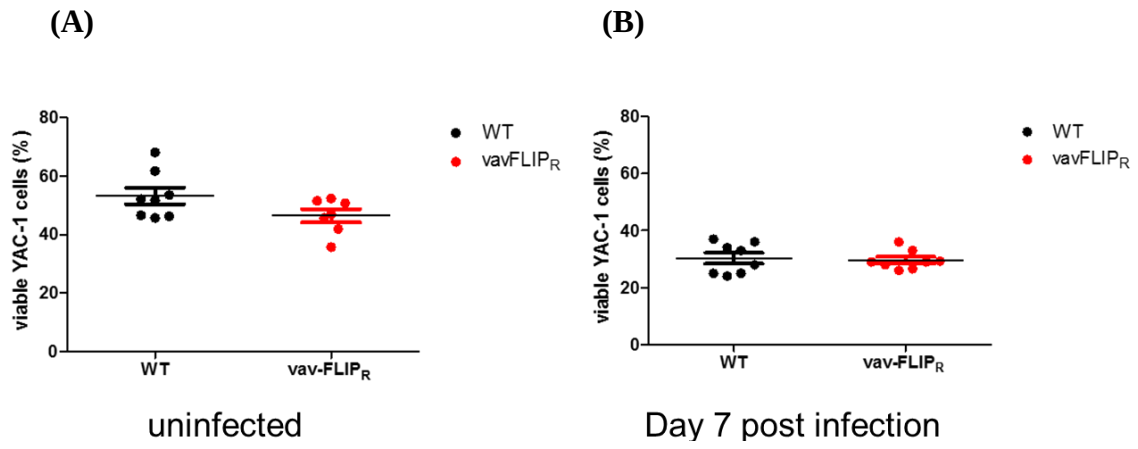

Figure 21. cFLIP$_R$ did not change the ability of NK cells to kill YAC-1 cells**.** NK cells of healthy (A) and IAV infected (B) vavFLIP$_R$ and WT littermates were incubated with YAC1 cells at the ratio of 1:8 for 16 hr. After the incubation time, cells were harvested and analyzed with flow cytometry.

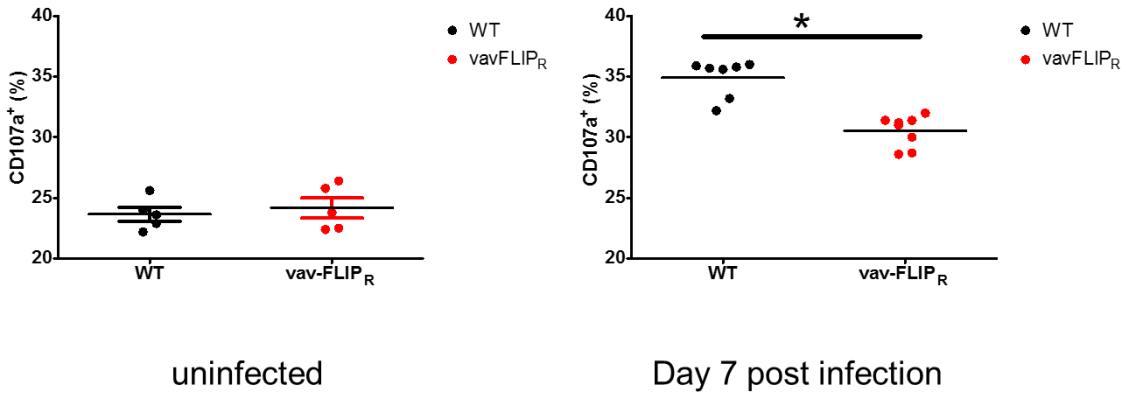

Figure 22. NK cell degranulation during influenza infection is impaired in vavFLIP$_R$ mice. NK cells from spleens of the uninfected and infected vavFLIP$_R$ and WT littermates were incubated with YAC-1 cells at an effector to target ratio of 1:1 in the presence of brefeldin A, monensin and BV-CD107a antibody for 2 hours. Surface expression of CD107a on the uninfected and infected NK cells of vavFLIP$_R$ mice and WT littermates were tested by FACS analysis using anti-CD107a antibody. The percentage of NK cells positive for CD107a were significantly lower in infected vavFLIP$_R$ mice compared to WT littermates. Statistical analyses were performed using two-tailed Mann-Whitney tests; *$p<0.05$.

3.10. Higher number of NK cells contribute to the severity of the influenza infection in vavFLIP$_R$ mice

Early studies showed that NK cells within the lung have a higher cytolytic activity following IAV infection and are important for survival, as their depletion from hamsters or mice with Anti-Asialo-GM1 antibody resulted in increased morbidity and mortality compared to undepleted controls [194,214]. Conversely, more recent studies have observed that NK cells contribute to the immunopathology in influenza infection [215,197]. To investigate the influence of a higher number of NK cells on the host outcome during influenza infection, mice were treated with Anti-Asialo-GM1 to deplete NK cells *in vivo* prior to and during influenza infection. Anti-Asialo-GM1 was reported effective at depletion of NK cells *in vivo* [216,217], as confirmed by our flow cytometric analysis of vavFLIP$_R$ and WT mice spleen (Figure 23A). Body weight of the NK cell depleted vavFLIP$_R$ and WT mice were recorded daily over a period of 14 days post infection (Figure 23B). As illustrated in Figure 23, weight loss curves in NK cell depleted-vavFLIP$_R$ and NK cell depleted-WT mice were similar and no significant difference could be observed in body weight loss/gain.

(A)

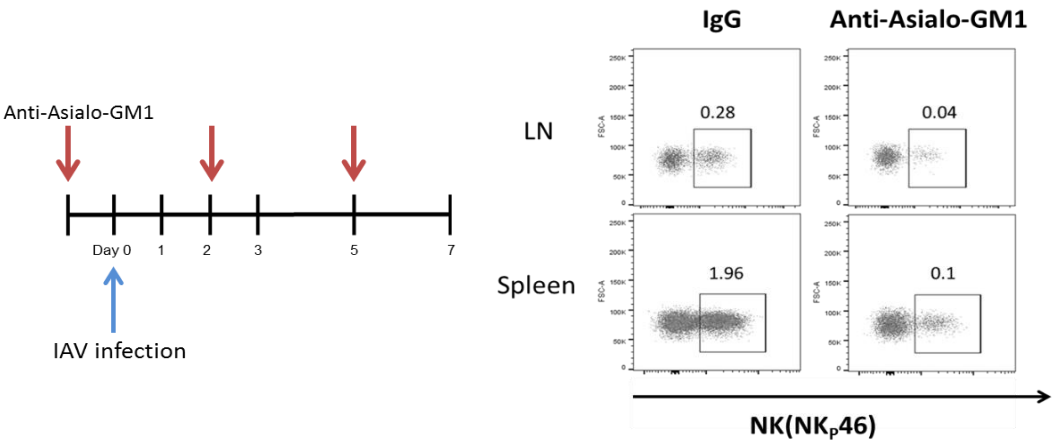

(B)

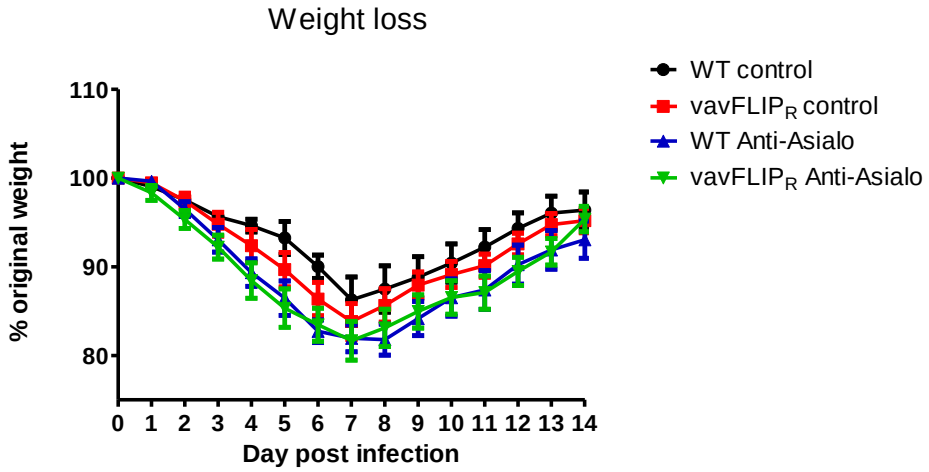

Figure 23. *In vivo* NK cells depletion with Anti-Asialo-GM1. Mice were inoculated i.p. with 20 µg Anti-Asialo-GM1 antiserum (or IgG control), 1 day prior to infection and received another 20 µg on day 2 and 5 p.i. The efficiency of depletion is shown in (A). (B) Following infection, mice were monitored daily for body weight. Both Anti-Asialo treated groups (vavFLIP$_R$ and WT) were more susceptible to influenza infection compared to controls. Notably in the absence of NK cells, the slight difference which was observed between infected vavFLIP$_R$ and WT mice disappeared. Data are presented as mean value +/- SEM. n= 5 per group of mice.

3.11. Improved outcomes for influenza-infected vavFLIP$_R$ mice by depletion of NK cells

Previous studies showed that different inbred mouse strains exhibit large differences in their response to 2x10^3 PFU PR8 infection [218]. To determine whether NK cells played a role in higher viral load at the peak of infection, NK cells were depleted using Anti-Asialo-GM1 antibody. Mice depleted of NK cell were infected with 2x10^3 FFU influenza virus and the viral load was measured on day 7 post infection with qPCR and foci assay. NK cell depletion resulted in a higher viral load in vavFLIP$_R$ and WT mice compared to IgG controls. Notably, although the viral load is higher the differences in vavFLIP$_R$ and WT mice disappeared, which suggested that an excessive number of NK cells are involved in higher viral load in vavFLIP$_R$ mice at the peak of infection.

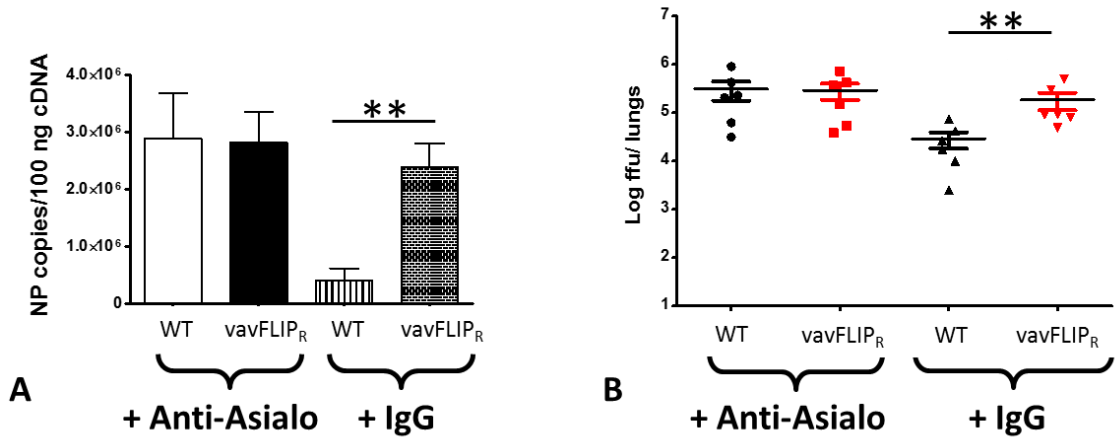

Figure 24. qPCR and foci assay analyses of the lungs of vavFLIP$_R$ and WT littermates. NK cell-depleted and control mice were infected with influenza virus. Virus titers determined by qPCR (A) and foci assay (B) on day 7 post-infection. In the absence of NK cells, vavFLIP$_R$ and wild type mice showed a similar viral load. Bar graphs represent the mean; error bars represent SEM. Statistical analyses were performed using two-tailed Mann-Whitney tests; *p<0.05, ***p<0.001.

3.12. Influenza virus can directly infect primary mouse NK cells

NK cells face influenza viruses within the microenvironment of infected cells, and are important for the host innate immunity during influenza virus infection. NK cells can recognize and kill influenza virus-infected cells [219,220]. To counteract this killing, however, influenza virus has developed an escape strategy that inhibits NK cell

cytotoxicity by increasing the binding of two inhibitory receptors to the infected cells after infection [221]. It is, therefore, important to investigate the direct effects of influenza virus on NK cells. First, it was studied whether influenza virus could directly infect NK cells. Freshly isolated primary NK cells were infected with H1N1 and subsequently washed and cultured. Using RT-PCR, the NP gene was detected in influenza virus-exposed NK cells but not in mock-treated NK cells. In parallel, purified resting primary mouse CD4 T cells, which cannot be directly infected by the influenza virus [222] were included as a negative control. No NP gene was detected in influenza virus-exposed CD4 T cells. After 6 hrs the supernatants from infected NK cells were collected and inoculated onto MDCK cells to determine if infectious progeny were produced. The results illustrated that influenza virus could replicate in primary NK cells.

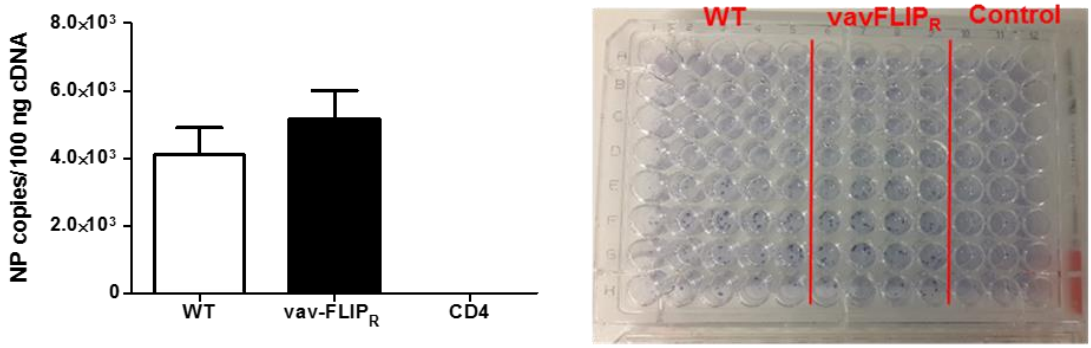

(A) **(B)**

Figure 25. Influenza virus directly infects primary murine NK cells. (A) NK cells from vavFLIP$_R$ mice and WT littermates were incubated with influenza virus H1N1 at a multiplicity of infection (MOI) of 2. After 1 hr of viral adsorption, unadsorbed viruses were washed away by excess phosphate buffered saline. CD4 cells were treated in parallel as a negative control. The expression of viral NP mRNA was detected by q-PCR in influenza virus-exposed NK cells but not in CD4 treated cells. (B) Additionally, the supernatants from infected NK cells were collected and inoculated onto MDCK cells to determine whether infectious progeny were produced and since infectious particles were detected, it was concluded that Influenza virus can replicate in primary NK cells.

3.13. NK cell depletion results in significantly more CD4 T cells in the lung during IAV Infection

It has been shown that NK cells can kill activated CD4 T cells during lymphocytic choriomeningitis virus (LCMV) infection [223]. To determine whether NK cells similarly reduce the number of CD4 and CD8 T cells during IAV infections, CD4 and CD8 T cells were quantified in NK-depleted and non-depleted mice. The number of CD8 T cells in the lung did not differ significantly between non-depleted and NK-depleted mice. However, there was a significant increase in the total number of CD4 T cells in the lungs of NK-depleted mice at day 7 p.i.

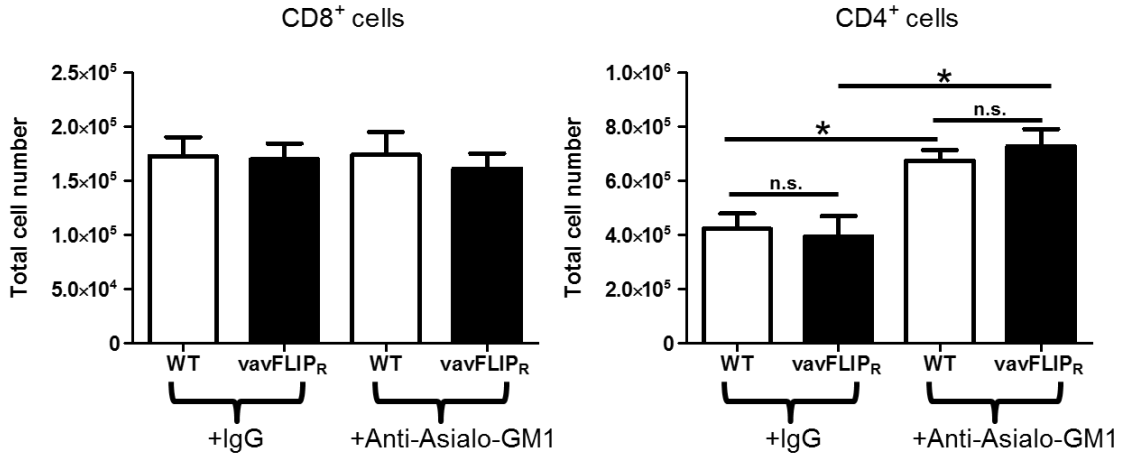

Figure 26. NK cell depletion results in significantly more CD4 T cells in the IAV infected lung. vavFLIP$_R$ and WT mice were depleted of NK cells or treated with IgG, 1 day prior to infection and received another 20 µg on day 2 and 5 p.i. (A) On day 7 post infection the number of CD4 and CD8 T cells in NK-depleted and non-depleted mice was enumerated by flow cytometry. The number of CD8 T cells in the lung did not alter in the NK-depleted mice compared to non-depleted mice. However, there was a significant increase in the total number of CD4 T cells in the lungs of NK-depleted mice at day 7 p.i. Bar graphs represent the mean; error bars represent SEM. Statistical analyses were performed using two-tailed Mann-Whitney tests; *$p<0.05$, ***$p<0.001$. n.s., not significant. Data were pooled from 2 independent experiments with a total of 4 mice per group

4. Discussion

4.1. Investigation of the role of c-FLIP in anti-viral immunity

Programmed cell death is a complex physiological cellular process that maintains homeostasis and plays an important role in the protection of multicellular organisms from diseases [224,225]. Apoptosis is the most prominent type of programmed cell death [224]. Apoptosis can be triggered by extrinsic signals, such as the binding of ligands to cell surface death receptors [34]. Deregulation of the apoptosis machinery has been found in different diseases [224]. Apoptosis has been often described as a mechanism of host defense, which can eliminate infected cells, reduce the spread of infection to neighboring cells and prevent pathogen persistence [226,227]. Different viruses have been shown to induce apoptosis in the host such as human cytomegalovirus, duck swollen head hemorrhagic disease virus and influenza A virus. [228–231]. In this respect, it has been demonstrated that influenza virus infection increases the expressions of both Fas and FasL on HeLa cells. Ligation of Fas/FasL on the surface of virus-infected cells mediates apoptosis [232–234]. Anti-Fas or FasL antibodies have been reported to partially suppress virus-induced apoptosis [235]. Notably, apoptosis has to be tightly regulated since too little or too much cell death may lead to pathology [14,240]. During the past few years many efforts have been made to study the molecular mechanisms of the apoptosis signaling pathway and its regulatory systems [74,237,238]. The anti-apoptotic c-FLIP proteins inhibit apoptosis in the extrinsic pathway by preventing initiator caspase-activation at the signaling complex of death receptors [239,240]. Although the physiological role of c-FLIP$_L$ and c-FLIP$_S$ is well characterized, the function of c-FLIP$_R$ in the immune system is poorly understood. In 2013 Telieps *et al*., could show that adult vavFLIP$_R$ mice, which constitutively express murine c-FLIP$_R$ in all hematopoietic cells, have normal numbers of immune cells in the steady state [173]. However, when challenged with *Listeria monocytogenes*, vavFLIP$_R$ mice exhibited better bacterial clearance, less liver necrosis and less caspase 3 activation compared with infected WT littermate. Thus, it was concluded that early apoptosis occurring during *Listeria monocytogenes* infection is restricting bacterial clearance and c-FLIP$_R$ expression in hematopoietic cells supports an efficient immune response against bacterial infections. Unexpectedly, in this work, challenging vavFLIP$_R$ mice with IAV infection resulted in a different outcome compared to bacterial infection. vavFLIP$_R$ mice were more susceptible to influenza

infection than WT mice, showing slightly increased weight loss at the peak of the infection. Additionally, vavFLIP$_R$ mice had a significantly higher viral load compared to WT mice at the peak of infection. Firstly, while some minor increases in viral titers were observed within the first 3 days following influenza virus infection, huge differences in viral titers were seen on day 5 and day 7 post infection. This data suggests that preventing apoptosis of the immune cells during influenza infections is in favor of influenza virus replication and does not have a beneficial effect on viral control. Notably, both vavFLIP$_R$ and WT mice could clear the virus by day 10 post infection and viral titers were below the level of detection on day 10 post infection. It is likely that a stronger adaptive immune response in vavFLIP$_R$ mice could control the viral replication after day 7 post infection.

4.2. Following influenza A infection, vavFLIP$_R$ mice have a higher number of NK cells

Upon influenza infection, the host develops innate and adaptive immune response, which aim at clearing the infection. CD8$^+$ and NK cells contribute mainly in elimination of influenza virus infected cells during influenza infection [148,214,215,241,242]. Upon influenza virus infection, CD8$^+$ cells are activated in the lymphoid tissue and recruited to the site of infection. CD8$^+$ T cell effector functions involve the ability to produce a variety of cytotoxic molecules such as perforin and granzymes, as well as the secretion of a variety of cytokines such as TNF-α and IFN-γ [148]. Clearance of the IAV infection in perforin deficient mice was impaired [148]. This indicates that perforin-dependent cytotoxicity plays a critical role in limiting IAV infection. Intrestingly, mice deficient in both granzyme A and B could effectively control infuenza A virus infection [243]. It is likely that other cell death pathways or other granzymes compensate for the absence of granzyme A and B and contribute to the control of the IAV infection. A more recent study uncovered that CD8$^+$ T cells can also utilize TRAIL to kill virally-infected cells [244].

In the context of this thesis, no significant difference was observed in the frequency or the total number of CD8$^+$ T cells between infected vavFLIP$_R$ and WT mice. Interestingly, frequencies and total cell numbers of the NK cells were significantly higher in the mediastinal lymph node, spleen and bronchoalveolar lavage of infected

vavFLIP$_R$ compared to WT mice. NK cells mediate host immune responses to viral infections through two main effector functions, natural cytotoxicity and cytokine production [245]. During the innate immune response against influenza infection, NK cells get activated, produce IFN-γ and fulfill cytotoxic reactions. The critical role of NK cell in influenza virus infection was further illustrated by a study, which showed that NK cells can kill influenza infected cells in vitro by the engagement of viral hemagglutinin with the NKp46 receptor on NK cells [246]. Recently it has been demonstrated that in response to influenza virus infection, conventional NK cells produce IL-22, which is epithelial regenerative and inflammation protective [247]. NK cells can also directly or indirectly affect the phenotype of numerous cell types, which play a role in immunity [248–250]. It has been documented that NK cells can increase DC and CD8 T cell migration to the DLN during IAV infection. However, the frequency and cell number of DCs were also comparable between influenza infected vavFLIP$_R$ and WT mice. The results of this thesis show that NK cells are actively recruited to the lung-draining LN during IAV infection. The higher frequency of NK cells in lung-draining LN was seen even on day 10 post infection. Although there were no statistical differences in the number of CD8 or DC in vavFLIP$_R$ mice, it is possible that a higher number of NK cells affected CD8 or DC cell function, which remains to be determined. Since the higher number of NK cells was the only difference that was founded between the vavFLIP$_R$ and WT mice, it was hypothesized that NK cells might contribute to the severity of influenza infection in vavFLIP$_R$ mice.

4.3. NK cells exacerbate the pathology of influenza virus infection in mice

The exact role of NK cells in the immune response against different virus families, including the orthomyxovirus is intricate. Shortly after viral infection, NK cells are recruited to the infection area, become activated and subsequently secret cytokines [251]. A critical role of NK cells in the development of the adaptive immune response against influenza virus infection has been demonstrated [196,249,252,253]. Several studies have pointed out the importance of NK cells in the control of IAV infection, in which depletion of NK cell or defect in NK cell activity can cause morbidity and mortality or delayed in viral clearance [214,215] . However, there were some examples, which illustrated that NK cells exacerbate pathology during influenza virus infection in mice [197–199].

These discrepancy between the results raise the interesting possibility that NK cells might have beneficial or deleterious function during influenza virus infection. Host genetic background, viral strain and infection viral dose are three important factors, which can be determinative. It has been demonstrated that different host genetic backgrounds result in different resistance to IAV infection and depletion of NK cells can result in totally different outcomes

depending on the host background [199,254]. Considering the infection dose, it has been reported that depletion of NK cells ameliorates the survival rate in high, but not medium or low-dose influenza infection [197]. Similarly, in another study, it has been shown that virus dosage can affect the immunoregulatory function of NK cells [223].

In this thesis NK cell depletion in vavFLIP$_R$ and WT mice resulted in an increase in viral load at the peak of infection compared to control mice (Figure 24). However, in the absence of NK cells, the viral load differences between vavFLIP$_R$ and WT mice disappeared. All together it was concluded that the higher number of NK cell was an unfavorable factor for the host in vavFLIP$_R$ mice. Comparing the kinetic of NK cells in high and low dose of influenza infections might be helpful in better understanding the two-sided role of NK cells in immunity during IAV infections.

4.4. IAV virus can infect and replicate in primary mouse NK cells

NK cells are considered as first line of defense against influenza A infection because they are able to act before T cell and B cell activation can happen. Being part of the host's innate immunity, NK cells can rapidly exterminate virus-infected cells, which limits viral replication and transmission. Viruses and NK cells are in constant combat. In response to NK cells activity, viruses develop different types of strategies to evade them [255,256]. In the case of Influenza, the virus increases its rate of replication during the acute phase of infection. Rapid viral synthesis provides enough time for the influenza virus to establish a stable virus titer [257]. A high number of virus particles overwhelms the limited number of surrounding NK cells [205,258]. The interaction of NKp46 with influenza HA is an important control strategy for NK cells to kill influenza-infected cell. However, Influenza can also modify its main surface proteins HA and NA frequently, in order to avoid antibody neutralization[259] . Moreover, the influenza virus stabilizes

MHC-I expression in infected cells, and therefore initiate signals that inhibit NK activation [221,257,260]. Additionally, there have been reports that the influenza A virus NS1 protein can inhibit apoptosis in infected cells [190,261,262]. However, other studies have concluded that the virus enhances apoptosis [185]. In this respect, it has been demonstrated that in the presence of an inhibitor that blocks caspase 3, influenza virus propagation was impaired [185]. It was concluded that apoptosis induction, specifically activation of caspase 3, is required for efficient influenza virus propagation.

In this thesis, it has been shown that influenza virus could directly infect and replicate in primary mouse NK cells. Direct viral infection of NK cells has been demonstrated for herpes simplex virus, Epstein-Barr virus, human immunodeficiency virus and ectromelia virus [263–266]. Among innate immune cells, influenza direct infection was first reported in macrophages [211,267,268]. Infection and killing the immune cells, including NK cells comprise a potential immune-evasive action.

In this study, using foci assay and qPCR, we demonstrated that NK cells are susceptible to influenza virus. Notably, using the same MOI for infection indicated that efficiency of influenza virus infection of NK cells is lower than MDCK cells. Virus replication in infected cell can be either productive or abortive. In this study, as evidenced by positive foci assay result, replication was productive.

4.5. Decreased cytotoxicity in vavFLIP$_R$ NK cells

NK cells from influenza infected vavFLIP$_R$ mice showed a significant reduction of their cytotoxicity against YAC-1 cells. As a response to influenza virus infection, virus-infected respiratory epithelial cells release inflammatory chemokines that recruit NK cells to the site of infection [192]. NK cells combat influenza infection by destroying the infected cells, which results in the release of viral particles that can be neutralized by antibodies. Upon NK cell stimulation, the activation signal mediates a downstream cascade of kinase activation, which results in exocytosis of cytotoxic granules and subsequently kills the target cells [135,269,270]. The balance between the inhibitory and activating receptors control the cytotoxicity of NK cells [269]. Following influenza infection, recognition of the missing self signal or the increased activating signals can advocate NK cells [271]. On the other hand, influenza virus develops evasion strategies,

which can enable the virus to impair the effector functions of NK cells. As a part of immune evasion strategies, the virus can directly infect NK cells and induces cell apoptosis [272]. Direct infection of NK cells by influenza virus can interfere with the ability of NK cells to effectively recognize and kill the host cells. It has been reported that influenza infected NK cells have less cytotoxicity against $EL4^{H60}$ cells compared to the mock-infected NK cells. $EL4^{H60}$ is a cell line which expresses H60, which is a known ligand for the NK cell activating receptor NKG2D. Similarly, it has been illuminated that the killing of YAC1 cells by influenza infected NK cells was down-regulated compared to uninfected NK cells [245]. Taken together, it has been agreed that direct influenza virus infection can decrease NK cells cytotoxic potential. This can explain the low efficiency of viral clearance, despite the fact that $vavFLIP_R$ mice have a higher number of NK cells. Moreover, a higher level of proinflamatory cytokines, as well as a higher level MIP-1α and RANTES were observed in $vavFLIP_R$ mice at the peak of the influenza infection. Many types of cytokines and chemokines are produced in response to influenza virus infection [273]. The connection between a strong immune response and severe disease following influenza virus infection in humans and animal models has been shown previously [274]. In the early stage of influenza virus infection, cytokines and chemokines have a protective role for the host. However, this shifts to a pathogenic role in the later stage of infection [206,275,276]. TNF-α is known to inhibit influenza virus replication and limit the spread of the virus [277]. However, several studies have been demonstrated the pathogenic roles for TNF-α during influenza virus infection [276]. It has been shown that using anti-TNF-α antibody in mice resulted in reduction of inflammatory cells recruitment, T cell cytokine production and subsequently higher morbidity in influenza infected mice [278]. Interestingly, no difference was observed in disease severity in mice deficient in TNFR1 or in both TNFR1 and TNFR2, following H5N1 infection [279]. Notably, mice that lack both IL-1R and TNFR displayed reduced cytokine production and morbidity compared to WT mice [280]. The reason for these disparate results can be the influenza virus strain or other unknown factors.

Antiviral activity of IFN-γ has been demonstrated for many years. In the early phase of influenza infection, IFN-γ is mainly produced by macrophages and natural killer cells, while after day 5 post infection $CD4^+$ and $CD8^+$ T cells are the main source of IFN-γ. IFN-γ treatment at early stages of influenza infection has been demonstrated to protect

mice from death [205]. Similarly, use of an agonist against the proteinase-activated receptor 2 (PAR2) *in vivo*, which increased IFN-γ production, was able to reduce influenza virus titer in comparison to infected WT mice [281]. However, several studies have reported that following influenza infection, virus clearance is comparable in IFN-γ deficient and WT mice [282–284]. NK cells secrete different anti-viral cytokines and pro-inflammatory chemokines during influenza infection [140,215,245]. Secretion of IFN-γ, TNF-α, MIP-1α, MIP-1β and RANTES has been demonstrated to decrease in PR8 infected NK cells [245]. This impairment of cytokine and chemokine secretion could be due to decreased ability of the PR8-infected NK cells to produce or secrete the cytokines and chemokines. Analyzing the levels of intracellular IFN-γ production in influenza infected NK cells revealed that IAV infection impaired generation of cytokines and chemokines [248,285]. Taken together, a comparison of the results in this thesis and other studies suggested that influenza-infected NK cells have less activity. Notably, the outcome can be different depending on the infection viral dose. The underlying mechanisms remain to be investigated.

4.6. Concluding remarks

The tight regulation of apoptosis is pivotal for multicellular organisms. Impaired apoptosis may result in cancer, autoimmune diseases, and developmental disorders. Cellular-FLIP proteins inhibit apoptosis directly at the death-inducing signaling complex of death receptors and play a role in apoptosis regulation during immune responses.

Influenza virus is the prototypic member of the orthomyxoviridae family. The severity of influenza A virus infection is also closely linked to the dysfunction of apoptosis regulation.

The physiological role of the c-FLIP$_R$ isoform in influenza virus infection was investigated in this thesis. Considering the data presented herein, mice with constitutive expression of c-FLIP$_R$ in all the hematopoietic cells were more susceptible to influenza virus infection. vavFLIP$_R$ mice had a higher number of NK cells at the peak of infection compared to WT mice. However, delayed viral clearance in vavFLIP$_R$ mice compared to WT mice was observed. Further in vitro study uncovered that murine NK cells are

susceptible to influenza virus infection. Additionally, it was demonstrated that influenza virus can replicate in primary murine NK cells. NK cells in vavFLIP$_R$ mice are more resistant to apoptosis. Less apoptosis in NK cells provided a reservoir for influenza virus to replicate in higher extent. It was concluded that early apoptosis occurring during influenza infection is supporting viral clearance.

These findings suggested that the influenza virus may have developed multiple strategies including infecting NK cells to evade NK cell innate immune defenses, which mediate viral transmission and may also contribute to pathogenesis.

Taken together, this thesis gives evidence for the hypothesis that NK cells can cause pathogenicity during viral infection. These findings underline the importance of strict regulation of apoptosis in immunity against viral infections.

5. Abbreviations

APAF1	Apoptotic peptidase activating factor 1
BAD	BCL-2 associated of cell death
BAK	BCL-2-antagonist/killer-1
BAX	BCL-2-associated X protein
BCA	Bicinchoninic acid
BCL	B-cell lymphoma
BCL-2	B-cell lymphoma-2
BCL-W	B-cell lymphoma-2-like-2
BCL-XL	B-cell lymphoma-extra-large protein
BH	BCL-2 homology domain
BID	BH3-interacting domain death agonist
BIK	BCL-2-interacting killer
BIM	BCL-2 interacting mediator of cell death
CARD	Caspase recruitment domain
CD95L	CD95 ligand
cFLIP	Cellular FLIP
$cFLIP_L$	Cellular FLIP long
$cFLIP_R$	Cellular FLIP Raji
$cFLIP_S$	Cellular FLIP short
CTL	Cytotoxic T lymphocyte

CMV	Cytomegalovirus
DC	Dendritic cell
DD	Death domain
DED	Death effector domain
DLN	draining lymph node
DISC	Death-inducing signaling complex
DLN	Draining Lymph node
FACS	Fluorescence-activated cell sorting
FADD	Fas-Associated Death Domain
FLICE	FADD-like IL-1β-converting enzyme
FLIP	FLICE-inhibitory protein
HA	Hemagglutinin
IAV	Influenza A virus
IFN	Interferon
i.n.	Intranasal
i.p.	Intraperitoneal
MHC	Major histocompatibility complex
NK	Natural killer
NCR	Natural cytotoxicity receptor
NA	Neuraminidase
OMM	Outer mitochondrial membrane

PAMP	Pathogen associated molecular patterns
pDC	plasmacytoid dendritic cell
PBS	Phosphate buffered saline
PCR	Polymerase chain reaction
p.i.	Post infection
qRT-PCR	Quantitative real-time polymerase chain reaction
TNF	tumor necrosis factor
TRAIL	TNF-related apoptosis-inducing ligand
TRAILR	TNF-related apoptosis-inducing ligand receptor
UBC	Ubiquitin-conjugating enzyme E2D 2A
WT	Wild type

6. References

1. Kroemer, G. *et al.* Classification of Cell Death 2009. *Cell Death Differ.* **16,** 3–11 (2009).

2. Clarke, P. G. H. Developmental cell death: morphological diversity and multiple mechanisms. *Anat. Embryol. (Berl).* **181,** 195–213 (1990).

3. Taylor, R. C., Cullen, S. P. & Martin, S. J. Apoptosis: controlled demolition at the cellular level. *Nat Rev Mol Cell Biol* **9,** 231–241 (2008).

4. Green, D. R., Ferguson, T., Zitvogel, L. & Kroemer, G. Immunogenic and tolerogenic cell death. *Nat. Rev. Immunol.* **9,** 353–363 (2009).

5. Das, G., Shravage, B. V. & Baehrecke, E. H. Regulation and Function of Autophagy during Cell Survival and. *Cold Spring Harb. Lab. Press* **4,** 22661635 (2012).

6. Klionsky, D. J., Eskelinen, E. L. & Deretic, V. Autophagosomes, phagosomes, autolysosomes, phagolysosomes, autophagolysosomes... Wait, I'm confused. *Autophagy* **10,** 549–551 (2014).

7. Sanchez-Wandelmer, J. & Reggiori, F. Amphisomes: out of the autophagosome shadow? *EMBO J.* **32,** 3116–8 (2013).

8. Fader, C. M. & Colombo, M. I. Autophagy and multivesicular bodies: two closely related partners. *Cell Death Differ.* **16,** 70–8 (2009).

9. Yang, Z. & Klionsky, D. J. in *Adeno Associated Virus Aav Vectors In Gene Therapy* **335,** 1–32 (2009).

10. Nikoletopoulou, V., Markaki, M., Palikaras, K. & Tavernarakis, N. Crosstalk between apoptosis, necrosis and autophagy. *Biochim. Biophys. Acta* **1833,** 3448–59 (2013).

11. Fink, S. L., Cookson, B. T., Fink, S. L. & Cookson, B. T. Eukaryotic Cells MINIREVIEW Apoptosis , Pyroptosis , and Necrosis : Mechanistic Description of Dead and Dying Eukaryotic Cells. **73,** 1907–1916 (2005).

12. Bergsbaken, T., Fink, S. L. & Cookson, B. T. Pyroptosis: host cell death and inflammation. *Nat. Rev. Microbiol.* **7,** 99–109 (2009).

13. McIlwain, D. R., Berger, T. & Mak, T. W. Caspase Functions in Cell Death and Disease. *Cold Spring Harb. Perspect. Biol.* **5,** a008656–a008656 (2013).

14. Elmore, S. Apoptosis: a review of programmed cell death. *Toxicol. Pathol.* **35,** 495–516 (2007).

15. Edinger, A. L. & Thompson, C. B. Death by design: apoptosis, necrosis and autophagy. *Curr. Opin. Cell Biol.* **16,** 663–9 (2004).

16. Krammer, P. H., Arnold, R. & Lavrik, I. N. Life and death in peripheral T cells.

Nat Rev Immunol **7,** 532–542 (2007).

17. Huang, D. C. S. *et al.* Activation of Fas by FasL induces apoptosis by a mechanism that cannot be blocked by Bcl-2 or Bcl-x(L). *Proc. Natl. Acad. Sci. U. S. A.* **96,** 14871–14876 (1999).

18. Orrenius, S., Nicotera, P. & Zhivotovsky, B. Cell death mechanisms and their implications in toxicology. *Toxicol. Sci.* **119,** 3–19 (2011).

19. Eckhart, L. *et al.* Identification of novel mammalian caspases reveals an important role of gene loss in shaping the human caspase repertoire. *Mol. Biol. Evol.* **25,** 831–841 (2008).

20. Li, J. & Yuan, J. Caspases in apoptosis and beyond. *Oncogene* **27,** 6194–6206 (2008).

21. Fuentes-Prior, P. & Salvesen, G. S. The protein structures that shape caspase activity, specificity, activation and inhibition. *Biochem. J.* **384,** 201–232 (2004).

22. Nicholson, D. W. Caspase structure, proteolytic substrates, and function during apoptotic cell death. *Cell Death Differ.* **6,** 1028–1042 (1999).

23. Boatright, K. M. & Salvesen, G. S. Mechanisms of caspase activation. *Curr. Opin. Cell Biol.* **15,** 725–731 (2003).

24. Pop, C. & Salvesen, G. S. Human caspases: Activation, specificity, and regulation. *J. Biol. Chem.* **284,** 21777–21781 (2009).

25. Nuñez, G., Benedict, M. a, Hu, Y. & Inohara, N. Caspases: the proteases of the apoptotic pathway. *Oncogene* **17,** 3237–3245 (1998).

26. Young, J. D., Damiano, A., DiNome, M. A., Leong, L. G. & Cohn, Z. A. Dissociation of membrane binding and lytic activities of the lymphocyte pore-forming protein (perforin). *J. Exp. Med.* **165,** 1371–1382 (1987).

27. Law, R. H. P. *et al.* The structural basis for membrane binding and pore formation by lymphocyte perforin. *Nature* **468,** 447–451 (2010).

28. Goping, I. S. *et al.* Granzyme B-Induced Apoptosis Requires Both Direct Caspase Activation and Relief of Caspase Inhibition. *Immunity* **18,** 355–365 (2003).

29. Shi, L. *et al.* Granzyme B (GraB) Autonomously Crosses the Cell Membrane and Perforin Initiates Apoptosis and GraB Nuclear Localization. *J. Exp. Med.* **185,** 855–866 (1997).

30. Voskoboinik, I., Whisstock, J. C. & Trapani, J. a. Perforin and granzymes: function, dysfunction and human pathology. *Nat. Rev. Immunol.* **15,** 388–400 (2015).

31. Kroemer, G., Galluzzi, L. & Brenner, C. Mitochondrial membrane permeabilization in cell death. *Physiol. Rev.* **87,** 99–163 (2007).

32. Chipuk, J. E., Moldoveanu, T., Llambi, F., Parsons, M. J. & Green, D. R. The

BCL-2 family reunion. *Mol. Cell* **37,** 299–310 (2010).

33. Kim, J.-S., He, L. & Lemasters, J. J. Mitochondrial permeability transition: a common pathway to necrosis and apoptosis. *Biochem. Biophys. Res. Commun.* **304,** 463–470 (2003).

34. Baig, S. *et al.* Potential of apoptotic pathway-targeted cancer therapeutic research: Where do we stand? *Cell Death Dis.* **7,** e2058 (2016).

35. Hsu, Y. T., Wolter, K. G. & Youle, R. J. Cytosol-to-membrane redistribution of Bax and Bcl-X(L) during apoptosis. *Proc. Natl. Acad. Sci. U. S. A.* **94,** 3668–3672 (1997).

36. Echeverry, N. *et al.* Intracellular localization of the BCL-2 family member BOK and functional implications. *Cell Death Differ.* **20,** 785–799 (2013).

37. Boatright, K. M. *et al.* A unified model for apical caspase activation. *Mol. Cell* **11,** 529–541 (2003).

38. Youle, R. J. & Strasser, A. The BCL-2 protein family: opposing activities that mediate cell death. *Nat. Rev. Mol. Cell Biol.* **9,** 47–59 (2008).

39. Nechushtan, A., Smith, C. L., Lamensdorf, I., Yoon, S. H. & Youle, R. J. Bax and Bak coalesce into novel mitochondria-associated clusters during apoptosis. *J. Cell Biol.* **153,** 1265–1276 (2001).

40. Wei, M. C. *et al.* Proapoptotic BAX and BAK: a requisite gateway to mitochondrial dysfunction and death. *Science* **292,** 727–30 (2001).

41. Vaux, D. L. Apoptogenic factors released from mitochondria. *Biochim. Biophys. Acta - Mol. Cell Res.* **1813,** 546–550 (2011).

42. Luna-Vargas, M. P. A. & Chipuk, J. E. The deadly landscape of pro-apoptotic BCL-2 proteins in the outer mitochondrial membrane. *FEBS J.* **283,** 2676–2689 (2016).

43. Schulze-Osthoff, K., Ferrari, D., Los, M., Wesselborg, S. & Peter, M. E. Apoptosis signaling by death receptors. *Eur. J. Biochem.* **254,** 439–459 (1998).

44. Guicciardi, M. E. & Gores, G. J. Life and death by death receptors. *FASEB J.* **23,** 1625–1637 (2009).

45. Gaur, U. & Aggarwal, B. B. Regulation of proliferation, survival and apoptosis by members of the TNF superfamily. *Biochem. Pharmacol.* **66,** 1403–1408 (2003).

46. Bremer, E. Targeting of the tumor necrosis factor receptor superfamily for cancer immunotherapy. *ISRN Oncol.* **2013,** 371854 (2013).

47. Igney, F. H. & Krammer, P. H. Death and anti-death: tumour resistance to apoptosis. *Nat Rev Cancer* **2,** 277–288 (2002).

48. Wilson, N. S., Dixit, V. & Ashkenazi, A. Death receptor signal transducers: nodes of coordination in immune signaling networks. *Nat. Immunol.* **10,** 348–355

(2009).

49. Wang, S. & El-Deiry, W. S. TRAIL and apoptosis induction by TNF-family death receptors. *Oncogene* **22,** 8628–33 (2003).

50. Donepudi, M., Mac Sweeney, A., Briand, C. & Grutter, M. G. Insights into the regulatory mechanism for caspase-8 activation. *Mol. Cell* **11,** 543–549 (2003).

51. Aggarwal, B. B. Signalling pathways of the TNF superfamily: a double-edged sword. *Nat. Rev. Immunol.* **3,** 745–756 (2003).

52. Locksley, R. M., Killeen, N. & Lenardo, M. J. The TNF and TNF receptor superfamilies: integrating mammalian biology. *Cell* **104,** 487–501 (2001).

53. Fischer, R., Kontermann, R. & Maier, O. Targeting sTNF/TNFR1 Signaling as a New Therapeutic Strategy. *Antibodies* **4,** 48–70 (2015).

54. Grell, M. *et al.* The transmembrane form of tumor necrosis factor is the prime activating ligand of the 80 kDa tumor necrosis factor receptor. *Cell* **83,** 793–802 (1995).

55. Apostolaki, M., Armaka, M., Victoratos, P. & Kollias, G. Cellular mechanisms of TNF function in models of inflammation and autoimmunity. *Curr. Dir. Autoimmun.* **11,** 1–26 (2010).

56. Scaffidi, C. The Role of c-FLIP in Modulation of CD95-induced Apoptosis. *J. Biol. Chem.* **274,** 1541–1548 (1999).

57. Goltsev, Y. V. *et al.* CASH, a novel caspase homologue with death effector domains. *J. Biol. Chem.* **272,** 19641–19644 (1997).

58. Inohara, N., Koseki, T., Hu, Y., Chen, S. & Núñez, G. CLARP, a death effector domain-containing protein interacts with caspase-8 and regulates apoptosis. *Proc. Natl. Acad. Sci. U. S. A.* **94,** 10717–22 (1997).

59. Golks, a *et al.* The role of CAP3 in CD95 signaling: new insights into the mechanism of procaspase-8 activation. *Cell Death Differ.* **13,** 489–98 (2006).

60. Wallach, D. *et al.* Tumor necrosis factor receptor and Fas signaling mechanisms. *Annu. Rev. Immunol.* **17,** 331–367 (1999).

61. Ueffing, N. *et al.* Mutational analyses of c-FLIPR, the only murine short FLIP isoform, reveal requirements for DISC recruitment. *Cell Death Differ.* **15,** 773–82 (2008).

62. Micheau, O. Cellular FLICE-inhibitory protein: an attractive therapeutic target? *Expert Opin. Ther. Targets* **7,** 559–573 (2003).

63. Safa, A. R. & Pollok, K. E. Targeting the Anti-Apoptotic Protein c-FLIP for Cancer Therapy. *Cancers (Basel).* **3,** 1639–1671 (2011).

64. Ozturk, S., Schleich, K. & Lavrik, I. N. Cellular FLICE-like inhibitory proteins (c-FLIPs): fine-tuners of life and death decisions. *Exp. Cell Res.* **318,** 1324–1331 (2012).

65. Irmler, M. *et al.* Inhibition of death receptor signals by cellular FLIP. *Nature* **388,** 190–195 (1997).

66. Budd, R. C., Yeh, W.-C. & Tschopp, J. cFLIP regulation of lymphocyte activation and development. *Nat. Rev. Immunol.* **6,** 196–204 (2006).

67. Djerbi, M., Darreh-Shori, T., Zhivotovsky, B. & Grandien, A. Characterization of the human FLICE-inhibitory protein locus and comparison of the anti-apoptotic activity of four different flip isoforms. *Scand. J. Immunol.* **54,** 180–189 (2001).

68. Krueger, A., Schmitz, I., Baumann, S., Krammer, P. H. & Kirchhoff, S. Cellular FLICE-inhibitory protein splice variants inhibit different steps of caspase-8 activation at the CD95 death-inducing signaling complex. *J. Biol. Chem.* **276,** 20633–20640 (2001).

69. Scaffidi, G. *et al.* Differential modulation of apoptosis sensitivity in CD95 type I and type II cells. *J. Biol. Chem.* **274,** 22532–22538 (1999).

70. Chang, D. W. *et al.* c-FLIP(L) is a dual function regulator for caspase-8 activation and CD95-mediated apoptosis. *EMBO J.* **21,** 3704–3714 (2002).

71. Schmitz, I. *et al.* Resistance of short term activated T cells to CD95-mediated apoptosis correlates with de novo protein synthesis of c-FLIPshort. *J. Immunol.* **172,** 2194–200 (2004).

72. Schleich, K. *et al.* Molecular architecture of the DED chains at the DISC: regulation of procaspase-8 activation by short DED proteins c-FLIP and procaspase-8 prodomain. *Cell Death Differ.* 1–14 (2015). doi:10.1038/cdd.2015.137

73. Matsuda, I. *et al.* The C-terminal domain of the long form of cellular FLICE-inhibitory protein (c-FLIPL) inhibits the interaction of the caspase 8 prodomain with the receptor-interacting protein 1 (RIP1) death domain and regulates caspase 8-dependent nuclear factor κB (NF-κ. *J. Biol. Chem.* **289,** 3876–87 (2014).

74. Hughes, M. A. *et al.* Co-operative and Hierarchical Binding of c-FLIP and Caspase-8: A Unified Model Defines How c-FLIP Isoforms Differentially Control Cell Fate. *Mol. Cell* **61,** 834–849 (2016).

75. Samji, T. Influenza A: Understanding the viral life cycle. *Yale J. Biol. Med.* **82,** 153–159 (2009).

76. Tumpey, T. M. *et al.* Pathogenicity of influenza viruses with genes from the 1918 pandemic virus: functional roles of alveolar macrophages and neutrophils in limiting virus replication and mortality in mice. *J. Virol.* **79,** 14933–14944 (2005).

77. Neuzil, K. M. *et al.* Burden of interpandemic influenza in children younger than 5 years: a 25-year prospective study. *J Infect Dis* **185,** 147–152 (2002).

78. LaForce, F. M., Nichol, K. L. & Cox, N. J. Influenza: virology, epidemiology, disease, and prevention. *Am. J. Prev. Med.* **10 Suppl,** 31–44 (1994).

79. Taubenberger, J. K. & Morens, D. M. The pathology of influenza virus infections. *Annu. Rev. Pathol.* **3,** 499–522 (2008).

80. Lee, H. Y. *et al.* Simulation and Prediction of the Adaptive Immune Response to Influenza A Virus Infection. *J. Virol.* **83,** 7151–7165 (2009).

81. Bosch, B. J. *et al.* Recombinant soluble, multimeric HA and NA exhibit distinctive types of protection against pandemic swine-origin 2009 A(H1N1) influenza virus infection in ferrets. *J. Virol.* **84,** 10366–74 (2010).

82. Webster, R. G. & Govorkova, E. A. Continuing challenges in influenza. *Ann. N. Y. Acad. Sci.* **1323,** 115–139 (2014).

83. Chen, W. *et al.* A novel influenza A virus mitochondrial protein that induces cell death. *Nat Med* **7,** 1306–1312 (2001).

84. Laver, W. G. & Valentine, R. C. Morphology of the isolated hemagglutinin and neuraminidase subunits of influenza virus. *Virology* **38,** 105–119 (1969).

85. Ping, J. *et al.* Development of high-yield influenza A virus vaccine viruses. *Nat. Commun.* **6,** 8148 (2015).

86. Lohmeyer, J., Talens, L. T. & Klenk, H. D. Biosynthesis of the influenza virus envelope in abortive infection. *J. Gen. Virol.* **42,** 73–88 (1979).

87. Stanley, P., Gandhi, S. S. & White, D. O. The polypeptides of influenza virus. VII. Synthesis of the hemagglutinin. *Virology* **53,** 92–106 (1973).

88. Gamblin, S. J. & Skehel, J. J. Influenza hemagglutinin and neuraminidase membrane glycoproteins. *Journal of Biological Chemistry* **285,** 28403–28409 (2010).

89. Shtyrya, Y. A., Mochalova, L. V & Bovin, N. V. Influenza Virus Neuraminidase : Structure and Function. 26–32 (2009).

90. Maines, T. R. *et al.* Pathogenesis of emerging avian influenza viruses in mammals and the host innate immune response. *Immunol. Rev.* **225,** 68–84 (2008).

91. Taubenberger, J. K. & Kash, J. C. Influenza Virus Evolution, Host Adaptation, and Pandemic Formation. *Cell Host Microbe* **7,** 440–451 (2010).

92. Lakadamyali, M., Rust, M. J. & Zhuang, X. Endocytosis of influenza viruses. *Microbes Infect.* **6,** 929–936 (2004).

93. Sieczkarski, B. S. & Whittaker, R. G. Characterization of the host cell entry of filamentous influenza virus. *Arch. Virol.* **150,** 1783–1796 (2005).

94. Arzt, S. *et al.* Combined results from solution studies on intact influenza virus M1 protein and from a new crystal form of its N-terminal domain show that M1 is an elongated monomer. *Virology* **279,** 439–446 (2001).

95. Boulo, S., Akarsu, H., Ruigrok, R. W. H. & Baudin, F. Nuclear traffic of influenza virus proteins and ribonucleoprotein complexes. *Virus Res.* **124,** 12–21

(2007).

96. Nayak, D. P., Hui, E. K.-W. & Barman, S. Assembly and budding of influenza virus. *Virus Res.* **106,** 147–165 (2004).

97. Pulendran, B. & Maddur, M. S. Innate immune sensing and response to influenza. *Curr. Top. Microbiol. Immunol.* **386,** 23–71 (2015).

98. Tripathi, S., White, M. R. & Hartshorn, K. L. The amazing innate immune response to influenza A virus infection. *Innate Immun.* **21,** 73–98 (2015).

99. McGill, J., Heusel, J. W. & Legge, K. L. Innate immune control and regulation of influenza virus infections. *J. Leukoc. Biol.* **86,** 803–12 (2009).

100. van de Sandt, C. E., Kreijtz, J. H. C. M. & Rimmelzwaan, G. F. Evasion of influenza A viruses from innate and adaptive immune responses. *Viruses* **4,** 1438–76 (2012).

101. Holt, P. G., Strickland, D. H., Wikstrom, M. E. & Jahnsen, F. L. Regulation of immunological homeostasis in the respiratory tract. *Nat Rev Immunol* **8,** 142–152 (2008).

102. Ganesan, S., Comstock, A. T. & Sajjan, U. S. Barrier function of airway tract epithelium. *Tissue Barriers* **1,** e24997 (2013).

103. Iwasaki, A. & Pillai, P. S. Innate immunity to influenza virus infection. *Nat. Rev. Immunol.* **14,** 315–28 (2014).

104. Tang, D., Kang, R., Coyne, C. B., Zeh, H. J. & Lotze, M. T. PAMPs and DAMPs: Signal 0s that Spur Autophagy and Immunity. *Immunol. Rev.* **249,** 158–175 (2012).

105. Sanders, C. J., Doherty, P. C. & Thomas, P. G. Respiratory epithelial cells in innate immunity to influenza virus infection. *Cell Tissue Res.* **343,** 13–21 (2011).

106. Blasius, A. L. & Beutler, B. Intracellular Toll-like Receptors. *Immunity* **32,** 305–315 (2010).

107. Pang, I. K. & Iwasaki, A. Inflammasomes as mediators of immunity against influenza virus. *Trends Immunol.* **32,** 34–41 (2011).

108. Takeuchi, O. & Akira, S. Innate immunity to virus infection. *Immunol. Rev.* **227,** 75–86 (2009).

109. Kawai, T. & Akira, S. Toll-like Receptors and Their Crosstalk with Other Innate Receptors in Infection and Immunity. *Immunity* **34,** 637–650 (2011).

110. Lund, J. M. *et al.* Recognition of single-stranded RNA viruses by Toll-like receptor 7. *Proc Natl Acad Sci U S A* **101,** 5598–5603 (2004).

111. Le Goffic, R. *et al.* Detrimental contribution of the Toll-like receptor (TLR)3 to influenza A virus-induced acute pneumonia. *PLoS Pathog.* **2,** e53 (2006).

112. Guillot, L. *et al.* Involvement of Toll-like receptor 3 in the immune response of

lung epithelial cells to double-stranded RNA and influenza A virus. *J. Biol. Chem.* **280,** 5571–5580 (2005).

113. Imai, Y. *et al.* Identification of Oxidative Stress and Toll-like Receptor 4 Signaling as a Key Pathway of Acute Lung Injury. *Cell* **133,** 235–249 (2008).

114. Hornung, V. *et al.* 5'-Triphosphate RNA Is the Ligand for RIG-I. *Science (80-.).* **314,** 994–997 (2006).

115. Rehwinkel, J. *et al.* RIG-I Detects Viral Genomic RNA during Negative-Strand RNA Virus Infection. *Cell* **140,** 397–408 (2010).

116. Kanneganti, T.-D. Central roles of NLRs and inflammasomes in viral infection. *Nat. Rev. Immunol.* **10,** 688–698 (2010).

117. Guarda, G. *et al.* Differential expression of NLRP3 among hematopoietic cells. *J. Immunol.* **186,** 2529–2534 (2011).

118. Pothlichet, J. *et al.* Type I IFN Triggers RIG-I/TLR3/NLRP3-dependent Inflammasome Activation in Influenza A Virus Infected Cells. *PLoS Pathog.* **9,** (2013).

119. Allen, I. C. *et al.* The NLRP3 Inflammasome Mediates *In Vivo* Innate Immunity to Influenza A Virus through Recognition of Viral RNA. *Immunity* **30,** 556–565 (2009).

120. Ichinohe, T., Pang, I. K. & Iwasaki, A. Influenza virus activates inflammasomes via its intracellular M2 ion channel. *Nat Immunol* **11,** 404–410 (2010).

121. McAuley, J. L. *et al.* Activation of the NLRP3 Inflammasome by IAV Virulence Protein PB1-F2 Contributes to Severe Pathophysiology and Disease. *PLoS Pathog.* **9,** (2013).

122. Leemans, J. C., Cassel, S. L. & Sutterwala, F. S. Sensing damage by the NLRP3 inflammasome. *Immunol. Rev.* **243,** 152–162 (2011).

123. Owen, D. M. & Gale, M. Fighting the Flu with Inflammasome Signaling. *Immunity* **30,** 476–478 (2009).

124. Fujisawa, H. Inhibitory role of neutrophils on influenza virus multiplication in the lungs of mice. *Microbiol. Immunol.* **45,** 679–688 (2001).

125. Hashimoto, Y., Moki, T., Takizawa, T., Shiratsuchi, A. & Nakanishi, Y. Evidence for phagocytosis of influenza virus-infected, apoptotic cells by neutrophils and macrophages in mice. *J. Immunol.* **178,** 2448–2457 (2007).

126. Mori, I. *In vivo* induction of apoptosis by influenza virus. 2869–2873 (1995).

127. Hufford, M. M. *et al.* Influenza-Infected Neutrophils within the Infected Lungs Act as Antigen Presenting Cells for Anti-Viral CD8+ T Cells. *PLoS One* **7,** (2012).

128. Holt, P. G. Inhibitory activity of unstimulated alveolar macrophages on T-lymphocyte blastogenic response. *Am. Rev. Respir. Dis.* **118,** 791–793 (1978).

129. Holt, P. G. *et al.* Downregulation of the antigen presenting cell function(s) of pulmonary dendritic cells *in vivo* by resident alveolar macrophages. *J. Exp. Med.* **177,** 397–407 (1993).

130. Strickland, D. H., Thepen, T., Kees, U. R., Kraal, G. & Holt, P. G. Regulation of T-cell function in lung tissue by pulmonary alveolar macrophages. *Immunology* **80,** 266–72 (1993).

131. Kay, A. W. *et al.* Enhanced natural killer-cell and T-cell responses to influenza A virus during pregnancy. *Proc. Natl. Acad. Sci. U. S. A.* **111,** 14506–11 (2014).

132. Cerwenka, A. & Lanier, L. L. Natural killer cells, viruses and cancer. *Nat. Rev. Immunol.* **1,** 41–49 (2001).

133. Vivier, E., Tomasello, E., Baratin, M., Walzer, T. & Ugolini, S. Functions of natural killer cells. *Nat. Immunol.* **9,** 503–510 (2008).

134. Crouse, J., Xu, H. C., Lang, P. A. & Oxenius, A. NK cells regulating T cell responses: mechanisms and outcome. *Trends Immunol.* **36,** 49–58 (2016).

135. Lanier, L. L. Up on the tightrope: natural killer cell activation and inhibition. *Nat. Immunol.* **9,** 495–502 (2008).

136. Natarajan, K., Dimasi, N., Wang, J., Mariuzza, R. A. & Margulies, D. H. Structure and function of natural killer cell receptors: multiple molecular solutions to self, nonself discrimination. *Annu. Rev. Immunol.* **20,** 853–885 (2002).

137. Moretta, L. *et al.* Human natural killer cells: Molecular mechanisms controlling NK cell activation and tumor cell lysis. *Immunol. Lett.* **100,** 7–13 (2005).

138. Belz, G. T. *et al.* Distinct migrating and nonmigrating dendritic cell populations are involved in MHC class I-restricted antigen presentation after lung infection with virus. *Proc. Natl. Acad. Sci. U. S. A.* **101,** 8670–5 (2004).

139. Arnon, T. I. *et al.* Recognition of viral hemagglutinins by NKp44 but not by NKp30. *Eur. J. Immunol.* **31,** 2680–2689 (2001).

140. Biron, C. A., Nguyen, K. B., Pien, G. C., Cousens, L. P. & Salazar-Mather, T. P. Natural killer cells in antiviral defense: function and regulation by innate cytokines. *Annu. Rev. Immunol.* **17,** 189–220 (1999).

141. Legge, K. L. & Braciale, T. J. Accelerated migration of respiratory dendritic cells to the regional lymph nodes is limited to the early phase of pulmonary infection. *Immunity* **18,** 265–277 (2003).

142. Kim, T. S. & Braciale, T. J. Respiratory dendritic cell subsets differ in their capacity to support the induction of virus-specific cytotoxic CD8+ T cell responses. *PLoS One* **4,** (2009).

143. Broeke, T., Wubbolts, R. & Stoorvogel, W. MHC Class II Antigen Presentation by Dendritic Cells Regulated through Endosomal Sorting. *Cold Spring Harb. Perspect. Biol.* 1–21 (2013). doi:10.1101/cshperspect.a016873

144. Joffre, O. P., Segura, E., Savina, A. & Amigorena, S. Cross-presentation by dendritic cells. *Nat Rev Immunol* **12,** 557–569 (2012).

145. Bender, A. *et al.* The distinctive features of influenza virus infection of dendritic cells. *Immunobiology* **198,** 552–567 (1998).

146. Banchereau, J. & Steinman, R. M. Dendritic cells and the control of immunity. *Nature* **392,** 245–252 (1998).

147. Doherty, P. C. in *Transgenic Models of Human Viral and Immunological Disease* (eds. Chisari, F. V & Oldstone, M. B. A.) 1–14 (Springer Berlin Heidelberg, 1996). doi:10.1007/978-3-642-85208-4_1

148. Topham, D. J., Tripp, R. A. & Doherty, P. C. CD8+ T cells clear influenza virus by perforin or Fas-dependent processes. *J. Immunol.* **159,** 5197–5200 (1997).

149. Lawrence, C. W., Ream, R. M. & Braciale, T. J. Frequency, specificity, and sites of expansion of CD8+ T cells during primary pulmonary influenza virus infection. *J. Immunol.* **174,** 5332–5340 (2005).

150. Legge, K. L. & Braciale, T. J. Lymph node dendritic cells control CD8+ T cell responses through regulated FasL expression. *Immunity* **23,** 649–659 (2005).

151. Graham, M. B. & Braciale, T. J. Resistance to and recovery from lethal influenza virus infection in B lymphocyte-deficient mice. *J. Exp. Med.* **186,** 2063–8 (1997).

152. Epstein, S. L., Lo, C. Y., Misplon, J. A. & Bennink, J. R. Mechanism of protective immunity against influenza virus infection in mice without antibodies. *J. Immunol.* **160,** 322–7 (1998).

153. Tripp, R. A., Sarawar, S. R. & Doherty, P. C. Characteristics of the influenza virus-specific CD8+ T cell response in mice homozygous for disruption of the H-2lAb gene. *J. Immunol.* **155,** 2955–2959 (1995).

154. Alam, S., Knowlden, Z. A. G., Sangster, M. Y. & Sant, A. J. CD4 T cell help is limiting and selective during the primary B cell response to influenza virus infection. *J. Virol.* **88,** 314–24 (2014).

155. Kaech, S. M. & Ahmed, R. Immunology. CD8 T cells remember with a little help. *Science* **300,** 263–265 (2003).

156. Tanchot, C. & Rocha, B. CD8 and B cell memory: same strategy, same signals. *Nature immunology* **4,** 431–432 (2003).

157. Román, E. *et al.* CD4 effector T cell subsets in the response to influenza: heterogeneity, migration, and function. *J. Exp. Med.* **196,** 957–968 (2002).

158. Mckinstry, K. K. *et al.* Memory CD4 + T cells protect against influenza through multiple synergizing mechanisms. **122,** 2847–2856 (2012).

159. Waffarn, E. E. & Baumgarth, N. Protective B cell responses to flu--no fluke! *J. Immunol.* **186,** 3823–9 (2011).

160. Wilson, I. A. & Cox, N. J. Structural basis of immune recognition of influenza

virus hemagglutinin. *Annu. Rev. Immunol.* **8,** 737–771 (1990).

161. Johansson, B. E., Bucher, D. J. & Kilbourne, E. D. Purified influenza virus hemagglutinin and neuraminidase are equivalent in stimulation of antibody response but induce contrasting types of immunity to infection. *J. Virol.* **63,** 1239–1246 (1989).

162. Hyland, L., Sangster, M., Sealy, R. & Coleclough, C. Respiratory virus infection of mice provokes a permanent humoral immune response. *J. Virol.* **68,** 6083–6 (1994).

163. Yu, X. *et al.* Neutralizing antibodies derived from the B cells of 1918 influenza pandemic survivors. *Nature* **455,** 532–536 (2008).

164. Zuercher, A. W., Coffin, S. E., Thurnheer, M. C., Fundova, P. & Cebra, J. J. Nasal-Associated Lymphoid Tissue Is a Mucosal Inductive Site for Virus-Specific Humoral and Cellular Immune Responses. *J. Immunol.* **168,** 1796–1803 (2002).

165. Rangel-Moreno, J. *et al.* Role of CXC Chemokine Ligand 13, CC Chemokine Ligand (CCL) 19, and CCL21 in the Organization and Function of Nasal-Associated Lymphoid Tissue. *J. Immunol.* **175,** 4904–4913 (2005).

166. Manicassamy, B. *et al.* Analysis of *in vivo* dynamics of influenza virus infection in mice using a GFP reporter virus. *Proc. Natl. Acad. Sci. U. S. A.* **107,** 11531–6 (2010).

167. Moyron-Quiroz, J. E. *et al.* Role of inducible bronchus associated lymphoid tissue (iBALT) in respiratory immunity. *Nat. Med.* **10,** 927–934 (2004).

168. Gerhard, W., Mozdzanowska, K., Furchner, M., Washko, G. & Maiese, K. Role of the B-cell response in recovery of mice from primary influenza virus infection. *Immunol. Rev.* **159,** 95–103 (1997).

169. Hinshaw, V. S., Olsen, C. W., Dybdahl-Sissoko, N. & Evans, D. Apoptosis: a mechanism of cell killing by influenza A and B viruses. *J. Virol.* **68,** 3667–73 (1994).

170. Schmitz, I., Kirchhoff, S. & Krammer, P. H. Regulation of death receptor-mediated apoptosis pathways. *Int. J. Biochem. Cell Biol.* **32,** 1123–1136 (2000).

171. Lavrik, I. *et al.* The active caspase-8 heterotetramer is formed at the CD95 DISC. *Cell Death Differ.* **10,** 144–145 (2003).

172. Ueffing, N. *et al.* A single nucleotide polymorphism determines protein isoform production of the human c-FLIP protein. *Blood* **114,** 572–579 (2009).

173. Telieps, T. *et al.* Cellular-FLIP, Raji isoform (c-FLIP R) modulates cell death induction upon T-cell activation and infection. *Eur. J. Immunol.* **43,** 1499–510 (2013).

174. Ogilvy, S. *et al.* Promoter elements of vav drive transgene expression *in vivo* throughout the hematopoietic compartment. *Blood* **94,** 1855–63 (1999).

175. Blazejewska, P. *et al.* Pathogenicity of different PR8 influenza A virus variants in mice is determined by both viral and host factors. *Virology* **412,** 36–45 (2011).

176. Zangemeister-Wittke, U. & Simon, H. U. Apoptosis--regulation and clinical implications. *Cell Death Differ.* **8,** 537–44 (2001).

177. He, M. X. & He, Y. W. A role for c-FLIPL in the regulation of apoptosis, autophagy, and necroptosis in T lymphocytes. *Cell Death and Differentiation* **20,** 188–197 (2013).

178. R Safa, A. Roles of c-FLIP in Apoptosis, Necroptosis, and Autophagy. *J. Carcinog. Mutagen.* (2013). doi:10.4172/2157-2518.S6-003

179. Majkut, J. *et al.* Differential affinity of FLIP and procaspase 8 for FADD's DED binding surfaces regulates DISC assembly. *Nat. Commun.* **5,** 3350 (2014).

180. Ueffing, N., Schuster, M., Keil, E., Schulze-Osthoff, K. & Schmitz, I. Up-regulation of c-FLIPshort by NFAT contributes to apoptosis resistance of short-term activated T cells. *Blood* **112,** 690–698 (2008).

181. Zang, F., Wei, X., Leng, X., Yu, M. & Sun, B. C-FLIP(L) contributes to TRAIL resistance in HER2-positive breast cancer. *Biochem. Biophys. Res. Commun.* **450,** 267–73 (2014).

182. Oztürk, S., Schleich, K. & Lavrik, I. N. Cellular FLICE-like inhibitory proteins (c-FLIPs): fine-tuners of life and death decisions. *Exp. Cell Res.* **318,** 1324–31 (2012).

183. Ewald, F. *et al.* The role of c-FLIP splice variants in urothelial tumours. *Cell Death Dis.* **2,** e245 (2011).

184. Wurzer, W. J. *et al.* NF-kappaB-dependent induction of tumor necrosis factor-related apoptosis-inducing ligand (TRAIL) and Fas/FasL is crucial for efficient influenza virus propagation. *J. Biol. Chem.* **279,** 30931–30937 (2004).

185. McLaughlin, B. *et al.* Caspase 3 activation is essential for efficient influenza virus propagation. *Proc Natl Acad Sci U S A* **100,** 715–720 (2003).

186. Herold, S., Ludwig, S., Pleschka, S. & Wolff, T. Apoptosis signaling in influenza virus propagation, innate host defense, and lung injury. *J. Leukoc. Biol.* **92,** 75–82 (2012).

187. Brydon, E. W. a, Morris, S. J. & Sweet, C. Role of apoptosis and cytokines in influenza virus morbidity. *FEMS Microbiol. Rev.* **29,** 837–50 (2005).

188. Tripp, R. A., Hou, S., McMickle, A., Houston, J. & Doherty, P. C. Recruitment and proliferation of CD8+ T cells in respiratory virus infections. *J. Immunol.* **154,** 6013–6021 (1995).

189. Tamura, S., Tanimoto, T. & Kurata, T. Mechanisms of broad cross-protection provided by influenza virus infection and their application to vaccines. *Jpn. J. Infect. Dis.* **58,** 195–207 (2005).

190. Zhirnov, O. P., Konakova, T. E., Wolff, T. & Klenk, H.-D. NS1 protein of influenza A virus down-regulates apoptosis. *J. Virol.* **76,** 1617–1625 (2002).

191. Zamarin, D., Ortigoza, M. B. & Palese, P. Influenza A virus PB1-F2 protein contributes to viral pathogenesis in mice. *J. Virol.* **80,** 7976–7983 (2006).

192. Gregoire, C. *et al.* The trafficking of natural killer cells. *Immunol Rev* **220,** 169–182 (2007).

193. Crome, S. Q., Lang, P. A., Lang, K. S. & Ohashi, P. S. Natural killer cells regulate diverse T cell responses. *Trends Immunol.* **34,** 342–349 (2013).

194. Stein-Streilein, J., Bennett, M., Mann, D. & Kumar, V. Natural killer cells in mouse lung: surface phenotype, target preference, and response to local influenza virus infection. *J. Immunol.* **131,** 2699–2704 (1983).

195. Tyznik, A. J., Verma, S., Wang, Q., Kronenberg, M. & Benedict, C. A. Distinct Requirements for Activation of NKT and NK Cells during Viral Infection. *J. Immunol.* **192,** 3676–3685 (2014).

196. Hwang, I. *et al.* Activation Mechanisms of Natural Killer Cells during Influenza Virus Infection. *PLoS One* **7,** (2012).

197. Zhou, G., Juang, S. W. W. & Kane, K. P. NK cells exacerbate the pathology of influenza virus infection in mice. *Eur. J. Immunol.* **43,** 929–38 (2013).

198. Duan, X. *et al.* NK-cells are involved in thymic atrophy induced by influenza A virus infection. *J. Gen. Virol.* **96,** 3223–3235 (2015).

199. Zhou, K. *et al.* Swift and Strong NK Cell Responses Protect 129 Mice against High-Dose Influenza Virus Infection. *J. Immunol.* **196,** 1842–1854 (2016).

200. Culley, F. J. Natural killer cells in infection and inflammation of the lung. *Immunology* **128,** 151–163 (2009).

201. Hennet, T., Ziltener, H. J., Frei, K. & Peterhans, E. A kinetic study of immune mediators in the lungs of mice infected with influenza A virus. *J. Immunol.* **149,** 932–939 (1992).

202. Carswell, E. A. *et al.* An endotoxin-induced serum factor that causes necrosis of tumors. *Proc. Natl. Acad. Sci. U. S. A.* **72,** 3666–70 (1975).

203. Kalliolias, G. D. & Ivashkiv, L. B. TNF biology, pathogenic mechanisms and emerging therapeutic strategies. *Nat. Rev. Rheumatol.* **12,** 49–62 (2015).

204. Seo, S. H. & Webster, R. G. Tumor necrosis factor alpha exerts powerful anti-influenza virus effects in lung epithelial cells. *J. Virol.* **76,** 1071–6 (2002).

205. Weiss, I. D. *et al.* IFN-γ Treatment at Early Stages of Influenza Virus Infection Protects Mice from Death in a NK Cell-Dependent Manner. *J. Interferon Cytokine Res.* **30,** 439–449 (2010).

206. Dinarello, C. a. Historical Review of Cytokines. *Eur. J. Immunol.* **37,** S34–S45 (2007).

207. de Jong, M. D. *et al.* Fatal outcome of human influenza A (H5N1) is associated with high viral load and hypercytokinemia. *Nat. Med.* **12,** 1203–1207 (2006).

208. de Jong, M. D. & Hien, T. T. Avian influenza A (H5N1). *J. Clin. Virol.* **35,** 2–13 (2006).

209. Kobasa, D. *et al.* Aberrant innate immune response in lethal infection of macaques with the 1918 influenza virus. *Nature* **445,** 319–323 (2007).

210. Peiris, J. S. M. *et al.* Re-emergence of fatal human influenza A subtype H5N1 disease. *Lancet (London, England)* **363,** 617–619 (2004).

211. Cheung, C. Y. *et al.* Induction of proinflammatory cytokines in human macrophages by influenza A (H5N1) viruses: a mechanism for the unusual severity of human disease? *Lancet (London, England)* **360,** 1831–1837 (2002).

212. Zimmer, J., Andrès, E. & Hentges, F. NK cell subsets and CD107a mobilization assay. *Leuk. Off. J. Leuk. Soc. Am. Leuk. Res. Fund, U.K* **19,** 1849–1851; author reply 1857 (2005).

213. Dons'koi, B. V, Chernyshov, V. P. & Osypchuk, D. V. Measurement of NK activity in whole blood by the CD69 up-regulation after co-incubation with K562, comparison with NK cytotoxicity assays and CD107a degranulation assay. *J. Immunol. Methods* **372,** 187–95 (2011).

214. Stein-Streilein, J. & Guffee, J. *In vivo* treatment of mice and hamsters with antibodies to asialo GM1 increases morbidity and mortality to pulmonary influenza infection. *J. Immunol.* **136,** 1435–1441 (1986).

215. Abdul-Careem, M. F. *et al.* Critical role of natural killer cells in lung immunopathology during influenza infection in mice. *J. Infect. Dis.* **206,** 167–177 (2012).

216. Kasai, M. *et al. In vivo* effect of anti-asialo GM1 antibody on natural killer activity. *Nature* **291,** 334–335 (1981).

217. Habu, S. *et al. In vivo* effects of anti-asialo GM1. I. Reduction of NK activity and enhancement of transplanted tumor growth in nude mice. *J. Immunol.* **127,** 34–38 (1981).

218. Srivastava, B. *et al.* Host genetic background strongly influences the response to influenza a virus infections. *PLoS One* **4,** (2009).

219. Arnon, T. & Achdout, H. The mechanisms controlling the recognition of tumor- and virus-infected cells by NKp46. *Blood* **103,** 664–673 (2004).

220. Draghi, M. *et al.* NKp46 and NKG2D Recognition of Infected Dendritic Cells Is Necessary for NK Cell Activation in the Human Response to Influenza Infection. *J. Immunol.* **178,** 2688–2698 (2007).

221. Achdout, H., Manaster, I. & Mandelboim, O. Influenza virus infection augments NK cell inhibition through reorganization of major histocompatibility complex class I proteins. *J Virol* **82,** 8030–8037 (2008).

222. Mock, D. J. *et al.* Macrophages Are Required for Influenza Virus Infection of Human Lymphocytes. **79,** 620–624 (1987).

223. Waggoner, S. N., Cornberg, M., Selin, L. K. & Welsh, R. M. Natural killer cells act as rheostats modulating antiviral T cells. *Nature* **481,** 394–398 (2012).

224. Fuchs, Y. & Steller, H. Live to die another way: modes of programmed cell death and the signals emanating from dying cells. *Nat. Rev. Mol. Cell Biol.* **16,** 329–344 (2015).

225. Peter, M. E. *et al.* The role of CD95 and CD95 ligand in cancer. *Cell Death Differ.* **22,** 549–59 (2015).

226. Alenzi, F. Q. *et al.* Role of Apoptosis in Microbial Infection. *Open J. Apoptosis* **3,** 32–38 (2014).

227. Lamkanfi, M. & Dixit, V. M. Manipulation of host cell death pathways during microbial infections. *Cell Host Microbe* **8,** 44–54 (2010).

228. Tripathi, S. *et al.* Influenza A virus nucleoprotein induces apoptosis in human airway epithelial cells: implications of a novel interaction between nucleoprotein and host protein Clusterin. *Cell Death Dis.* **4,** e562 (2013).

229. Koyama, A. H. *et al.* Role of virus-induced apoptosis in a host defense mechanism against virus infection. *J. Med. Invest.* **45,** 37–45 (1998).

230. Li, C. *et al.* Host cell apoptosis induced by infection with duck swollen head hemorrhagic disease virus. *Prog. Nat. Sci.* **19,** 47–53 (2009).

231. Odeberg, J. *et al.* Human cytomegalovirus inhibits neuronal differentiation and induces apoptosis in human neural precursor cells. *J. Virol.* **80,** 8929–8939 (2006).

232. Takizawa, T. *et al.* Induction of programmed cell death (apoptosis) by influenza virus infection in tissue culture cells. *J. Gen. Virol.* **74 (Pt 11,** 2347–2355 (1993).

233. Fujimoto, I., Takizawa, T., Ohba, Y. & Nakanishi, Y. Co-expression of Fas and Fas-ligand on the surface of influenza virus-infected cells. *Cell Death Differ.* **5,** 426–431 (1998).

234. Wada, N. *et al.* Transcription stimulation of the Fas-encoding gene by nuclear factor for interleukin-6 expression upon influenza virus infection. *J. Biol. Chem.* **270,** 18007–18012 (1995).

235. Takizawa, T., Fukuda, R., Miyawaki, T., Ohashi, K. & Nakanishi, Y. Activation of the apoptotic Fas antigen-encoding gene upon influenza virus infection involving spontaneously produced beta-interferon. *Virology* **209,** 288–96 (1995).

236. Pistritto, G., Trisciuoglio, D., Ceci, C., Garufi, A. & D'Orazi, G. Apoptosis as anticancer mechanism : function and dysfunction of its modulators and targeted therapeutic strategies. *Aging (Albany. NY).* **8,** 1–17 (2016).

237. Ewald, F. *et al.* Constitutive expression of murine c-FLIPR causes autoimmunity in aged mice. *Cell Death Dis.* **5,** e1168 (2014).

238. Troeger, A. *et al.* Up-regulation of c-FLIPS+R upon CD40 stimulation is associated with inhibition of CD95-induced apoptosis in primary precursor B-ALL. *Blood* **110,** 384–387 (2007).

239. Huang, Y. *et al.* Overcoming resistance to TRAIL-induced apoptosis in solid tumor cells by simultaneously targeting death receptors, c-FLIP and IAPs. *Int. J. Oncol.* **49,** 153–163 (2016).

240. Lv, X.-Q., Qiao, X.-R., Su, L. & Chen, S.-Z. Honokiol inhibits EMT-mediated motility and migration of human non-small cell lung cancer cells in vitro by targeting c-FLIP. *Acta Pharmacol. Sin.* (2016). doi:10.1038/aps.2016.81

241. Parzych, E. M. *et al.* Influenza Virus Specific CD8 + T Cells Exacerbate Infection Following High Dose Influenza Challenge of Aged Mice. **2013,** (2013).

242. Ge, M. Q. *et al.* NK cells regulate CD8+ T cell priming and dendritic cell migration during influenza A infection by IFN-γ and perforin-dependent mechanisms. *J. Immunol.* **189,** 2099–109 (2012).

243. Jenkins, M. R., Trapani, J. A., Doherty, P. C. & Turner, S. J. Granzyme K expressing cytotoxic T lymphocytes protects against influenza virus in granzyme AB-/- mice. *Viral Immunol.* **21,** 341–346 (2008).

244. Brincks, E. L., Katewa, A., Kucaba, T. A., Griffith, T. S. & Legge, K. L. CD8 T cells utilize TRAIL to control influenza virus infection. *J. Immunol.* **181,** 4918–25 (2008).

245. Guo, H. *et al.* The functional impairment of natural killer cells during influenza virus infection. *Immunol. Cell Biol.* **87,** 579–89 (2009).

246. Achdout, H. *et al.* Killing of avian and Swine influenza virus by natural killer cells. *J. Virol.* **84,** 3993–4001 (2010).

247. Kumar, P., Thakar, M. S., Ouyang, W. & Malarkannan, S. IL-22 from conventional NK cells is epithelial regenerative and inflammation protective during influenza infection. *Mucosal Immunol.* **6,** 69–82 (2013).

248. Gerosa, F. *et al.* Reciprocal activating interaction between natural killer cells and dendritic cells. *J. Exp. Med.* **195,** 327–333 (2002).

249. Mocikat, R. *et al.* Natural killer cells activated by MHC class I-low targets prime dendritic cells to induce protective CD8 T cell responses. *Immunity* **19,** 561–569 (2003).

250. Adam, C. *et al.* DC-NK cell cross talk as a novel CD4+ T-cell-independent pathway for antitumor CTL induction. *Blood* **106,** 338–344 (2005).

251. Pommerenke, C. *et al.* Global transcriptome analysis in influenza-infected mouse lungs reveals the kinetics of innate and adaptive host immune responses. *PLoS One* **7,** e41169 (2012).

252. Robbins, S. H. *et al.* Natural killer cells promote early CD8 T cell responses against cytomegalovirus. *PLoS Pathog.* **3,** 1152–1164 (2007).

253. Piccioli, D. Contact-dependent Stimulation and Inhibition of Dendritic Cells by Natural Killer Cells. *J. Exp. Med.* **195,** 335–341 (2002).

254. Horby, P., Nguyen, N. Y., Dunstan, S. J. & Baillie, J. K. The role of host genetics in susceptibility to influenza: a systematic review. *PLoS One* **7,** e33180 (2012).

255. Jonjić, S., Babić, M., Polić, B. & Krmpotić, A. Immune evasion of natural killer cells by viruses. *Curr. Opin. Immunol.* **20,** 30–38 (2008).

256. Lodoen, M. B. & Lanier, L. L. Viral modulation of NK cell immunity. *Nat. Rev. Microbiol.* **3,** 59–69 (2005).

257. Guo, H., Kumar, P. & Malarkannan, S. Evasion of natural killer cells by influenza virus. *J. Leukoc. Biol.* **89,** 189–194 (2011).

258. Toapanta, F. R. & Ross, T. M. Impaired immune responses in the lungs of aged mice following influenza infection. *Respir. Res.* **10,** 112 (2009).

259. Carrat, F. & Flahault, A. Influenza vaccine: the challenge of antigenic drift. *Vaccine* **25,** 6852–6862 (2007).

260. Karre, K., Ljunggren, H. G., Piontek, G. & Kiessling, R. Selective rejection of H-2-deficient lymphoma variants suggests alternative immune defence strategy. *Nature* **319,** 675–678 (1986).

261. Ehrhardt, C. *et al.* Influenza A virus NS1 protein activates the PI3K/Akt pathway to mediate antiapoptotic signaling responses. *J. Virol.* **81,** 3058–67 (2007).

262. Zhirnov, O. P. & Klenk, H.-D. Control of apoptosis in influenza virus-infected cells by up-regulation of Akt and p53 signaling. *Apoptosis* **12,** 1419–1432 (2007).

263. York, I. A. & Johnson, D. C. Direct contact with herpes simplex virus-infected cells results in inhibition of lymphokine-activated killer cells because of cell-to-cell spread of virus. *J. Infect. Dis.* **168,** 1127–1132 (1993).

264. Isobe, Y. *et al.* Epstein-Barr Virus Infection of Human Natural Killer Cell Lines and Peripheral Blood Natural Killer Cells. *Cancer Res.* **64,** 2167–2174 (2004).

265. Chehimi, J. *et al.* In vitro infection of natural killer cells with different human immunodeficiency virus type 1 isolates. *J. Virol.* **65,** 1812–1822 (1991).

266. Parker, A. K., Yokoyama, W. M., Corbett, J. A., Chen, N. & Buller, R. M. L. Primary naive and interleukin-2-activated natural killer cells do not support efficient ectromelia virus replication. *J. Gen. Virol.* **89,** 751–759 (2008).

267. Zhou, J. *et al.* Differential expression of chemokines and their receptors in adult and neonatal macrophages infected with human or avian influenza viruses. *J. Infect. Dis.* **194,** 61–70 (2006).

268. Perrone, L. A., Plowden, J. K., García-Sastre, A., Katz, J. M. & Tumpey, T. M.

H5N1 and 1918 Pandemic Influenza Virus Infection Results in Early and Excessive Infiltration of Macrophages and Neutrophils in the Lungs of Mice. *PLoS Pathog* **4,** e1000115 (2008).

269. Mao, H. *et al.* Inhibition of human natural killer cell activity by influenza virions and hemagglutinin. *J Virol* **84,** 4148–4157 (2010).

270. Leibson, P. J. Signal transduction during natural killer cell activation: inside the mind of a killer. *Immunity* **6,** 655–661 (1997).

271. Bryceson, Y. T., March, M. E., Ljunggren, H.-G. & Long, E. O. Activation, coactivation, and costimulation of resting human natural killer cells. *Immunol. Rev.* **214,** 73–91 (2006).

272. Mao, H. *et al.* Influenza virus directly infects human natural killer cells and induces cell apoptosis. *J. Virol.* **83,** 9215–9222 (2009).

273. Chan, M. C. *et al.* Proinflammatory cytokine responses induced by influenza A (H5N1) viruses in primary human alveolar and bronchial epithelial cells. *Respir Res* **6,** 135 (2005).

274. La Gruta, N. L., Kedzierska, K., Stambas, J. & Doherty, P. C. A question of self-preservation: immunopathology in influenza virus infection. *Immunol. Cell Biol.* **85,** 85–92 (2007).

275. Gao, R. *et al.* Cytokine and chemokine profiles in lung tissues from fatal cases of 2009 pandemic influenza A (H1N1): role of the host immune response in pathogenesis. *Am. J. Pathol.* **183,** 1258–68 (2013).

276. Szretter, K. J. *et al.* Role of host cytokine responses in the pathogenesis of avian H5N1 influenza viruses in mice. *J Virol* **81,** 2736–2744 (2007).

277. Matikainen, S. *et al.* Tumor necrosis factor alpha enhances influenza A virus-induced expression of antiviral cytokines by activating RIG-I gene expression. *J. Virol.* **80,** 3515–3522 (2006).

278. Hussell, T., Pennycook, A. & Openshaw, P. J. Inhibition of tumor necrosis factor reduces the severity of virus-specific lung immunopathology. *Eur. J. Immunol.* **31,** 2566–2573 (2001).

279. Salomon, R., Hoffmann, E. & Webster, R. G. Inhibition of the cytokine response does not protect against lethal H5N1 influenza infection. *Proc. Natl. Acad. Sci.* **104,** 12479–12481 (2007).

280. Perrone, L. A., Szretter, K. J., Katz, J. M., Mizgerd, J. P. & Tumpey, T. M. Mice Lacking Both TNF and IL-1 Receptors Exhibit Reduced Lung Inflammation and Delay in Onset of Death following Infection with a Highly Virulent H5N1 Virus. *J. Infect. Dis.* **202,** 1161–1170 (2010).

281. Khoufache, K. *et al.* Protective role for protease-activated receptor-2 against influenza virus pathogenesis via an IFN-gamma-dependent pathway. *J. Immunol.* **182,** 7795–7802 (2009).

282. Price, G. E., Gaszewska-Mastarlarz, a & Moskophidis, D. The role of alpha/beta and gamma interferons in development of immunity to influenza A virus in mice. *J. Virol.* **74,** 3996–4003 (2000).

283. Bot, A., Isobe, H. & Bona, C. Immunodeficient mouse models in the characterization of the protective immunity to influenza virus. *Folia Microbiol. (Praha).* **43,** 477–478 (1998).

284. Nguyen, H. H. *et al.* Gamma interferon is not required for mucosal cytotoxic T-lymphocyte responses or heterosubtypic immunity to influenza A virus infection in mice. *J. Virol.* **74,** 5495–5501 (2000).

285. Pulendran, B. & Maddur, M. S. Innate immune sensing and response to influenza. *Curr. Top. Microbiol. Immunol.* **386,** 23–71 (2015).